NATIONAL COOPERATIVE HIGHWAY RESEARCH PROGRAM
REPORT 108

TENTATIVE DESIGN PROCEDURE FOR RIPRAP-LINED CHANNELS

HIGHWAY RESEARCH BOARD
NATIONAL RESEARCH COUNCIL
NATIONAL ACADEMY OF SCIENCES—NATIONAL ACADEMY OF ENGINEERING

NATIONAL COOPERATIVE HIGHWAY RESEARCH PROGRAM
REPORT 108

TENTATIVE DESIGN PROCEDURE FOR RIPRAP-LINED CHANNELS

ALVIN G. ANDERSON, AMREEK S. PAINTAL,
AND JOHN T. DAVENPORT
UNIVERSITY OF MINNESOTA
MINNEAPOLIS, MINNESOTA

RESEARCH SPONSORED BY THE AMERICAN ASSOCIATION
OF STATE HIGHWAY OFFICIALS IN COOPERATION
WITH THE FEDERAL HIGHWAY ADMINISTRATION

SUBJECT CLASSIFICATIONS
HIGHWAY DESIGN
HIGHWAY DRAINAGE

HIGHWAY RESEARCH BOARD
DIVISION OF ENGINEERING NATIONAL RESEARCH COUNCIL
NATIONAL ACADEMY OF SCIENCES—NATIONAL ACADEMY OF ENGINEERING
1970

NATIONAL COOPERATIVE HIGHWAY RESEARCH PROGRAM

Systematic, well-designed research provides the most effective approach to the solution of many problems facing highway administrators and engineers. Often, highway problems are of local interest and can best be studied by highway departments individually or in cooperation with their state universities and others. However, the accelerating growth of highway transportation develops increasingly complex problems of wide interest to highway authorities. These problems are best studied through a coordinated program of cooperative research.

In recognition of these needs, the highway administrators of the American Association of State Highway Officials initiated in 1962 an objective national highway research program employing modern scientific techniques. This program is supported on a continuing basis by funds from participating member states of the Association and it receives the full cooperation and support of the Federal Highway Administration, United States Department of Transportation.

The Highway Research Board of the National Academy of Sciences-National Research Council was requested by the Association to administer the research program because of the Board's recognized objectivity and understanding of modern research practices. The Board is uniquely suited for this purpose as: it maintains an extensive committee structure from which authorities on any highway transportation subject may be drawn; it possesses avenues of communications and cooperation with federal, state, and local governmental agencies, universities, and industry; its relationship to its parent organization, the National Academy of Sciences, a private, nonprofit institution, is an insurance of objectivity; it maintains a full-time research correlation staff of specialists in highway transportation matters to bring the findings of research directly to those who are in a position to use them.

The program is developed on the basis of research needs identified by chief administrators of the highway departments and by committees of AASHO Each year, specific areas of research needs to be included in the program are proposed to the Academy and the Board by the American Association of State Highway Officials. Research projects to fulfill these needs are defined by the Board, and qualified research agencies are selected from those that have submitted proposals Administration and surveillance of research contracts are responsibilities of the Academy and its Highway Research Board.

The needs for highway research are many, and the National Cooperative Highway Research Program can make significant contributions to the solution of highway transportation problems of mutual concern to many responsible groups. The program, however, is intended to complement rather than to substitute for or duplicate other highway research programs.

NCHRP Report 108

Project 15-2 FY '66
ISBN 0-309-01896-X
L. C. Card No 76-608896

Price: $4.00

Published reports of the

NATIONAL COOPERATIVE HIGHWAY RESEARCH PROGRAM

are available from:

Highway Research Board
National Academy of Sciences
2101 Constitution Avenue
Washington, D.C. 20418

(See last pages for list of published titles and prices)

FOREWORD

By Staff

Highway Research Board

The tentative procedures for the design of riprap-lined roadside drainage channels detailed in this report will be of particular interest to hydraulic engineers. It contains a thorough analysis of previous research and other information on tractive forces and sediment transport in channels that was considered pertinent to the problem of erosion control in roadside ditches. The tentative design criteria developed from this analysis were verified by limited experimental testing in the hydraulics laboratory. A field testing program is under way and will be covered by a subsequent report. In view of the fact that this report contains design charts for determining the suitability of locally available aggregates for erosion protection of drainage channels handling less than 1,000 cfs, it should be of considerable value to practicing engineers of highway departments, consulting engineering firms, and other agencies that are confronted with drainage design problems.

Water moving over a soil surface causes erosion that often results in two undesirable consequences—damage to the soil surface, and silting or the depositing of the eroded soil in another waterway, such as a stream or a lake. Natural waterway channels are generally stabilized due to the action of erosion over long periods of time, and much of the earth's land area is protected from erosion by vegetative cover. When highway construction interferes with the natural flow of water, drainage channels must be designed and built to redirect the water to a natural waterway. Highway drainage channels should be made erosion resistant, usually by the installation of a protective lining, to prevent damage to the channel and silting of some other waterway or body of water.

The most extensively used protective linings for roadside ditches currently are turf cover, either by sodding or other methods of establishment, and various types of pavement. These linings are quite effective for a wide variety of conditions but have certain limitations, such as (1) turf cover is very difficult to establish in arid areas and over sandy soil, (2) turf cover is only effective at relatively low flow velocities, (3) paved ditch linings are usually difficult to construct and rather costly, and (4) paved ditch linings at times require extensive maintenance due to undercutting. As a result, there is a need for a type of economical protective lining for roadside channels suitable for conditions intermediate between those for which turf cover performs satisfactorily and those for which paved channels or pipe flumes are more economical The objective of this study was the development of criteria and design procedures for the use of aggregate or riprap linings for this intermediate category.

The University of Minnesota researchers approached the problem by first analyzing the theory of open channel flow and pertinent experimental data reported in the literature on forces acting on noncohesive particles in a flowing stream. On the basis of the analysis and interpretation of available data, equations were developed for determining the characteristics of a noncohesive assemblage of discrete particles that should not be moved by the forces generated by specified flow in a channel of a designated shape and longitudinal slope. Experimental verification of the tentative design method was undertaken on model segments of channels in a flume of the University of Minnesota St. Anthony Falls Hydraulic Laboratory. Experimental studies on linings, designed in accordance with the proposed procedures, failed at discharges of approximately twice the design discharges for uniform riprap material and at 1.5 times the design discharges for graded riprap material. The graded material was found to be more effective than uniform material in the prevention of leaching. A layer whose thickness is equivalent to three mean diameters appears adequate to prevent leaching of sand through the lining.

In addition to the development and experimental verification of the tentative design procedures, charts were prepared to provide a simplified means for establishing channel size and selecting suitable riprap material for a given channel flow and slope. Design charts are included in this report for regular trapezoidal channels with a maximum discharge of 1,000 cfs and wide triangular channels with a maximum discharge of 100 cfs—both with maximum slopes of 0.10 ft/ft. Design considerations for nonsymmetrical channels and channel bends are also included.

A field evaluation phase of the study is under way to provide further verification and possible modification of the tentative design procedures. A number of roadside channels are expected to be designed and built by state highway departments. Experience with regard to the economics, maintenance, and performance of these channels will be compiled and submitted in a subsequent report.

CONTENTS

1 SUMMARY

PART I

1 CHAPTER ONE Introduction—Review of Theory and Literature

Nature of Channel Erosion

Symbols Used

Characteristics of Open-Channel Flow

Uniform Flow

Forces Acting on Bed Particles in a Flowing Stream

Critical Boundary Shear

Distribution of Boundary Shear

Ratio of Critical Shear on Side Slopes to Critical Shear on the Bed

Shear Distribution in Bends

Leaching

Channel Freeboard

17 CHAPTER TWO Research Approach and Findings

Development of Design Procedure

Example 1. Trapezoidal Channel

Example 2. Trapezoidal Channel

Example 3. Trapezoidal Channel

Example 4. Triangular Channel

Experimental Verification of Design Procedures

Design of the Prototype Drainage Channel

Conclusions

Experiments on the Leaching of Base Material

69 CHAPTER THREE Application of Design Charts to Channel Design

70 CHAPTER FOUR Recommendations for Further Research

Field Testing

Channels of Large Capacity

Laboratory Research

70 REFERENCES

PART II

72 APPENDIX A Size Distribution and Gradation Limits for Eight Standard Aggregates

ACKNOWLEDGMENTS

The research reported herein was performed under NCHRP Project 15-2 by the University of Minnesota, with Alvin G. Anderson, Professor of Civil Engineering, as principal investigator. Amreek S. Paintal, Research Assistant, conducted the experimental research and analyzed the results. John T. Davenport, Research Assistant, was instrumental in working out the design charts. The experimental research on the mechanics of leaching, summarized in Chapter Two, was conducted by Dr Josef Zaruba of the Institute of Hydrodynamics, Czechoslovak Academy of Sciences, Prague, Czechoslovakia, during his study leave at the St. Anthony Falls Hydraulic Laboratory. A bibliography of pertinent literature was compiled by Warren Q. Dahlin, Research Engineer. The facilities of the St. Anthony Falls Hydraulic Laboratory of the University of Minnesota (Edward Silberman, Director) were used and the research was carried out with the able assistance of its staff

TENTATIVE DESIGN PROCEDURE FOR RIPRAP-LINED CHANNELS

SUMMARY

In some areas and in certain circumstances it is necessary, to prevent erosion of highway drainage channels, to provide a protective erosion-resistant lining. One such type, the protective qualities of which lie between those of a grassed drainage channel and a concrete-lined drainage channel, is the so-called riprap lining. It consists of a layer of discrete fragments of rock of sufficient size to resist the erosive forces of the flow. The design of such riprap-lined drainage channels involves the interrelationship between the discharge, the longitudinal slope, the size and shape of the channel, and the size distribution of the riprap lining This report describes these interrelationships and develops design criteria by which a riprap-lined drainage channel can be proportioned and the riprap lining can be specified for a given discharge and longitudinal slope. The relationships so developed have been reduced to design charts, the use of which permits rapid and simple establishment of channel shape and size as well as of the properties of the riprap lining.

Highway drainage channels are divided into two groups. In the first group are those that serve as median or side ditches for the drainage of the roadways. These are relatively small and often approach a triangular cross section because of the relatively flat side slopes and generally small bottom width. In the second group are large drainage channels that convey a larger discharge and are usually trapezoidal in cross section. A set of design charts for each type has been prepared.

Limited experimental data are presented which serve to verify the design procedure, to test the efficacy of channels designed according to this procedure, and to examine somewhat more closely the phenomenon of leaching of base material through the riprap interstices. These experiments, although preliminary in character, indicate that the design procedures are suitable and incorporate sufficiently large factors of safety to provide stable channels.

CHAPTER ONE

INTRODUCTION–REVIEW OF THEORY AND LITERATURE

NATURE OF CHANNEL EROSION

The purpose of highway drainage channels is to transport excess water from the highway surface and surrounding area to places of disposal, such as natural streams or other declivities. Such channels constructed through local natural materials must be designed to convey the prescribed discharges without serious erosion of the boundaries It is the purpose of this report to discuss the characteristics of flow in open channels and the means by which erosion-resistant channels may be designed. The suggested design procedure as outlined is based on information and prac-

tices that have been reported in the literature and on limited experimentation in areas where the literature appeared to be deficient in some respect. Stable channels represent a special case of the sediment transport problem and much of the data come from this discipline A number of papers (*1, 2*) on this and related aspects have been helpful in organizing the data and developing the procedure

Erosion results when the dynamic forces generated by the velocity of the fluid acting on the boundary are greater than the resistive forces of the boundary material. The materials through which a channel may be constructed or which may exist on the boundary may, from the point of view of erosivity, be loosely classified as noncohesive sediments or cohesive sediments As the term implies, noncohesive sediments are those consisting of discrete particles, of whatever size, the movement of which for given erosive forces depends only on the particle properties (such as shape, size, density) and on the relative position of the particle with respect to surrounding particles. Sands and gravels of stream beds that have been previously transported, deposits laid down by wind or water, and even crushed rock in the form of riprap may be included in this class

Cohesive sediments, on the other hand, are those for which the resistance to initial movement or erosion depends on the strength of the cohesive bond that may exist between the particles, as well as on the properties of individual particles The resisting force due to the cohesive bond may far outweigh the influence of the physical properties of the individual particles, so that erosion of cohesive soils can often be considered a function only of the soil properties that give rise to cohesion Cohesive sediments include residual soils containing cohesive materials such as clay In the broad sense, cohesive materials may also include soils protected by a vegetative cover, either natural or cultivated, as well as artificial substances used to define channel boundaries, such as concrete or bituminous materials, whose resistance depends on the internal strength of the substance itself In general, cohesive sediments are considerably more resistant to erosion than are corresponding noncohesive sediments. In fact, many practices designed to lessen the rate of erosion in canals or channels have the purpose of increasing the erosion-resisting forces where necessary by the promotion of vegetable growth, such as grass lining or other artificial cover (*3*)

From this point of view, then, erosion-resistant channels also can be divided into two groups: (1) those in which the boundary consists of an assemblage of discrete particles, the resistance of which depends on the particle properties such as weight and size and position, and (2) those channels in which the boundaries are resistant to erosion by virtue of the cohesive forces of whatever nature inherent in the boundary material. In the first category are those channel boundaries protected by a layer of coarser particles, commonly called riprap, which are large enough of themselves to withstand the dynamic forces In the second category are those channels in which the boundaries are protected by the addition of cohesive elements such as the natural soil, grass, or other vegetative linings, membranes or fabrics; bituminous materials; and finally, probably the most resistant to erosion, concrete lining. All these different types are found in practice, each designed to serve a particular purpose.

This report is limited to a discussion of erosion-resistant channels whose boundaries are protected by a noncohesive assemblage of discrete particles, of such a size that they will not be moved by the forces generated in the flow.

SYMBOLS USED

The symbols used in the equations in this report are defined after the equations and, for the reader's convenience, are also defined in the following:

A = cross-sectional area, ft^2;
B = bottom width, ft,
B_s = surface width, ft,
C_d' = drag or lift coefficient,
C_f = skin friction coefficient;
D = drag force on particle, lb,
d = particle size, mm, ft,
d_{50} = particle size, of which 50 percent is finer by weight, mm, ft,
F_1, F_2 = hydrostatic force, lb,
g = gravitational acceleration, ft/sec^2;
H = total head, ft,
H_o = specific head, ft;
h_L = frictional losses, ft;
L = lift force on particle, lb,
n = Manning's coefficient of roughness,
P = wetted perimeter, ft,
p = pressure, psf,
Q = discharge, ft^3/sec;
q = transport rate of base material, lb/ft sec;
R = hydraulic radius, ft,
R_o = mean radius of bend, ft;
S = slope, ft/ft,
ΔS = length along channel, ft;
S_b = bed slope, ft/ft,
S_e = energy slope, ft/ft,
S_w = water surface slope, ft/ft;
V = velocity, fps,
V_c = critical velocity, fps;
W = weight, lb,
y = depth, ft,
y_c = critical depth, ft,
y_c = vertical distance from bed to elevation of velocity vector,
y_m = mean depth, ft,
y_o = normal depth, ft;
Δy = superelevation in bends, ft;
z = distance from datum to bed, ft;
z_* = effective side slope,
Z = side slope z horizontal. 1 vertical (Z:1).
α_1 = area shape factor for riprap,
α_2 = proportionality factor,
α_3 = volumetric shape factor for riprap,
β = bed slope angle, degrees;
γ = unit weight of water, pcf;
γ_s = unit weight of riprap, pcf,

ζ = coefficient;
θ = angle of repose, degrees;
ϕ = angle of side slope, degrees;
ρ = density of water;
σ = standard deviation;
τ = shear stress, psf;
τ_* = dimensionless shear stress,
τ_o = average shear stress, psf;
τ_c = critical shear stress, psf,
τ_b = shear stress on bottom, psf; and
τ_s = shear stress on side slope, psf.

CHARACTERISTICS OF OPEN-CHANNEL FLOW

As an introduction to the design of riprap-protected channels, the erosion-producing forces generated by flow in open channels are briefly described. Such a description may properly begin with the Bernoulli equation, which, in turn, may be derived from the equations of motion (*4*). This relationship applied to a particular section of a particular stream tube can be written as

$$\frac{V^2}{2g}+\frac{p}{\gamma}+z=H \qquad (1)$$

in which V is taken as the mean velocity in the stream tube assumed to be infinitesimal in cross section, g is the acceleration due to gravity, p is the pressure, γ is the specific weight of the water, and z is the elevation of the stream line above some arbitrary datum. The sum of these terms is equal to H, commonly called the total head or total energy in foot-pounds per pound of fluid of the flow at the section in question. The equations of motion also can be written for the stream tube and integrated with respect to the distance along the stream tube, with the following results:

$$\frac{V_1^2}{2g}+\frac{p_1}{\gamma}+z_1=\frac{V_2^2}{2g}+\frac{p_2}{\gamma}+z_2+\frac{\tau}{\gamma R}\Delta S \qquad (2)$$

in which, in addition to the terms previously defined, τ is the unit shear on the boundary of the stream tube of which R is the hydraulic radius, and ΔS is the distance between the points 1 and 2 along the stream tube. Here, the last term on the right-hand side represents the head loss or energy loss due to frictional shear on the boundary of the stream tube.

If the stream lines are straight, the pressure will be hydrostatically distributed so that $p/\gamma=y_s$, in which y_s is the vertical distance from the free water surface to the stream tube under consideration. Then $p/\gamma+z=y_s+z_s$, in which y_s+z_s is the distance to the free water surface from the arbitrary datum This applies to all stream lines passing through the channel cross section. As the location of the stream line changes, y_s and z_s correspondingly change, so that y_s+z_s is always a constant. If y_s is taken equal to the depth and z_s is the elevation of the stream bed, Eq. 2 can be written in the form

$$\frac{\alpha_1 V_1^2}{2g}+y_1+z_1=\frac{\alpha_2 V_2^2}{2g}+y_2+z_2+\frac{\tau}{\gamma R}\Delta S \qquad (3)$$

in which V_1 and V_2 are the mean velocities in sections 1 and 2, respectively, and α_1 and α_2 are the energy coefficients to account for the velocity profile. With sufficient accuracy they can be taken as unity. The geometrical relationships of these dynamic properties are shown in Figure 1.

It is apparent from Figure 1 that

$$\frac{\tau}{\gamma R}\Delta S=S_e\,\Delta S \qquad (4)$$

so that the unit shear generated on the bed of the open channel by the flow can be expressed as

$$\tau_o=\gamma R S_e \qquad (5)$$

in which τ_o is the mean shear around the wetted perimeter, acting parallel to the bed in the direction of flow, γ is the specific weight of the water, R is the hydraulic radius defined as A/P (in which A is the cross-sectional area and P is the wetted perimeter), and S_e is the slope of the energy gradeline. The distribution of τ_o around the wetted perimeter is discussed in a later section. Eq 5, however, indicates the origin and the magnitude of the shear which acts on the boundary material giving rise to the erosive forces.

Now, if Eq. 1 is applied to an open channel flow for which the pressure is hydrostatically distributed and for

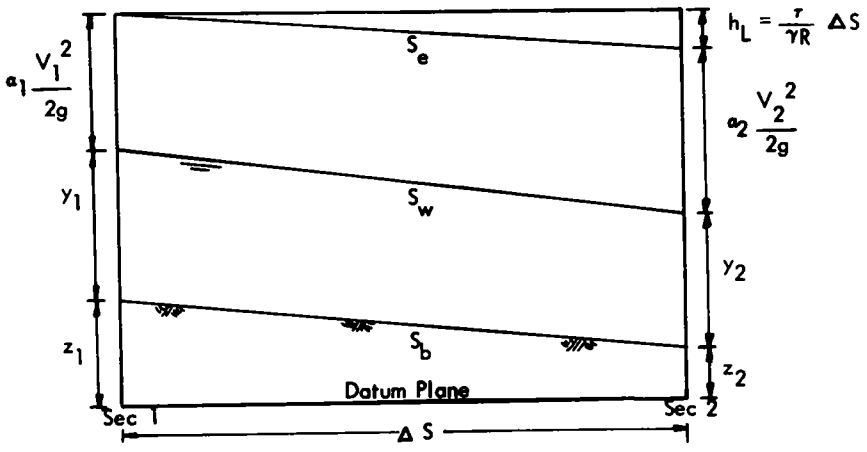

Figure 1 Energy relationships between two sections in open channel flow

which the arbitrary datum is fixed at the channel bed, one has, as before, p/γ equal to y_s, the distance from the water surface to the point in question, and z_s, its elevation with respect to the bottom of the channel. The equation can then be written in simple, but significant, form as

$$\frac{V^2}{2g} + y = H_o \tag{6}$$

in which $y_s + z_s = y$ is a constant equal to the depth, commonly known as the specific energy equation. This equation simply states that the energy of the flow with respect to the bed at a particular cross section is equal to the sum of the velocity head and the flow depth. It appears from this that for a given discharge, the flow may occur in different sections at any one of an infinite combination of velocities and depths. Using the discharge as a parameter, Eq 6 can also be plotted as in Figure 2 in the form of the familiar specific energy diagram showing specific head, H_o, as a function of y Of significance is the fact that a minimum specific energy exists The depth corresponding to this minimum specific energy is called the critical depth and plays a very important role in open-channel hydraulics.

Critical flow can be evaluated from Eq. 6 by differentiation as that condition for which

$$A^3/B_s = Q^2/g \tag{7}$$

in which A is the cross-sectional area and B_s is the surface width at critical flow. Inasmuch as both A and B_s are known functions of the depth, the value of y which satisfies Eq. 7, in which both Q and g are known, is the critical depth. Tables (*5*) have been prepared for the solution of Eq. 7 which greatly facilitate the computation of the critical depth in channels of various geometrical shapes. For depths less than the critical depth, the flow is described as being supercritical and is characterized by high velocities and small depths, as can be seen from Figure 2. For depths greater than the critical depth the flow is described as subcritical and is characterized by large depths and small velocities An examination of Eq 7 shows that for critical conditions

$$\frac{A}{B_s} = y_m = \frac{Q^2}{gA^2} = \frac{V_c^2}{g} \tag{8}$$

in which y_m is the mean depth for critical flow, and V_c is the critical velocity, or $(V_c^2/gy_m) = 1$. The expression V^2/gy_m, called the Froude number, is a dimensionless parameter that characterizes the flow and is of great significance in all phases of open-channel flow. When the Froude number is equal to unity the flow is in the critical state at a minimum specific energy; when the Froude number is less than unity the flow is subcritical; and when the Froude number is greater than unity the flow is supercritical.

The preceding equations describing the local boundary shear and the specific energy deal with the flow at a particular section and relate the frictional forces to the local hydraulic conditions Eq. 1 can also be used to study the interrelationships between the variations downstream in the longitudinal direction Differentiation of Eq 1 with respect to the longitudinal direction and simplification leads to the following equation for the water surface profile.

$$\frac{dy}{dx} = \frac{S_b - S_e}{1 - (V^2/gy_m)} \tag{9}$$

in which dy/dx is the rate of change of depth with respect to distance, S_b and S_e are the slopes of the bed and energy gradeline, respectively, and V^2/gy_m is the Froude number of the flow. Both the slope of the energy gradeline and the Froude number can change as the flow proceeds downstream, so that the depth will also change. Examination of Eq. 9 shows that two significant limits exist Whenever $S_e = S_b$, that is, when the energy gradeline is parallel to the bed, $dy/dx = 0$. This means that the depth is then constant, the flow is uniform, and the rate of energy loss is equal to the change in bed elevation The depth for which the slopes are equal and the depth remains constant is called the normal depth, y_o The normal depth may, of course, be greater or less than the critical depth. When the normal depth, y_o, is less than critical depth, the slope of the bed must be greater than the critical slope so that normal flow is supercritical This is called a steep or supercritical slope When the normal depth is greater than the critical, the slope of the bed is less than the critical slope, the normal flow is subcritical, and the bed slope is called a mild or subcritical slope. For a given discharge in a particular channel of given shape and roughness, there will then be only one depth at which uniform flow at constant depth will occur. The second limit occurs when the Froude number in the denominator approaches unity so that $dy/dx = \infty$. This means that theoretically the water surface profile crosses the critical depth vertically. In reality the water surface intersects the critical depth line at an angle considerably less than 90°.

The water surface profiles that may exist in channels in which the normal depth for uniform flow is greater or less

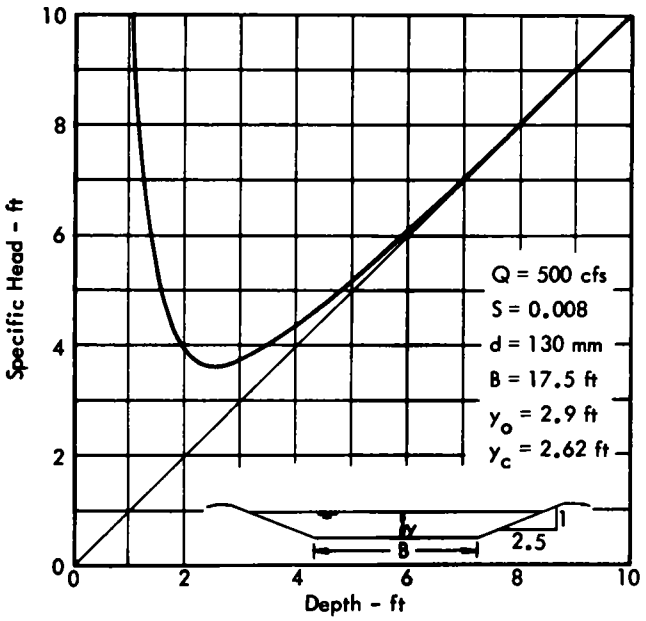

Figure 2. Variation of specific head in terms of flow depth for trapezoidal channels at a given discharge

than the critical depth are shown in Figure 3. It will be observed that for both the mild and steep slopes the actual depths leave or approach the normal depth asymptotically. The diagrams also show that in the absence of major channel controls the depth will tend to approach uniform flow Although, because of minor variations in channel shape, cross-sectional size, and roughness properties, the flow can never be exactly uniform, uniformity and normal depth are the conditions to which all flows in open channels tend. In the case of artificial channels of appreciable length, particularly in channels of large roughness protuberances, it can be assumed with negligible error that the flow does occur at normal depth. Therefore, channel design in general needs to be concerned only with uniform flow at normal depth.

UNIFORM FLOW

It can be seen from Eq 9 that when the slope of the energy gradeline is equal to the slope of the bed, the depth of flow will be constant along the channel and so, consequently, will be the velocity This depth, called the normal depth, is such that the rate of energy loss is exactly equal to the rate of change of bed elevation. It might be expected then that the normal depth would depend on the discharge, slope, channel geometry, and roughness. For uniform flow the total boundary shear is the only force acting on the body of fluid to counteract the weight of the fluid inasmuch as the pressure forces are equal and opposite and all accelerations are zero. This situation is shown in Figure 4 from which

$$\tau_o P \Delta S = \gamma A \Delta S \sin \theta \qquad (10a)$$

Because for small angles $\sin \theta = \tan \theta = S_b$,

$$\tau_o = \gamma R S_b \qquad (10b)$$

in which τ_o is the mean boundary shear acting over the wetted perimeter, R is the hydraulic radius, and S_b is the slope of the channel bed. The expression for mean boundary shear given in Eq. 10b is seen to be the same as that developed in Eq. 5 when uniform flow exists and the slope of the energy gradeline is equal to that of the bed. Inasmuch as the boundary shear is due to the drag of the fluid over the boundary surface, it can be expected that the boundary shear also depends on some characteristic velocity in the channel as well as the channel properties given in Eq. 10b The relationship of shear to velocity is by dimensional reasoning

$$\tau_o = C_f \rho V^2 \qquad (11)$$

in which ρ is the fluid density, V is the mean velocity in the channel, and C_f is a friction coefficient that depends, by analogy to flow over flat plates, on the channel roughness

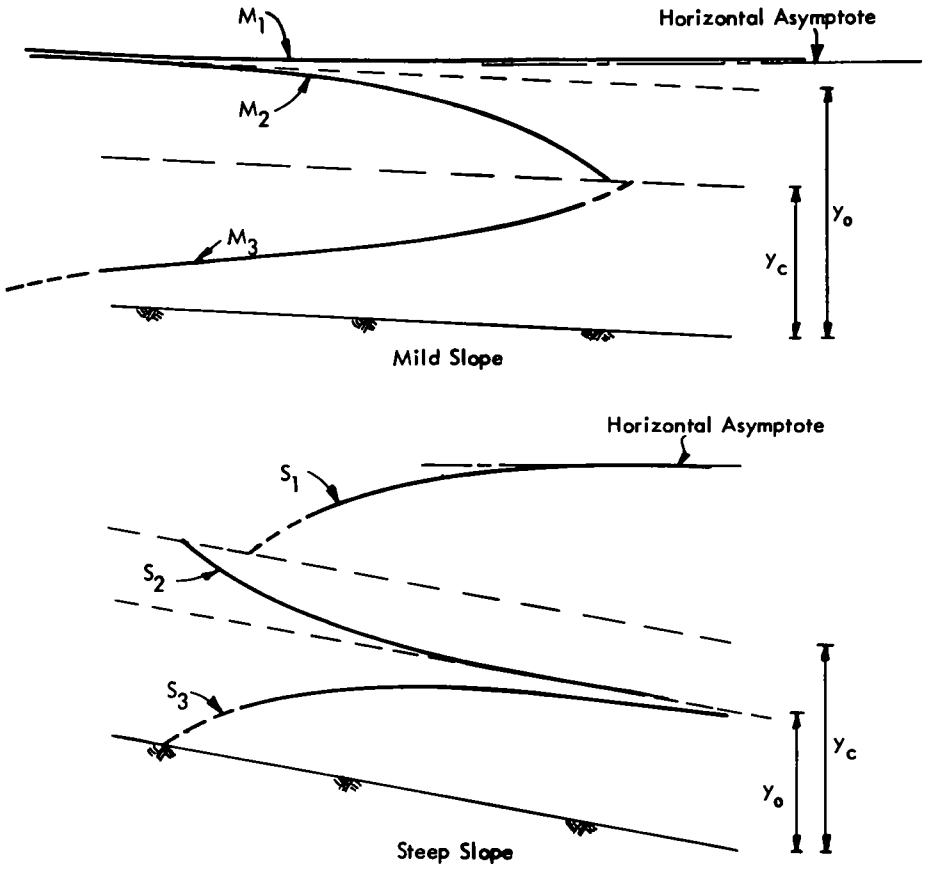

Figure 3 Water surface profile on mild slopes and steep slopes

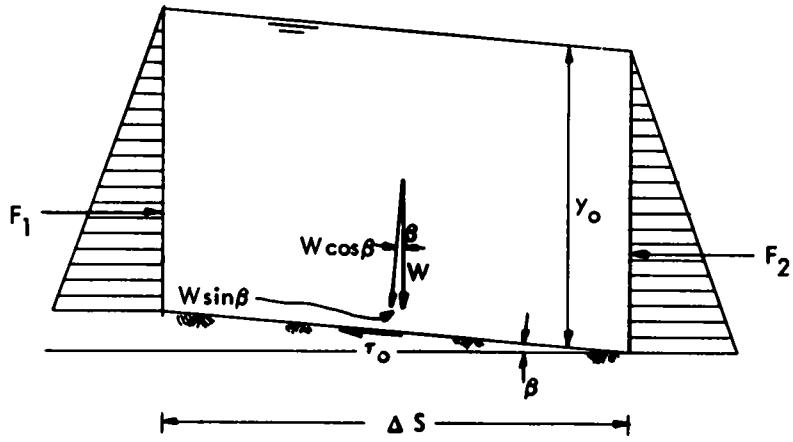

Figure 4 Forces acting on fluid mass flowing at normal depth

and a characteristic Reynolds number. Using Eqs 10 and 11, the mean channel velocity for uniform flow can be written in terms of the channel geometry as

$$V = C\sqrt{gRS_b} \tag{12}$$

Eq. 12 then defines the normal depth and specifies the relationship between mean velocity and channel characteristics for a given discharge. The coefficient C becomes a measure of channel resistance in that the larger the C the greater the mean velocity for a given depth. The smaller the coefficient the greater would be the depth of flow for a given discharge. If C has the form $\frac{1.49\,R^{1/6}}{n\sqrt{g}}$ the familiar Manning formula results. In this expression n is the so-called Manning roughness coefficient which must have the dimensions of $(L)^{1/6}$ Introducing this coefficient the Manning formula as commonly used is

$$V = \frac{1.49}{n} R^{2/3} S_b^{1/2} \tag{13}$$

With the proper choice of n, Eq. 13 relates the mean velocity for normal flow to the channel roughness, hydraulic radius, and bed slope

Innumerable observations in natural streams as well as large artificial channels and laboratory flumes have been made to relate the roughness coefficient n to the channel properties (*6-14*). In natural streams the Manning coefficient would depend on, in addition to boundary roughness, such properties as channel alignment, resistant outcrops, bank vegetation, and overbank conditions, as well as variations in channel size. In artificial channels, however, only channel roughness as related to channel size would be significant and n should be a relatively simple function of the actual size of channel roughness elements. Experiment has borne out the expectation in that for straight, prismatic channels of uniform boundary texture flowing less than bank full, the n in the Manning equation can be expressed as

$$n = Kd^{1/6} \tag{14}$$

in which d is a characteristic size of the boundary particles and K is a coefficient. The results of measurement in a variety of channels over a wide range in relative size are shown in Figure 5, in which the Manning form of the roughness coefficient in Eq. 12 is plotted in terms of the relative roughness, y/d_{50}. In this plot it was assumed that the hydraulic radius could be approximated by the depth and the effective grain size could be represented by the median or 50-percent size. Although there is some scatter among the data of the various investigators, the trend relating n to the grain diameter over a large range of relative size is very good. As was expected, a trend line drawn through the data could be fitted so that

$$n = 0.0395\,d_{50}^{1/6} \tag{15}$$

The data of Figure 5 and other data are plotted in Figure 6 in terms of n directly as a function of the effective grain size d_{50} with Eq. 15 fitted to the points. In this plot the roughness coefficient for channels ranging from laboratory flumes to large rivers is included The grain size ranged from less than 0.001 ft to nearly 1.0 ft. With the aid of Eq. 15, knowing the effective size of the riprap or boundary material (d_{50}, ft) covering the bed and side slopes in a given artificial channel, one can determine the mean velocity and hydraulic radius for any prescribed discharge.

FORCES ACTING ON BED PARTICLES IN A FLOWING STREAM

If one considers an assemblage of discrete particles immersed in a moving fluid such that they form the lower boundary or bed, certain forces are generated by the fluid on the particles. In Figure 7 some of these forces are shown schematically as they might be applied to a particular particle. A characteristic velocity profile in the neighborhood of the bed is also shown The velocity profile represents the temporal mean velocity at each point and shows the characteristic decrease in velocity as the boundary is approached. Because of the irregularity of the boundary, elevations are measured from an arbitrary da-

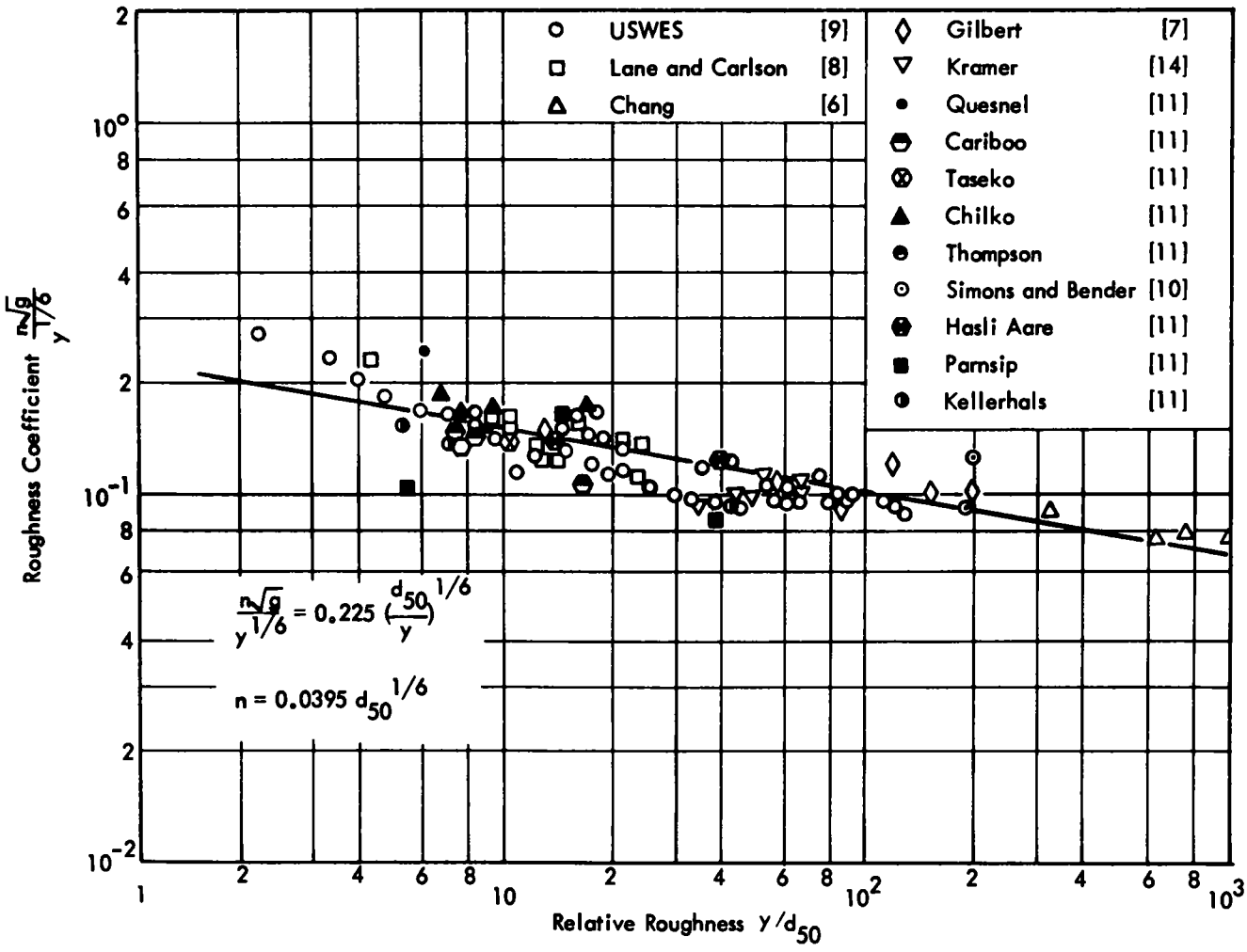

Figure 5 Variation of Manning's n *with relative roughness of the bed*

tum. Superimposed on this temporal mean velocity field are the turbulent velocity fluctuations which may or may not cause instantaneous local modifications of velocity field about the particle. As the flow passes the particle, the stream lines are deflected upward and around the particle, thus forming a downstream wake. The size of the wake depends on the point of separation of the local boundary layer developed on the particle, which in turn depends on the shape of the particle and the local Reynolds number.

As a result of the mean velocity field, forces are generated on the particle which may be decomposed into a drag force in the direction of the mean velocity and the lift force perpendicular to the mean velocity. The drag force is composed of a skin friction drag and a form drag, and its location with respect to the center of gravity of the particle depends on the relative magnitude of the two effects, which again depends on the local Reynolds number and the shape and relative position of the particle. If the form drag predominates, the resultant drag force will pass through a point approaching the center of gravity of the exposed portion of the particle The effect of the skin friction component is to raise the point of application toward the top of the grain.

The lift force is the resultant of the pressure differences between the upper and lower sides of the particle. On the upper side the pressure is reduced below the static pressure by virtue of the curvature of the stream lines and increased velocity around the particle. On the lower side of the particle, because the flow through the interstices of the bed is small, the pressure approaches the static pressure of the flow. The lift force is normally directed upward, but with the turbulent velocity fluctuations superimposed on the mean velocity field, the lift and the drag are actually fluctuating quantities both in magnitude and in location of the point of application. In fact, it is conceivable that at certain instances one or both might be reversed in direction.

The force resisting motion of noncohesive particles is the submerged weight of the particle plus any downward force component caused by contact with other particles in the bed. The submerged weight depends on the size, shape, and density of the particle. In an aggregation of natural particles the shape, and particularly the size, can vary over

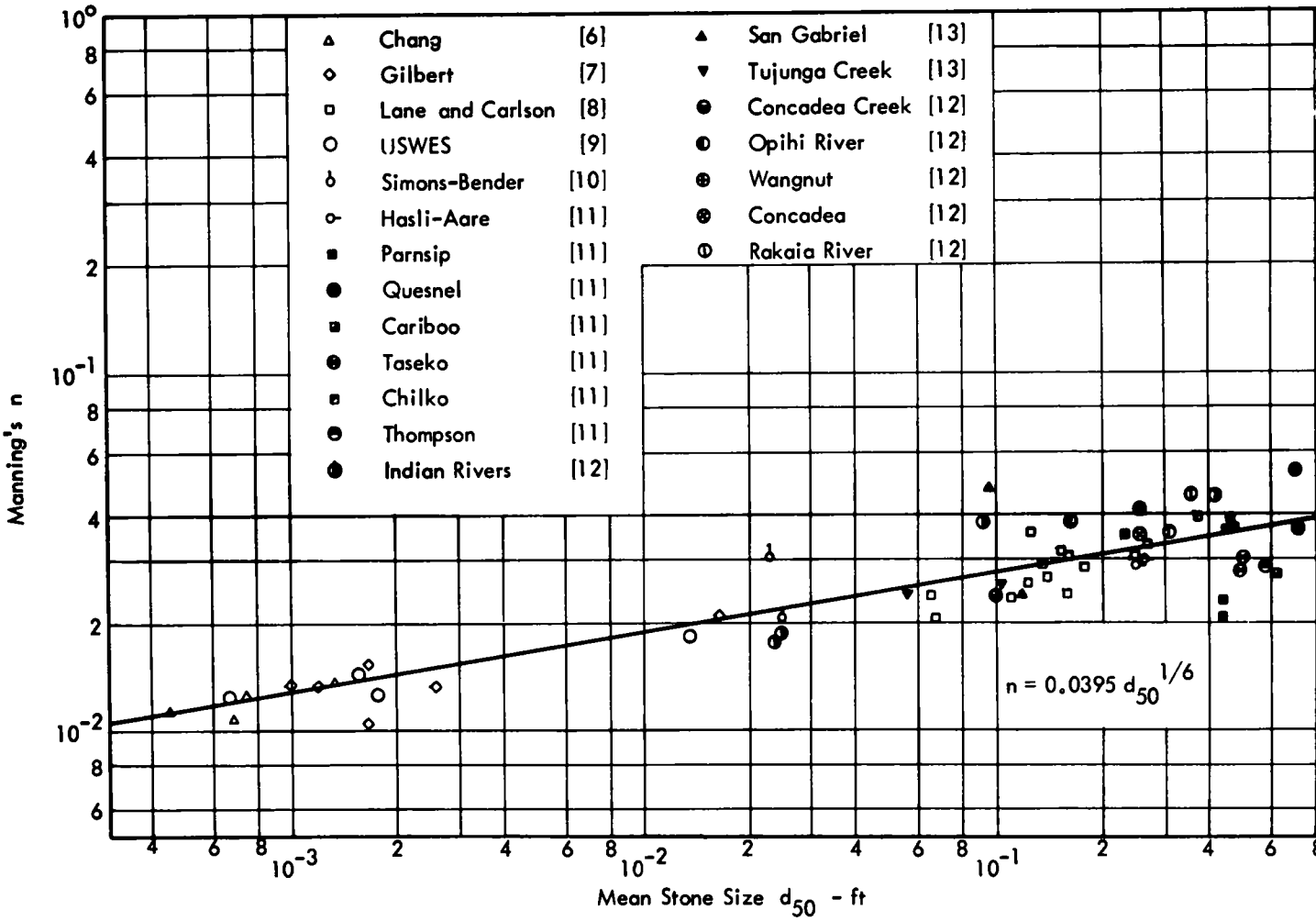

Figure 6 Variation of Manning's n *with size of stones composing the bed*

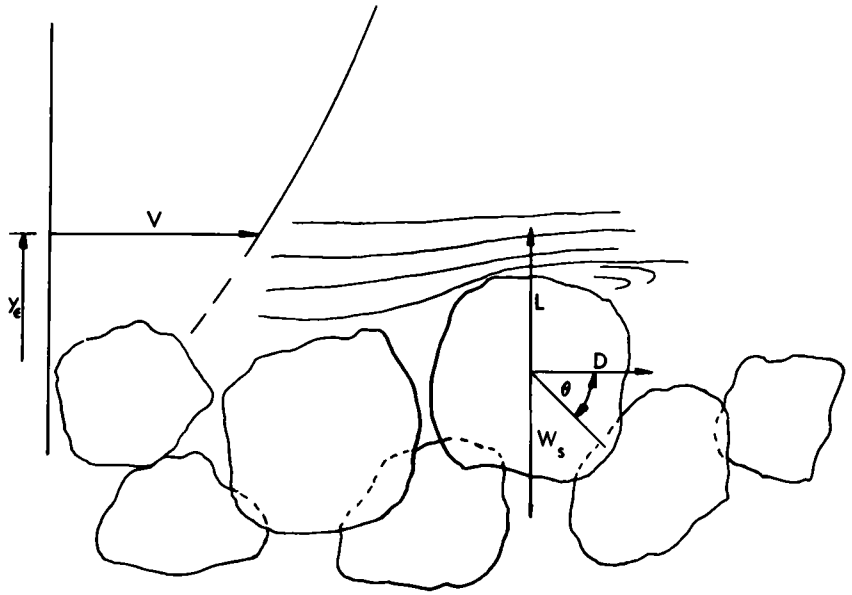

Figure 7 Diagrammatic description of forces on a typical bed particle in a flowing stream

a wide range. In addition, the degree of exposure to the fluid forces depends on the relative position of the particle in the bed and can vary from that of being completely exposed on the surface to that of being completely submerged in the bed. Consequently, considering the flow characteristics also, the force system that determines the motion of the particles is a complex function of time, space, and the properties of the particles that make up the aggregation.

Referring again to Figure 7, the movement of the indicated particle will depend on the instantaneous relative magnitudes of the forces acting and may occur in one of several ways If the moment of the resultant of the lift and drag about the point of contact is greater than the moment of the submerged weight about the same point, the particle will be rolled from its initial position to some point downstream where the combination of forces, including its own momentum, is such that it is once more stable. If the lift force at any instant becomes larger than the submerged weight, the particle will be lifted bodily from the bed and carried upward. The drag force acting on the particle will also tend to move it downstream so that its motion will be in the nature of a hop. Because of the possible variations of the forces generated by the fluid flowing about the typical particle, the instant of movement is rather indeterminate Considering the bed as a whole, particles will move whenever and wherever the dynamic forces are greater than the resisting forces. General movement might be defined as that state where particles at all points of the bed are moving with equal frequency and at which time the effective lift and drag may be represented by some mean value

Because the mean drag force or mean lift force can be defined by

$$D = C_1 \alpha_1 \rho d^2 \frac{V^2}{2} \tag{16}$$

in which C_1 is a drag or a lift coefficient, α_1 represents a shape factor describing the exposed cross-sectional area of the particle such that $A = \alpha_1 d^2$, d is the particle size, and V is the characteristic velocity of the flow. Because the local bed shear, τ_0, is also a function of the mean velocity (Eq. 11), Eq. 16 shows that the drag is proportional to the local bed shear and the size of the particles making up the bed over which the shear is acting From Eqs. 11 and 16 the drag can be described approximately by

$$D = \zeta d^2 \tau_0 \tag{17a}$$

in which ζ incorporates the drag coefficient, shape factor, and fluid properties, d is the size of the exposed particle, and τ_0 is the local bed shear per unit area. The stability of the material used to line a drainage channel then depends on the interaction of the local bed shear, τ_0, and the size and position of the riprap material.

CRITICAL BOUNDARY SHEAR

The critical boundary shear, τ_c, is defined as that value of the bed shear at which there is a general movement of the particles that make up the bed. As indicated previously, this value is rather indefinite because of the variation in both dynamic forces and properties and position of the individual particles. However, the range of mean shear required to initiate movement is sufficiently narrow in general to justify the use of the critical boundary shear concept. The value of the mean shear for the beginning of such movement may be estimated by visual observation of the condition of general movement or by extrapolating the curve showing transport rate as a function of bed shear to the condition of zero transport and evaluating the shear for this condition. Shields (*15*) developed a functional relationship by comparing the drag force as described in Eq. 17a to the effective weight of the submerged particle at incipient motion. Here ζ in Eq. 17a is a function of particle shape and local Reynolds number, or

$$\zeta = f\left(\alpha_1, \sqrt{\frac{\tau_c}{\rho}}\frac{d}{\nu}\right) \tag{17b}$$

and W is the submerged weight of the same particle so that

$$W = \alpha_3(\gamma_s - \gamma)d^3 \tag{18}$$

in which α_3 is a volumetric shape factor, γ_s is the specific weight of the bed particle, and γ is the specific weight of water. At incipient motion the drag can be taken as proportional to the submerged weight. Therefore,

$$f\left(\alpha_1, \frac{\sqrt{\frac{\tau_c}{\rho}}d}{\nu}\right) d^2\tau_c = \alpha_2\alpha_3(\gamma_s - \gamma)d^3 \tag{19a}$$

in which α_2 is the proportionality factor, or

$$\frac{\tau_c}{(\gamma_s - \gamma)d} = f\left(\alpha_1, \alpha_2, \alpha_3, \frac{\sqrt{\frac{\tau_c}{\rho}}d}{\nu}\right) \tag{19b}$$

In general, especially for larger rock particles, α_1, α_2, and α_3 can be taken as constants, and also for the larger particles of immediate concern the drag becomes independent of the local Reynolds number, so that

$$\frac{\tau_c}{(\gamma_s - \gamma)d} = \text{constant} \tag{20}$$

It is significant that for rock having a given specific weight the critical shear is directly proportional to the effective rock size. Figure 8 shows data (*14-21*) on the critical boundary shear in terms of the grain size, d_{50}. The plot clearly shows that for particles greater than about 0.001 ft the critical shear, τ_c, is proportional to the particle size. The range of data includes rock up to about 0.5 ft, so that extrapolation to larger sizes appears justified.

The critical boundary shear for various stone sizes as shown in Figure 8 represents the condition of motion (that is, the existing shear when particles are actually in motion), and can be represented by

$$\tau_c = 5\, d_{50} \tag{21}$$

In the design of stable channels, however, the rock size should be such that the rocks do not move for the given boundary shear. In effect, this means that the line shown in Figure 8 should be moved downward to some lower value to represent stone sizes that are stable for the given shear. Such a line has been drawn to encompass practically

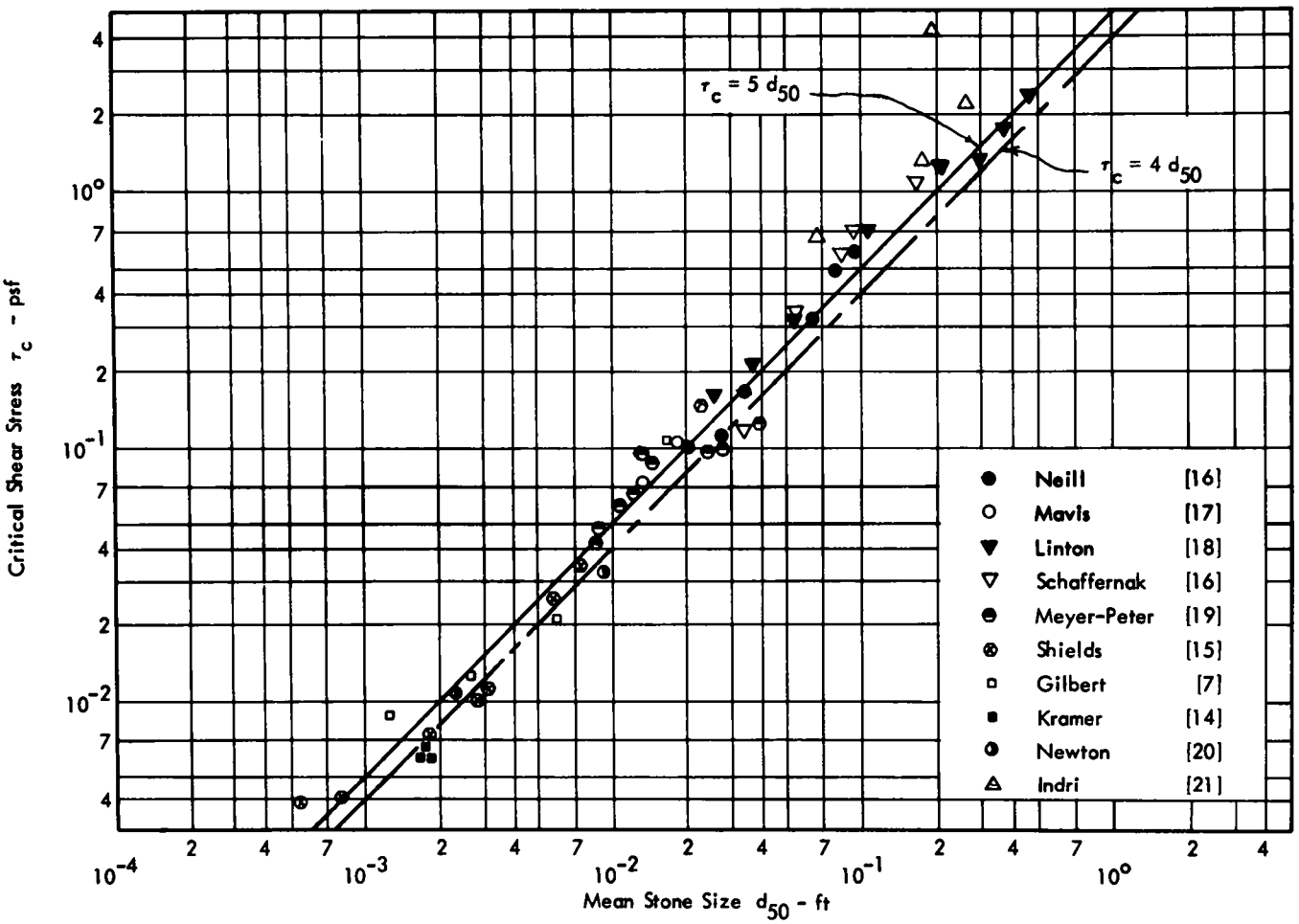

Figure 8 Critical boundary shear at incipient movement of riprap in terms of effective size

all the plotted data and should represent the upper limit of stable bed riprap. For comparison with Eq. 21 this relationship can be written as

$$\tau_c = 4\ d_{50} \qquad (22)$$

The studies of Lane and Carlson (*8*) on the San Luis Valley channels represented the critical boundary shear in terms of d_{75} as being more characteristic of the riprap mixture. It may be argued, however, that for channels in which sediment is moved the composition of the bed becomes coarser. In the case that the channel bed is stable, so that there is no movement, the bed composition remains constant and the initial d_{75} approaches d_{50} after a period of operation. At any rate, using d_{75} tends toward the conservative side.

It has been common practice to establish the velocity at which erosion of canal bed material begins. The so-called permissible velocities are generally based on observation. By means of the Manning equation and Eqs. 10 and 15, these permissible velocities can be reduced to permissible shear stresses. Some of these formulations (*15, 16, 17, 21-25*) are plotted in Figure 9 for comparison with the curve for the critical shear given in Eq. 22. It appears that the value based on the critical shear stress represents an approximate mean of those previously suggested.

DISTRIBUTION OF BOUNDARY SHEAR

In the development of Eq. 10 it was assumed that the shear equal to the mean shear was uniformly distributed around the wetted perimeter Because of the shape of the channel and the velocity distribution, it is unlikely that the shear would be uniformly distributed but would depend on the channel shape. In an attempt to develop the perimetric shear distribution, Olsen and Florey (*26*) applied membrane analogy methods to channel cross sections of various bottom widths and side slopes, including triangular channels. The results showed that the shear is not uniformly distributed but tends toward zero at the corners and a maximum on the center line of the bed, with lesser maxima at about the lower third point on the side slopes. Additional studies using finite difference methods adapted to digital computers by Replogle and Chow (*27*) have provided additional results for trapezoidal channels. This distribution compares well with previous experiments showing shear

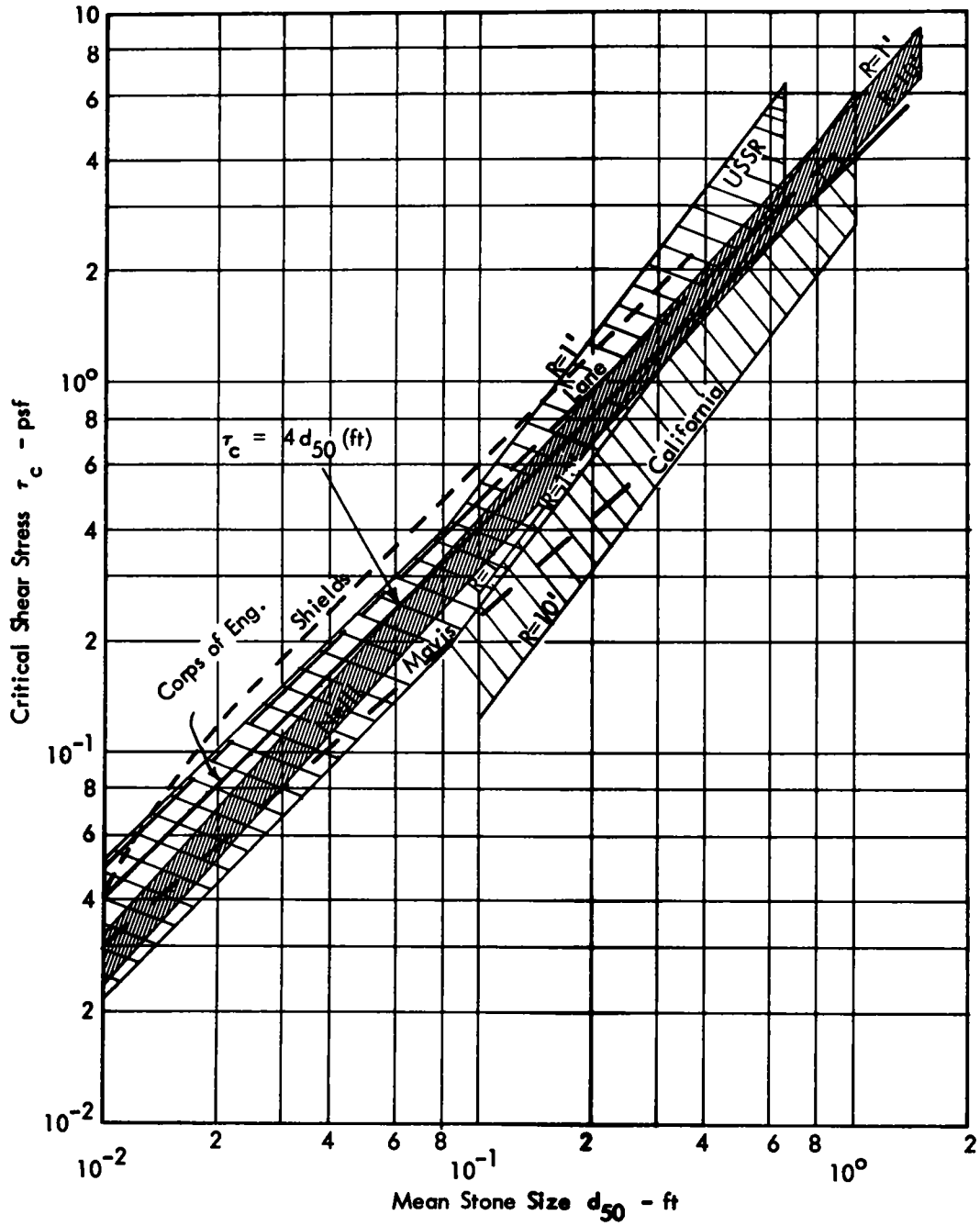

Figure 9 Comparison of various published formulations of critical boundary shear.

distribution. The side slopes of the channels investigated by Olsen and Florey (*26*) covered a range considerably smaller than that of interest in this study, so an attempt has been made to extrapolate the results to flatter side slope. In Figure 10 the relative shear as computed on the side of triangular channels in terms of the depth is plotted in terms of the side slope. A smooth curve connecting the given points has been extrapolated up to $Z = 10$, assuming that $C_{Rs} \rightarrow 1$ as Z becomes large. The Olsen and Florey results for the shear distribution on the sides of the triangular channels combined with the shear distribution in trapezoidal channels with relatively steep side slopes are plotted in Figures 11 and 12 in terms of the hydraulic radius to show the maximum shear on the sides and bottoms for various B/y ratios. The results of Olsen and Florey were transformed in this way in order that they might be used in Eq. 10 to determine the maximum local shear in terms of the hydraulic characteristics. It appears from Figures 11 and 12 that the maximum value of the boundary shear occurs on the bed and depends on the B/y ratio and the

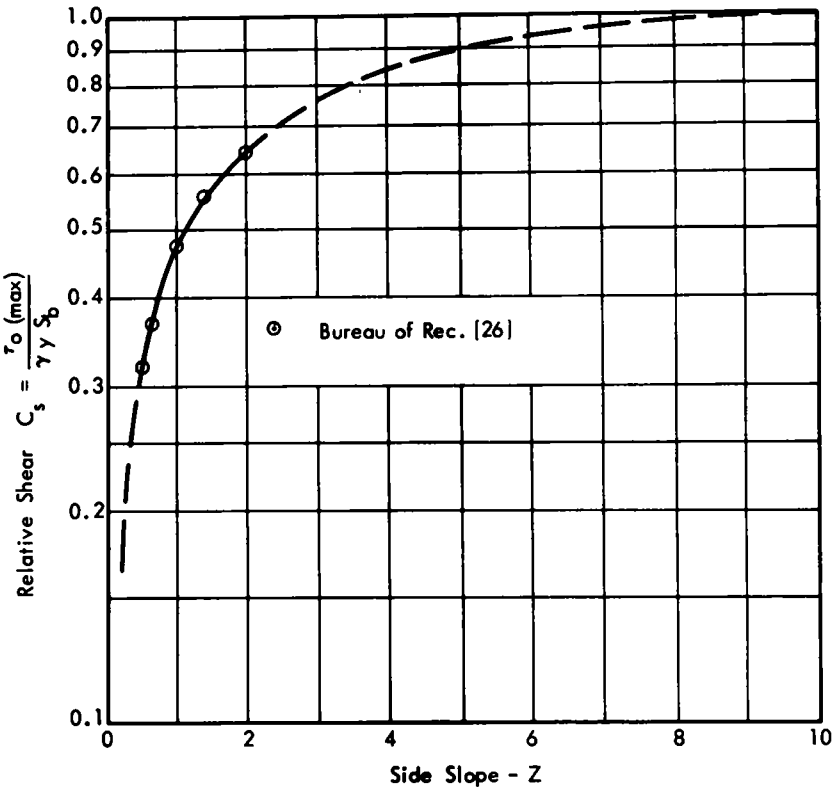

Figure 10 Maximum boundary shear stress on sides of triangular channels

side slopes. As the channel gets narrower (less than 1:2) the shear on the bed decreases, whereas that on the sides tends to increase relative to the mean. Because the trapezoidal channels of interest have values of B/y greater than 2 and side slopes steeper than 1:4 the value of maximum shear can be conservatively approximated as

$$\tau_{o(\max)} = 1.5\,\gamma R S_b \tag{23}$$

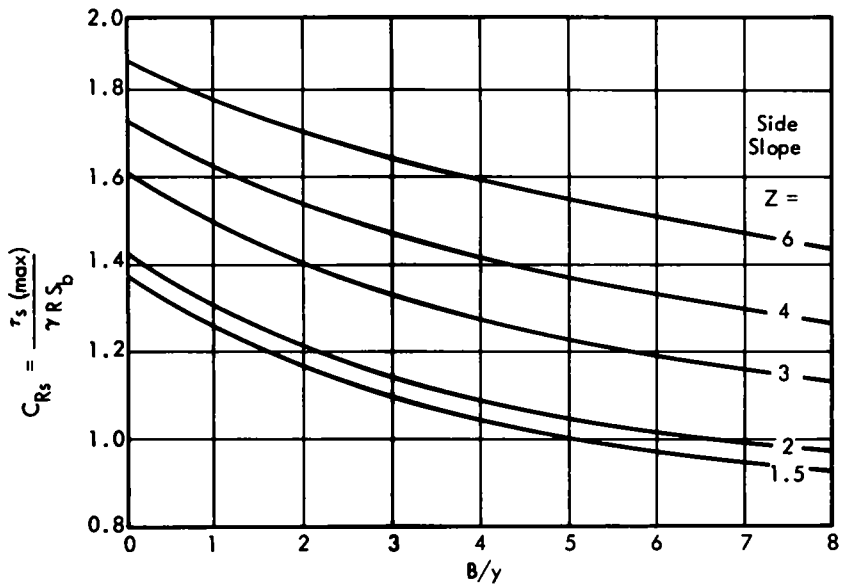

Figure 11 Maximum boundary shear stress on sides of trapezoidal channels

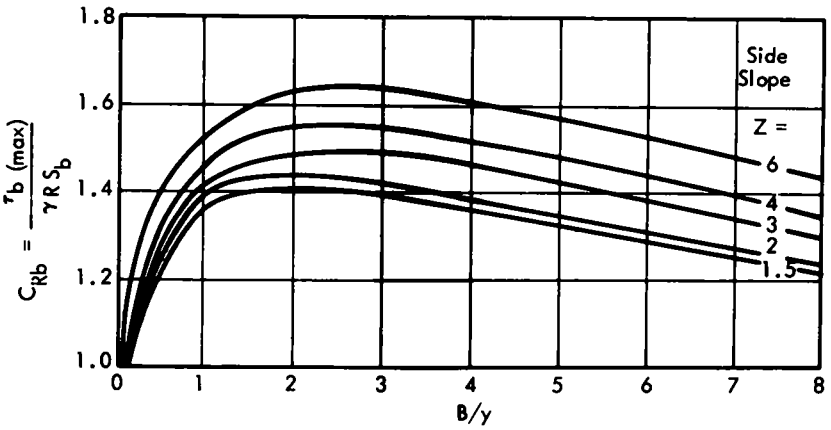

Figure 12 Maximum boundary shear stress on bottom of trapezoidal channels

This is further substantiated by measurements (*28*) of the shear distribution in trapezoidal channels of relatively steep side slopes reproduced in Figure 13 The range of data for the several channels is included in the shaded portion. From this diagram it also appears that the maximum shear on the bed may be taken as 1 5 times the mean shear on the entire wetted perimeter.

The stability of the riprap lining of a trapezoidal channel implies that the riprap on the sloping sides of the channel will be as resistant to motion as that on the bottom. The ratio of the maximum shear on the sides to the maximum shear on the bed can be determined from Figures 11 and 12 for corresponding side slopes and values of B/y. These data are plotted in Figure 14, which further shows that except for the smaller values of B/y the maximum bed shear is greater than the maximum side shear. Again, considering the range of values of side slope and B/y of concern the ratio of these shears can be approximated by a single value as being representative of a large number of channels. This representative value can be taken, somewhat arbitrarily in view of the approximations used in establishing the curves, as

$$\frac{\tau_{s(max)}}{\tau_{b(max)}} = 0.8 \qquad (24)$$

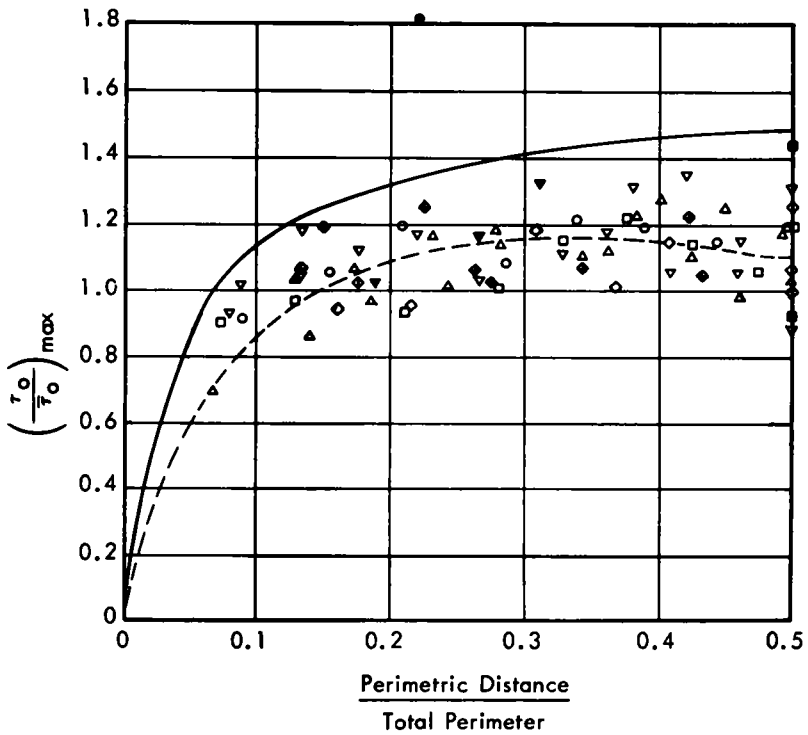

Figure 13 Distribution of boundary shear stress in trapezoidal channels

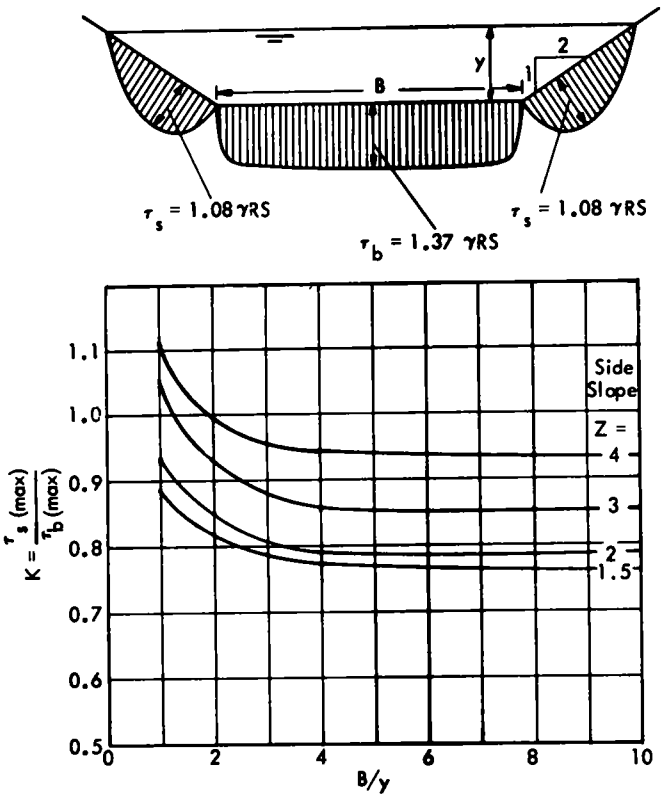

Figure 14. Distribution of boundary shear around wetted perimeter and maximum unit shear on sides and bottom of trapezoidal channels.

This implies that the riprap on the side slopes should have a resistance to motion approximately 0.8 times that on the bottom for all the riprap to be uniformly stable.

RATIO OF CRITICAL SHEAR ON SIDE SLOPES TO CRITICAL SHEAR ON THE BED

A noncohesive particle resting on the side slope of an open channel is subjected to two forces: (1) the boundary shear acting in the direction of flow, and (2) the gravitational force component parallel to the slope which tends to make the particle roll down the slope. To estimate the relative values of the critical shear on side slopes and on the bed, studies have been made by various investigators. The studies of the Bureau of Reclamation (*21*) resulted in the ratio

$$K = \frac{\tau_{cs}}{\tau_{cb}} = \sqrt{1 - \frac{\sin^2\phi}{\sin^2\theta}} \qquad (25)$$

in which ϕ is the angle of inclination of the sloping side, and θ is the angle of repose of the material that forms the side slope. The result shows that the critical shear for a given particle is less when the particle is on the side slope than when it is on the bottom. The nature of Eq. 25 showing the variation of K in terms of side slope and angle of repose is shown in Figure 15. As would be expected, the ratio increases and approaches unity as the side slopes become flatter or the angle of repose becomes greater.

The data for angle of repose of riprap are relatively scarce, but two published sets of curves (*10, 21*) are shown in Figure 16. In general, the angle of repose is greater as

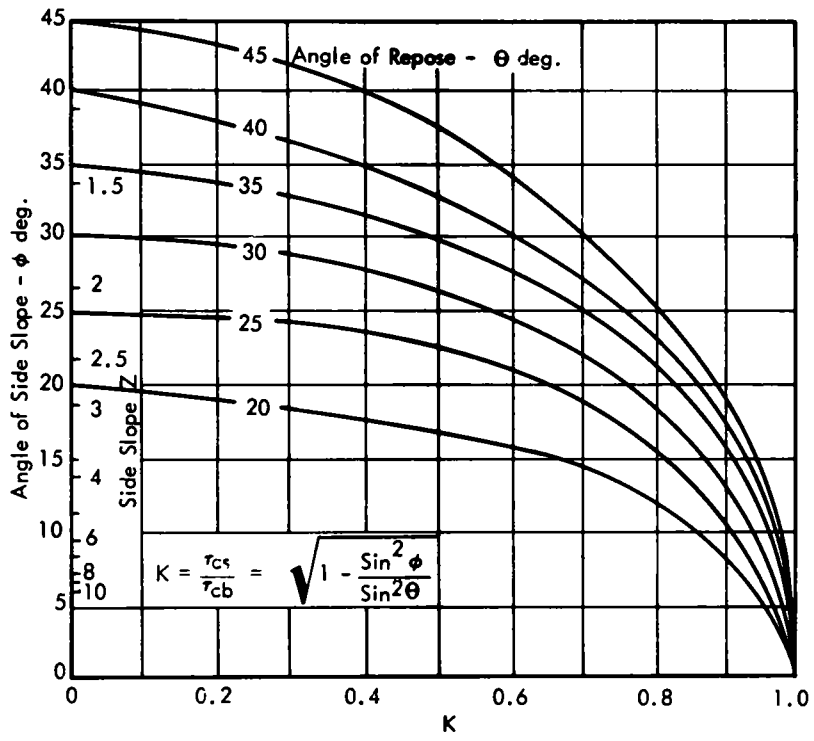

Figure 15 Ratio of critical shear on sides to critical shear on bottom for noncohesive sediment

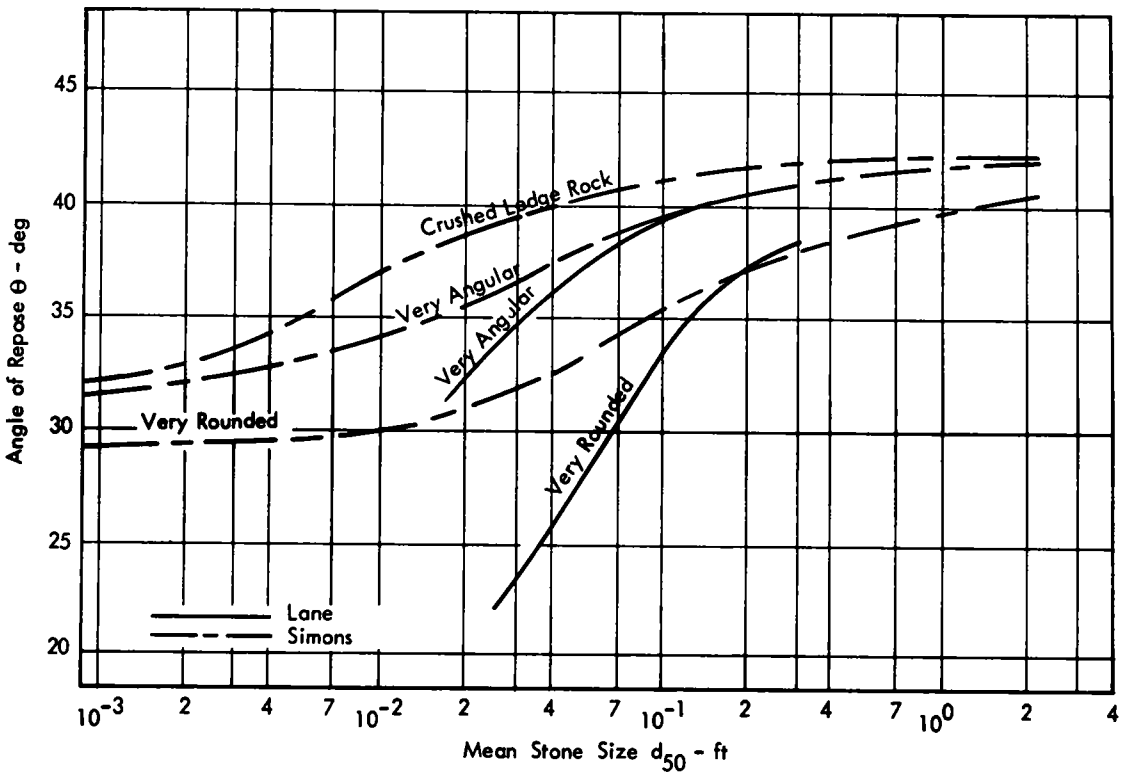

Figure 16 Angle of repose of stones of different angularity for various sizes (10, 21).

the particles are more irregular—as in crushed rock—and as they increase in size. The curves differ more for smaller sizes than for the larger. Based on these data a set of approximate curves can be drawn.

SHEAR DISTRIBUTION IN BENDS

Because of the curvature of the streamlines and the development of secondary currents, the boundary shear in a bend is not uniformly distributed in a cross section or in the longitudinal direction. Most of the work published in this area (*28, 29, 30, 31*) has been descriptive and experimental in nature

When water flows around a bend in an open channel, the centrifugal force causes the water level to rise at the outside of the bend and fall at the inside. This gives rise to secondary currents and, in some cases, separation of the flow at the inside boundary. The superelevation of the water surface can be expressed approximately as

$$\Delta y = \frac{V^2 B_s}{g R_o} \tag{26}$$

in which Δy is the superelevation, V is the mean velocity, B_s is the surface width, and R_o is the mean radius of the bend. For trapezoidal channels the superelevation is somewhat reduced because of the increased effective radius and the modification of the secondary currents as the water flows upward on the sloping sides. In addition, these secondary currents modify the velocity and the shear pattern, so that the trace of the maximum shear stress that is near the inside at the beginning of the bend tends to drift toward the outside as the flow leaves the bend. The general pattern of shear stress distribution is similar in rough and smooth channel bends (*28*). Experimental data for smooth channel bends (*28*) and bends in alluvial meandering channels (*29*) are plotted in Figure 17 in terms of $(\tau_o/\bar{\tau}_o)_{max}$ and B_s/R_o. In this plot, τ_o is the local boundary shear at any point and $\bar{\tau}_o$ is the mean boundary shear in a straight cross section leading to the bend. The maximum value of this ratio for each bend is plotted as a function of B_s/R_o from measurements. It is apparent that as B_s/R_o increases —that is, as the bend becomes sharper—the maximum shear stress also tends to increase. The curve fitted to the data has been extended to the value of $(\tau_o/\bar{\tau}_o)_{max} = 1.5$ for $B_s/R_o = 0$. This corresponds to the finding that the maximum value of the local shear on the bed of a straight channel is 1 5 times the mean shear (Eq. 23 and Fig. 13).

A theoretical analysis of the flow in an open channel bend, taking into account the secondary currents generated by the centrifugal forces, has been undertaken to verify the experimental results and predict the shear pattern for other geometries. A result that gives the maximum relative shear for one value of the ratio B_s/R_o is shown in Figure 17. It is in reasonably good agreement with laboratory measurements (*28*), but is somewhat larger than the values obtained from field measurements (*29*). The solution of the three-dimensional equations of motion given in cylindrical coordinates must be adapted for computer operation before complete results can be obtained.

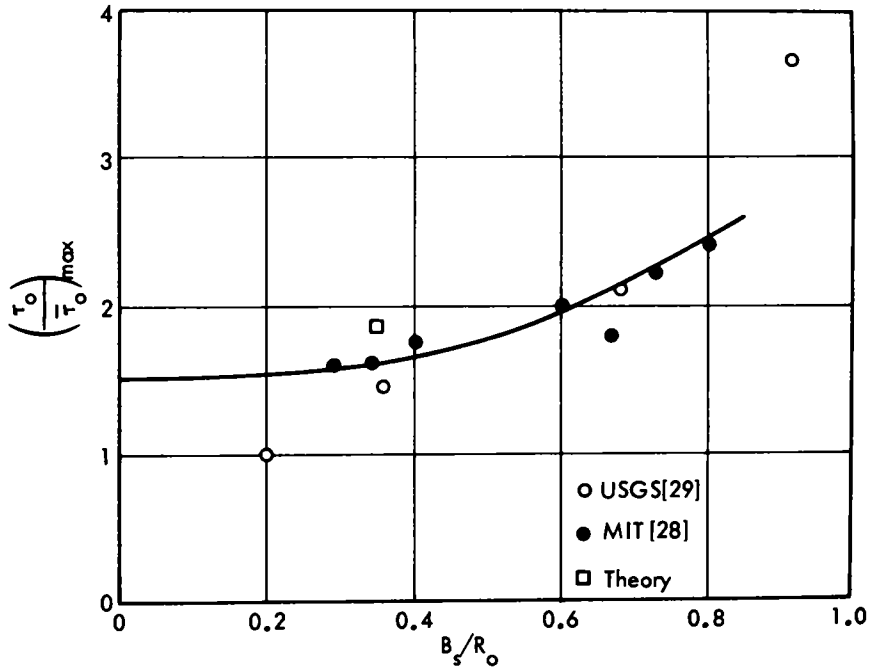

Figure 17 Ratio of maximum boundary shear stress to the mean shear stress for flow in bends

LEACHING

Leaching is the process by which the finer material underlying the riprap is picked up and carried away by turbulent eddies and jets that penetrate the riprap blanket through the interstices of the rock particles. It is apparent that leaching will be minimized if (1) the blanket is thick enough; (2) the interstices are closed or reduced in size;

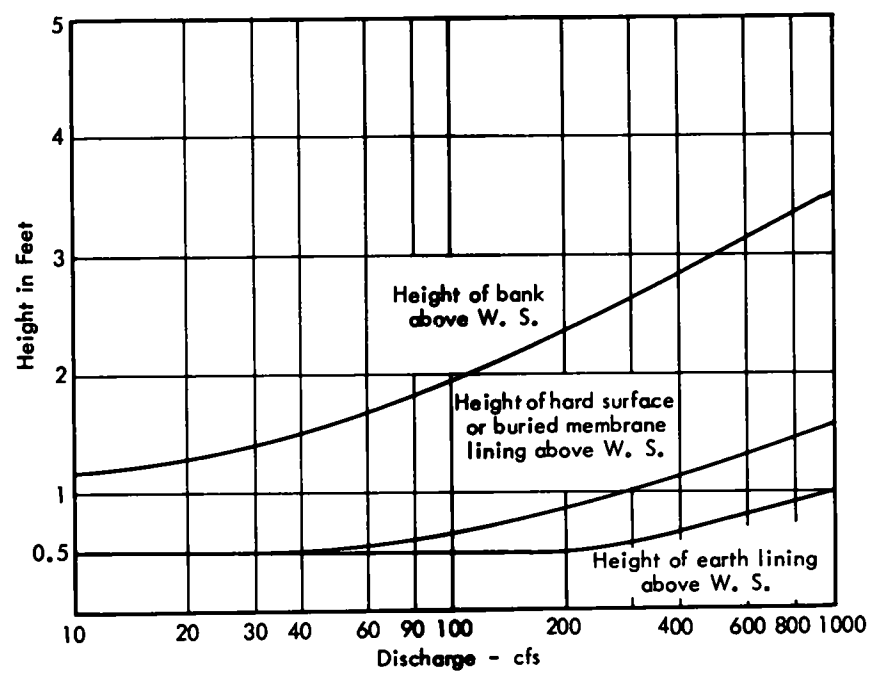

Figure 18. Bank height for canals and freeboard for hard-surface, buried membrane, and earth linings (36)

(3) a protective layer of intermediate-sized material is interposed between the base material and the riprap, or (4) the base material is sufficiently cohesive to prevent its raveling and the erosion of the individual particles. All these methods have application in various situations

An experiment (*37*) has suggested that if a layer of uniform material is placed three or more stones thick, leaching will be reduced to a minimum On the other hand, if the interstices were reduced by adding approximately 25 percent by weight of finer material, the mean size of which was about one-fourth of that of the riprap proper, the leaching was reduced to a negligible rate, even when the armor layer was only one stone thick.

It is common practice in providing protection to slopes subject to flowing water to use a filter layer under the riprap to prevent leaching if the difference in size between the riprap layer and the base material is appreciable. This serves the purpose of reducing the size of the interstices A rational design of such filter layers has been developed through the work of the Bureau of Reclamation (*33*) and the Corps of Engineers (*34*) and can be defined as follows.

$$\frac{d_{15}\ \text{Filter}}{d_{85}\ \text{Base}} < 5 < \frac{d_{15}\ \text{Filter}}{d_{15}\ \text{Base}} < 40$$

$$\frac{d_{50}\ \text{Filter}}{d_{50}\ \text{Base}} < 40$$

in which d_{15}, d_{50}, and d_{85} are the sizes of filter and base material of which 15, 50, and 85 percent are finer. If these criteria are not met by the combination of the riprap lining and the base material a filter layer is necessary If more than one filter is required the preceding conditions must hold for successive layers.

The thickness of the riprap layer over the filter layer to prevent leaching seems to be based largely on experience. Recommendations of layer thickness range from about 1 3 to 2 times the d_{50} size of the riprap. California practice (*24*) requires approximately two times the effective size for rounded cobbles Lindner (*35*) recommends two median diameters with a minimum thickness of 1½ diameters. Some (*1*) suggest a thickness great enough to accommodate the largest stone (stones equal to or larger than the computed riprap size can constitute up to 50 percent by weight, but no stone should be more than twice the weight of the computed size). The Corps of Engineers practice (*2*) is that as a general guide the thickness of the blanket should be 1.5 d_{max}, in which d_{max} is the size of the largest particle.

CHANNEL FREEBOARD

Freeboard is provided in channel design to encompass unexpected surface fluctuations or surface waves that may be generated by the flow. There is no universally accepted rule for the determination of freeboard, because the surface fluctuations may originate for various reasons. Freeboard normally will be governed by the canal size and other special conditions such as water table fluctuations, wind action, and soil characteristics. For lined canals the height of the riprap lining above the water surface will depend on similar factors, including flow velocity. The recommendation of the Bureau of Reclamation (*36*) for the freeboard to be provided on canals is shown in Figure 18.

CHAPTER TWO

RESEARCH APPROACH AND FINDINGS

DEVELOPMENT OF DESIGN PROCEDURE

Basic Design Assumptions

The design charts developed in this chapter summarize and apply the experimental information and the theory of open channel flow described in Chapter One to the design of riprap-lined drainage channels. The experimental data are used in conjunction with the characteristics of flow to describe the characteristics of the riprap lining and the channel dimensions necessary to convey a given discharge on a given slope. Based on these relationships it is assumed that, for purposes of design, the following conditions are applicable:

1. The drainage channel to be designed will be essentially straight and of trapezoidal or triangular cross section. It is recognized that in practice certain modifications will be made These two channel shapes were chosen as typical and are used for the development of a design procedure. The effect of bends in the alignment of the channel on the resulting design is treated as a corrective factor that will be applied to the design.

2 The flow will be essentially uniform and can be described by the Manning flow formula:

$$V = \frac{1\,49}{n} R^{2/3} S_b^{1/2} \qquad (13)$$

in which the symbols are as previously defined and listed in Chapter One. It is recognized that certain precautions must be taken at the entrance and outlet of the drainage channel and consideration must be given to these regions of possible

nonuniform flow The design of appropriate stilling basins and spillway crests is considered to be a special problem that is not within the scope of this report.

3. Because it is presumed that the riprap used in the proposed drainage channel will be stable and that the channel alignment is essentially straight, Manning's n, the roughness coefficient, will depend only on the effective size of the rock fragments that make up the riprap and can be expressed as

$$n = 0.0395\, d_{50}^{1/6} \tag{15}$$

The effective size of the riprap mixture, d_{50}, is that size of which 50 percent of the material is finer by weight and is measured in feet or millimeters, as may be designated.

4. The critical boundary shear, τ_c, which represents the maximum shear for which the riprap will be stable, is, in the region of interest, directly proportional to the effective size, d_{50}, or

$$\tau_c = 4\, d_{50} \tag{22}$$

5. The boundary shear stress is not uniformly distributed around the wetted perimeter of the channel. The magnitude and location of the maximum shear on the boundary depends on the shape of the cross section. For the wider trapezoidal channels the maximum shear occurs at the center of the bed, with lesser maxima on the side slopes. For narrow trapezoidal channels and triangular channels the maximum shear occurs on the side slope The excess of the maximum boundary shear over the mean shear varies somewhat with the width-depth ratio. To simplify the computation and design charts, the ratio of the maximum boundary shear stress is taken to be 1 5 times the mean for all trapezoidal channels and 2 times the mean for triangular channels

$$\tau_{o(\max)} = 1.5\gamma R S_b \text{ (trapezoidal)} \tag{23}$$

$$\tau_{o(\max)} = 2\gamma R S_b \text{ (triangular)} \tag{39}$$

6 Because of the component of the force of gravity acting on the riprap in the direction of the side slope, the critical boundary shear stress for the riprap on the sloping side is less than that for riprap on the bed. The ratio of the critical boundary shear on the sloping side to the critical boundary shear acting on a similar particle on the bed is

$$K = \frac{\tau_{cs}}{\tau_{cb}} = \sqrt{1 - \frac{\sin^2 \phi}{\sin^2 \theta}} \tag{25}$$

7. The discharge to be conveyed in the channel and the topographic slope on which it is to be constructed are prescribed by external conditions; that is, they are independent variables Under certain circumstances the size of the riprap that may be available may also be considered an independent variable and the channels may be designed to take this into account

8. The ratio of width to depth for trapezoidal channels must be limited to practical values. This may be done arbitrarily within certain limits The ratio P/R (in which P is the wetted perimeter and R is the hydraulic radius) is a minimum for a triangular channel. For channels with side slopes of 2.5:1, P/R (min) equals 11.6, for 3:1, P/R (min) equals 13.3; and for side slopes of 4:1, P/R (min) equals 17. Because trapezoidal channels with side slopes of 4·1 or less are relatively rare, the minimum P/R ratio is taken as 13 3. The upper limit of P/R is set at 30, because wider channels become uneconomical. In practice, the ultimate design probably will be between these limits.

To facilitate the design of channels a series of design charts has been developed from which the channel properties can be determined. Although the basic requirements are the same, separate sets of charts have been developed for the larger trapezoidal channels with steeper side slopes designed to transport relatively large discharges and for the wide triangular channels that convey small discharges from the immediate highway surfaces

Development of Design Charts—Trapezoidal Channels

The development of design charts for trapezoidal channels is founded on the basic equations described in Chapter One. The combination of these equations with the equation of continuity for the flow results in a relationship between the principal variables of discharge, slope, shape of channel, and size of riprap material.

Starting with the basic Manning formula (Eq. 13), the roughness coefficient defined by Eq 15 may be introduced, with the result that

$$V = \frac{37.7}{d_{50}^{1/6}} R^{2/3} S_b^{1/2} \tag{27}$$

Further, because the stability of the riprap depends on the boundary shear not exceeding the critical boundary shear for the riprap, the condition for stability is that

$$\tau_c = \tau_{o(\max)} \tag{28}$$

The combination of Eqs. 22 and 23 results in an expression for R in the form

$$R = \frac{4 d_{50}}{1.5\gamma S_b} = 0.0428\, \frac{d_{50}}{S_b} \tag{29}$$

When Eq. 29 for the hydraulic radius is substituted into Eq 27 the mean velocity can be expressed, in terms of the size of the riprap and the longitudinal slope of the channel, as

$$V = 4\,60\, \frac{d_{50}^{1/2}}{S_b^{1/6}} \tag{30}$$

Introducing the equation of continuity for the flow defined as

$$Q = VA = VPR = VR^2(P/R) \tag{31}$$

into Eq 30 using Eq. 29 results in an equation relating the discharge, the longitudinal slope of the channel, the size of the riprap, and the shape of the channel as defined by P/R in the form

$$Q = \frac{1}{118}\, \frac{d_{50}^{5/2}}{S_b^{13/6}}\, \frac{P}{R} \tag{32}$$

This equation shows that, for a given discharge and slope, the size of riprap that is needed to protect the channel depends also on the channel shape. For given values of P/R, Eq. 32 can be plotted with the discharge, Q, as a function of the slope, S_b, with d_{50} as a parameter. The val-

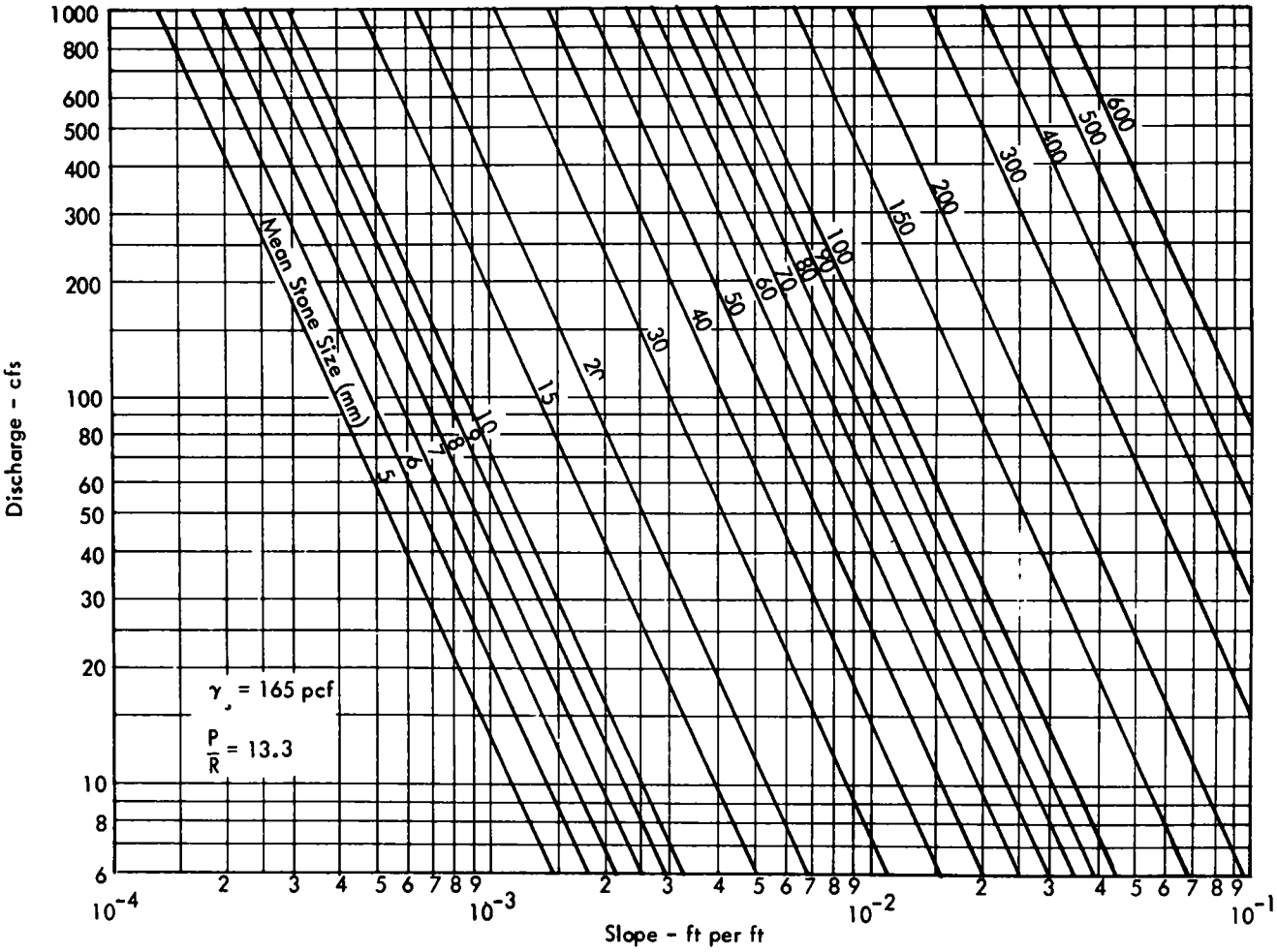

Figure 19. Minimum size (mean) of stone riprap that will be stable in trapezoidal channels with P/R=13.3 for various combinations of discharge and slope.

ues of P/R to be used can be taken as the upper and lower limits of practical channels. These limits have been taken as $P/R = 13.3$ and $P/R = 30$ for the reasons given previously. Figures 19 and 20 represent Eq. 32 for $P/R = 13.3$ and $P/R = 30$, respectively For these values of P/R the charts show the size of riprap required to line a channel having the given discharge, Q, and slope, S_b, such that the riprap is stable. The determination of d_{50} from each chart provides two limits within which the actual size must fall. Once the size of riprap between these two limits has been chosen, the velocity and the hydraulic radius can be determined from Figures 21 and 22, which are graphical representations of Eqs 29 and 30 and which give V and R in terms of the known values of d_{50} and S_b. Having the mean velocity from Figure 21, one obtains the required cross-sectional area from Figure 23, which is a graphical representation of the continuity equation.

The required side slopes are obtained from Figures 24 and 25, which are obtained by combining Eq. 24 and Eq. 25. The shear stress on the sloping sides is appreciably less than that on the bottom (Eq. 24). At the same time, the critical shear stress for riprap on the side of the trapezoidal channel is also less than that for the same size on the bed. Now, if the side slopes are adjusted so that the ratio of critical shear on the side to that on the bed is equal to the ratio of the boundary shears on the side to that on the bottom, then the riprap will be equally stable on the side and on the bottom. The result is shown in Figures 24 and 25. Given the size of riprap, d_{50}, and its angularity, the angle of repose is taken from Figure 24. Using this angle of repose the side slope is determined from Figure 25. The curve in Figure 25 represents the actual variation between angle of repose and side slope, but for practical reasons the range of side slopes was divided into three groups and each was assigned a value. It appears that the side slope is not very sensitive to the angle of repose.

Having chosen the side slope and having determined the cross sectional area and the hydraulic radius, one obtains the channel geometry directly from the appropriate chart of Figures 26a through 26e. In these design charts the side slope is established so that the riprap on the side is as stable as that on the bottom and the size of the riprap is a minimum consistent with the superimposed discharge and slope. If for any reason it is desirable to make the side slopes

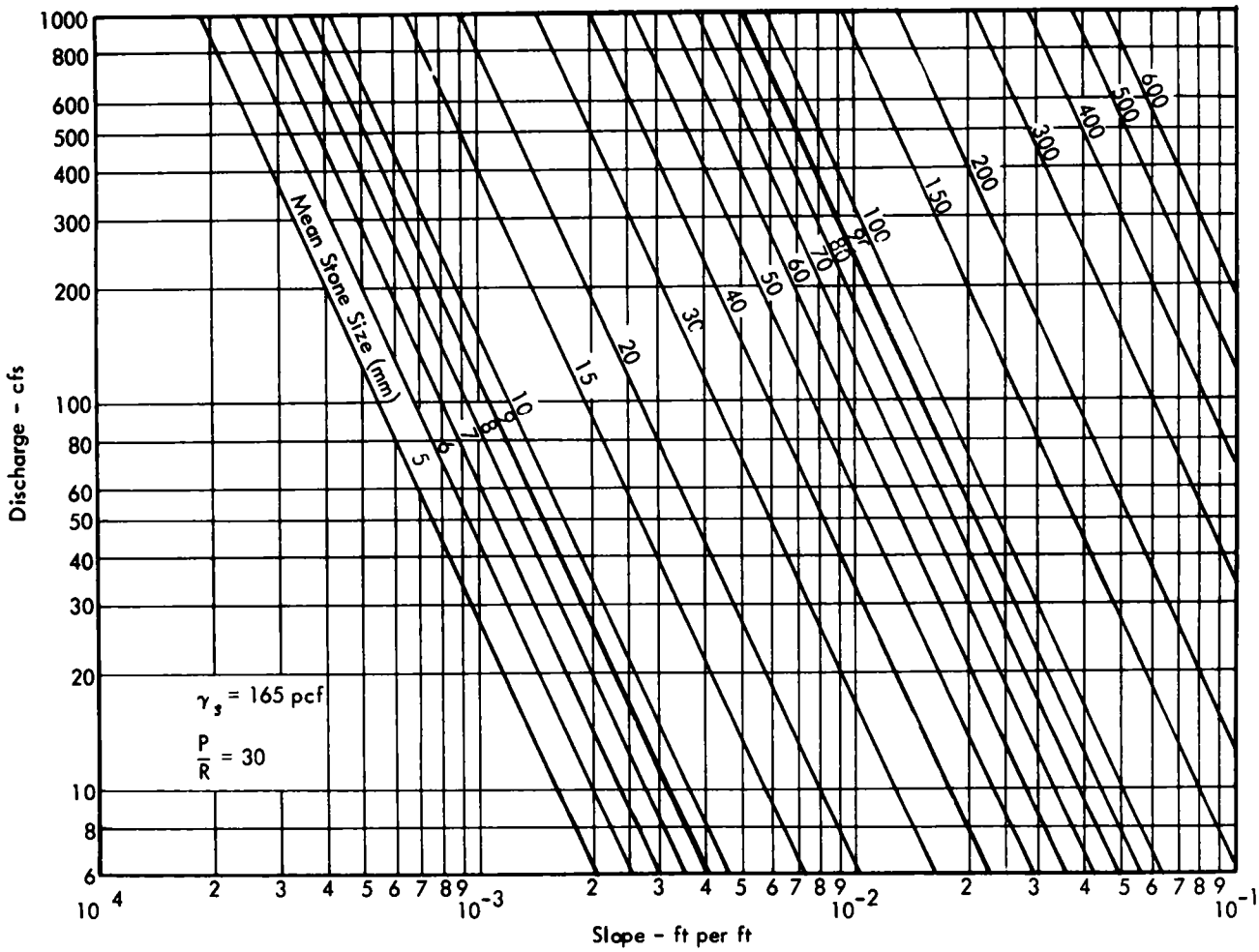

Figure 20. Minimum size (mean) of stone riprap that will be stable in trapezoidal channels with P/R=*30 for various combinations of discharge and slope*

steeper than what is given by the design charts, the size of the riprap can be increased to accommodate the increased side slope at the cost of some loss of efficiency on the channel bottom. Assuming that the angle of repose is a constant, the value of K in Figure 15 can be determined for both the design slope and the desired steeper slope. Assuming further that the riprap on the bottom remains unchanged, K becomes proportional to the critical boundary shear stress of the side riprap, and therefore, through Eq 22, also proportional to d_{50} Therefore,

$$d_{50}' = d_{50}\frac{K}{K'} \tag{33}$$

in which d_{50}' is the required size of riprap on the steeper side slope.

Development of Design Charts—Triangular Channels

The drainage channels in highway practice used to transport small discharges are commonly those used to drain the roadway and are constructed in the median strip of divided highways or as side ditches for both divided and undivided highways. In their design there are certain nonhydraulic factors to be considered. These have to do primarily with safety, but may also include construction techniques and land cost Safety considerations require that the side slopes of highway embankments be relatively flat and wide enough so that vehicles leaving the roadway can recover and return to the driving lanes or be stopped without serious danger to the occupants. These side slopes will also constitute part of the drainage channel. The requirements for width of recovery zone and relatively flat side slopes suggest that shallow triangular sections which can be modified into appropriate trapezoidal channels be used. In addition, construction techniques for triangular channels probably can be simplified through the use of ordinary grading machinery for excavating the channel and distributing the riprap lining. Finally, wide, shallow swales parallel to the highway are probably more esthetic than narrower, deeper channels.

The design of erosion-resistant channels depends primarily on the discharge and the longitudinal slope, but the side slope may also be prescribed. The remaining dependent variables then are the size of the riprap to be used and the depth of flow that must be provided for.

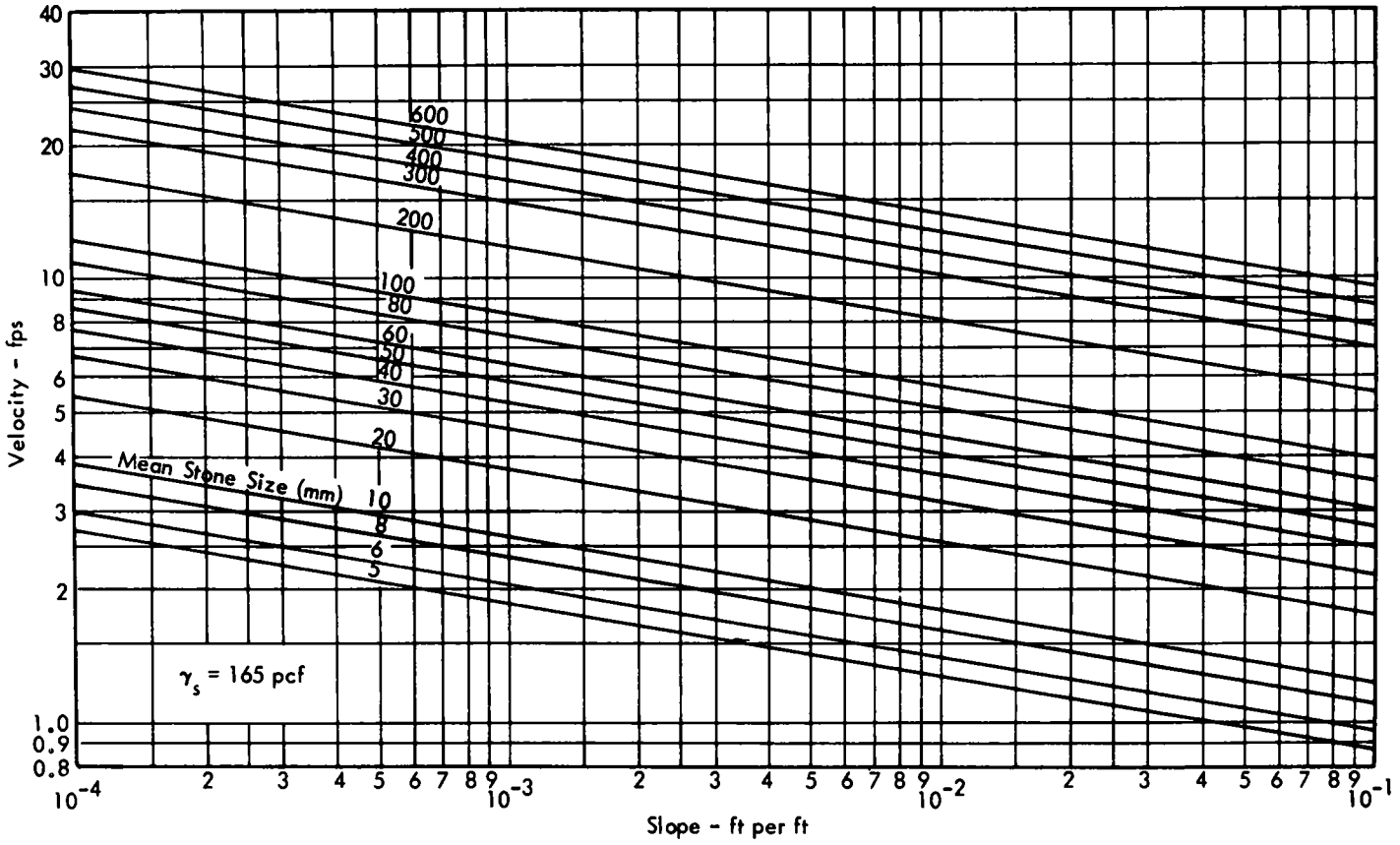

Figure 21 Maximum mean velocity for stable riprap in trapezoidal channels for various mean stone sizes and slopes.

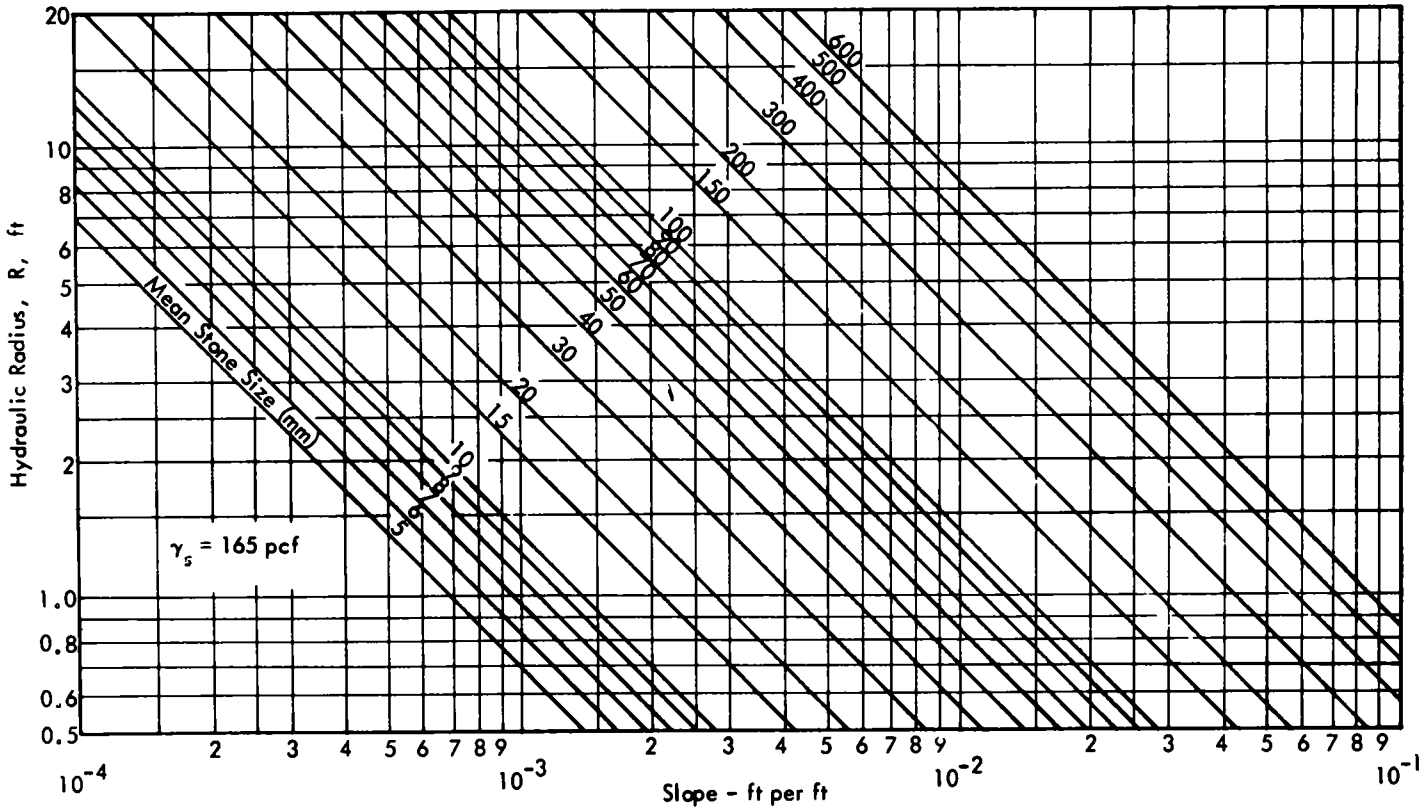

Figure 22 Hydraulic radius for trapezoidal channels in terms of mean stone size and slope.

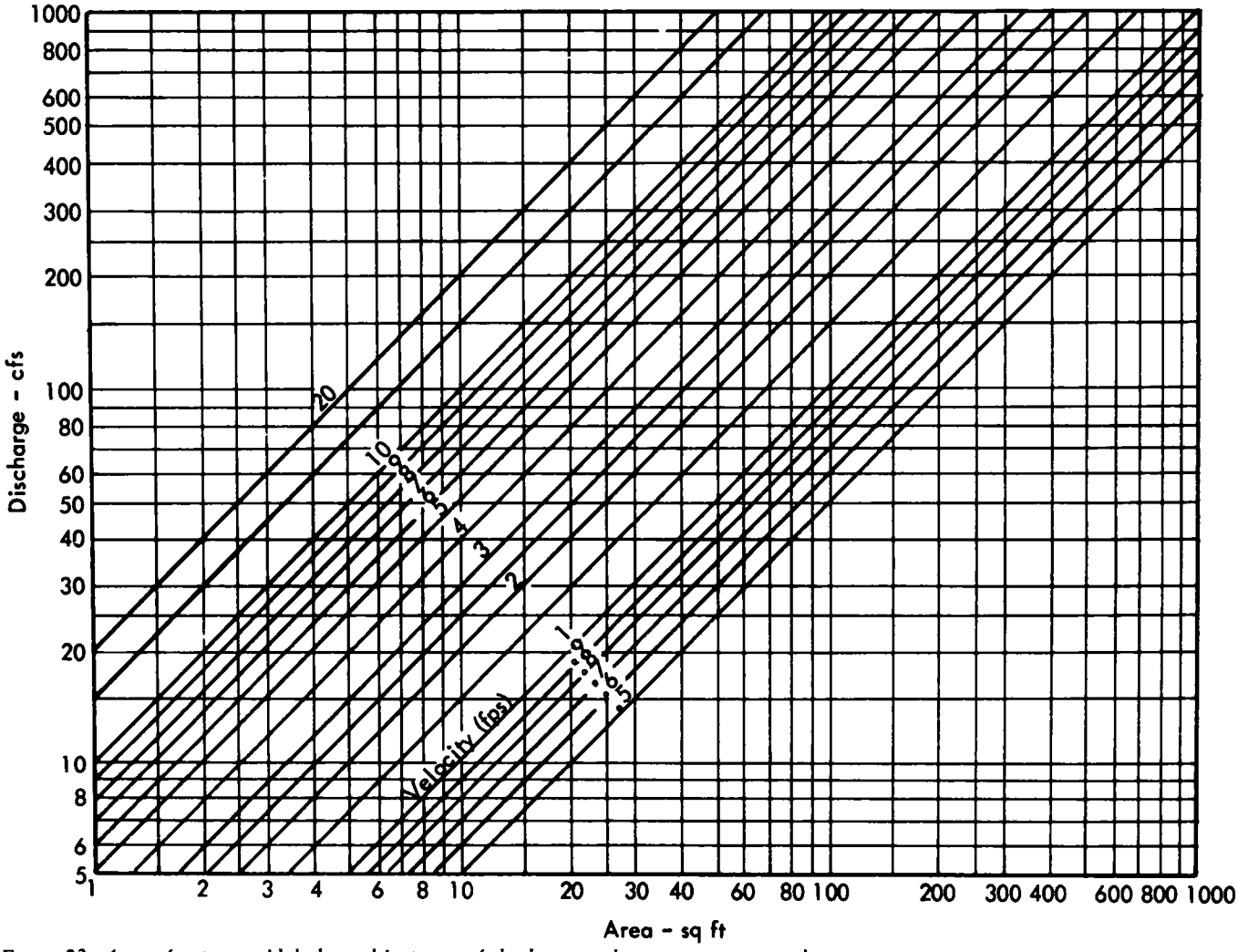

Figure 23. Area of a trapezoidal channel in terms of discharge and maximum mean velocity

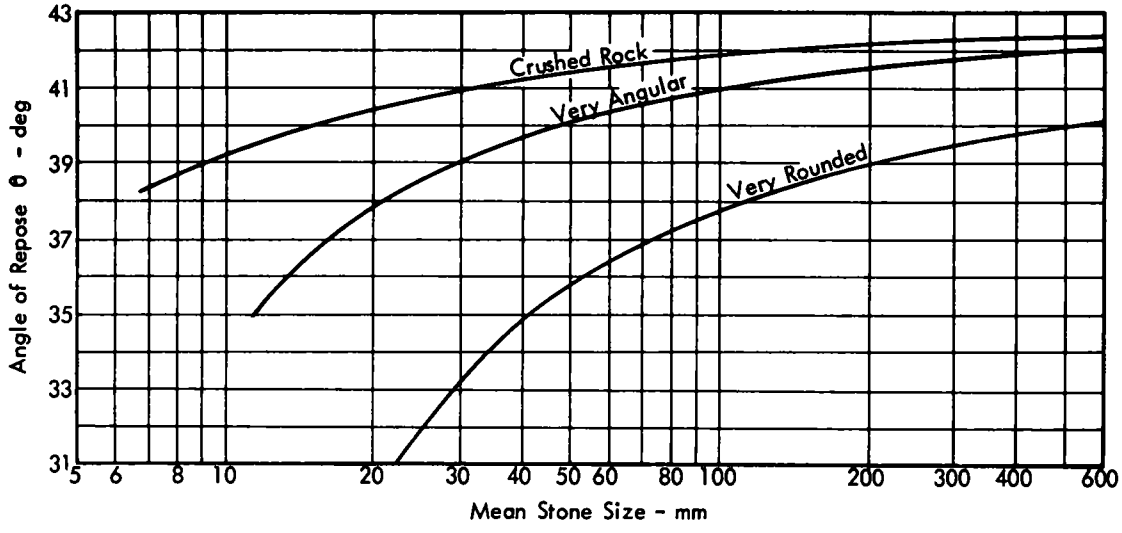

Figure 24 Angle of repose of riprap in terms of mean size and shape of stone

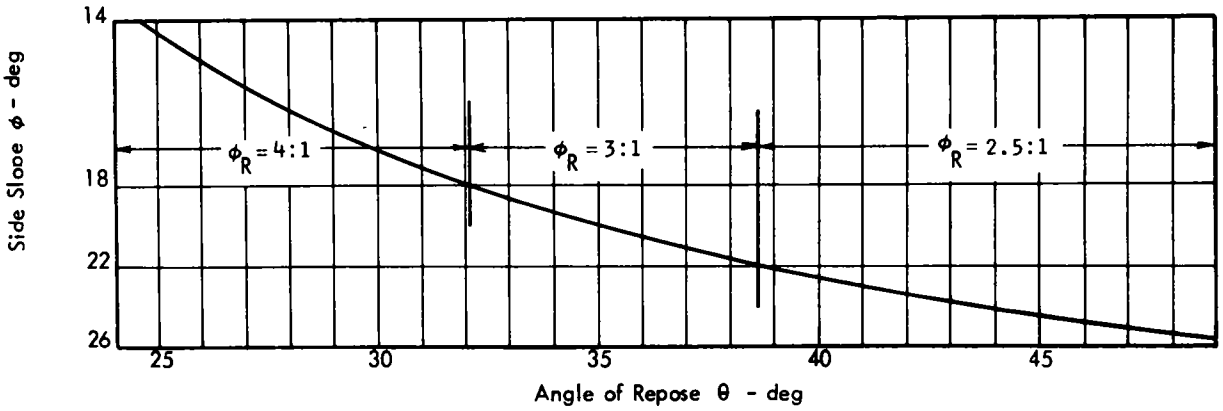

Figure 25. Recommended side slopes of trapezoidal channels in terms of riprap angle of repose

The area contributory to the local drainage channels along the highway is usually relatively small, so that the discharges considered in the design of these channels are limited to a range from 1 to 100 cfs.

Topographic slopes are chosen to conform to those commonly used in highways and are limited to those from 0.001 to 0.10. If slopes of less than 0.001 occur, the minimum slope of 0.001 can be used in the design or the channel properties can be computed from the equations to be developed. The upper limit of the slope is justified by the fact that AASHO recommends [1] that rural highways have a center-line slope of less than 0.09, even for low speeds in mountainous topography.

In the review of the literature, riprap was characterized by the geometric mean diameter, d_{50}, without regard to size distribution in the mixture or availability of the material. To simplify the design of these small channels, standard sizes of coarse aggregate having standard gradations will be used whenever possible. Because the range of mean diameters needed to cover the prescribed range of discharges and longitudinal slopes was nearly the same as that specified by AASHO for other purposes, an attempt has been made to use these specifications in the design procedure. For this purpose AASHO designation M 43-54, "Standard Sizes of Coarse Aggregate for Highway Construction," was chosen.

[1] American Association of State Highway Officials, *A Policy on Geometric Design of Rural Highways* (1965)

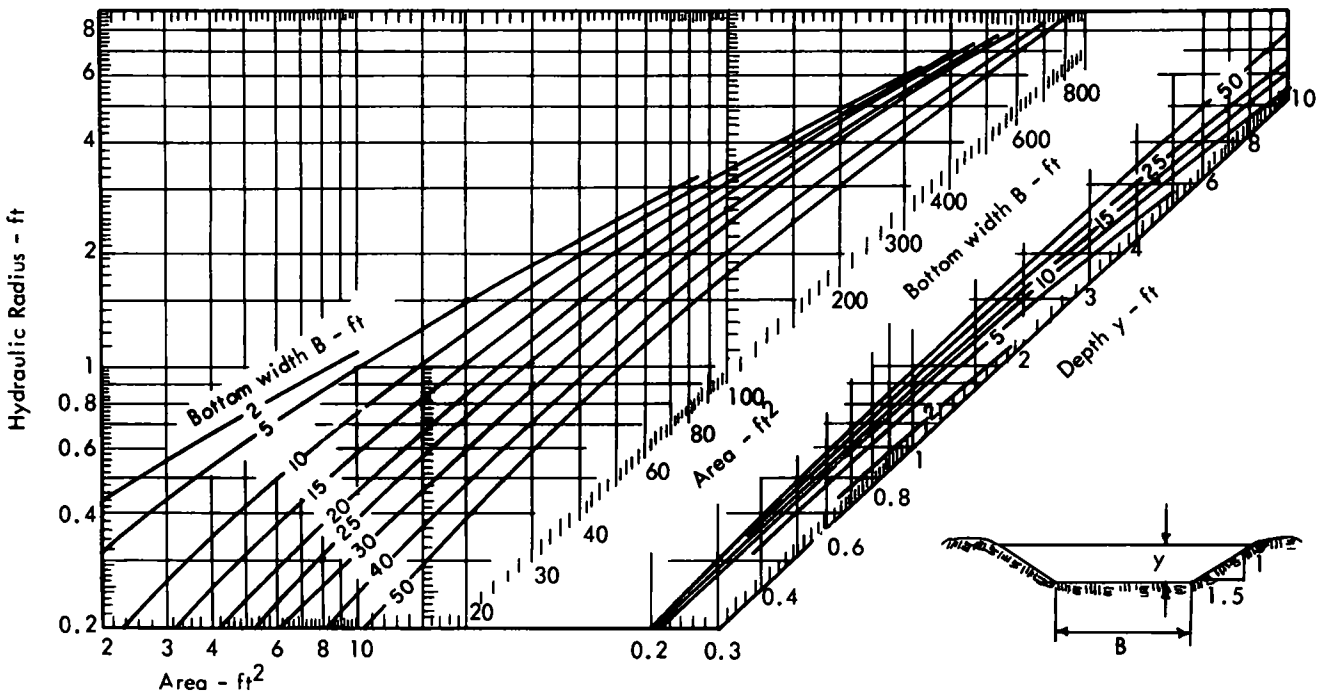

Figure 26a. Geometry of trapezoidal channels with 1.5:1 side slopes (3).

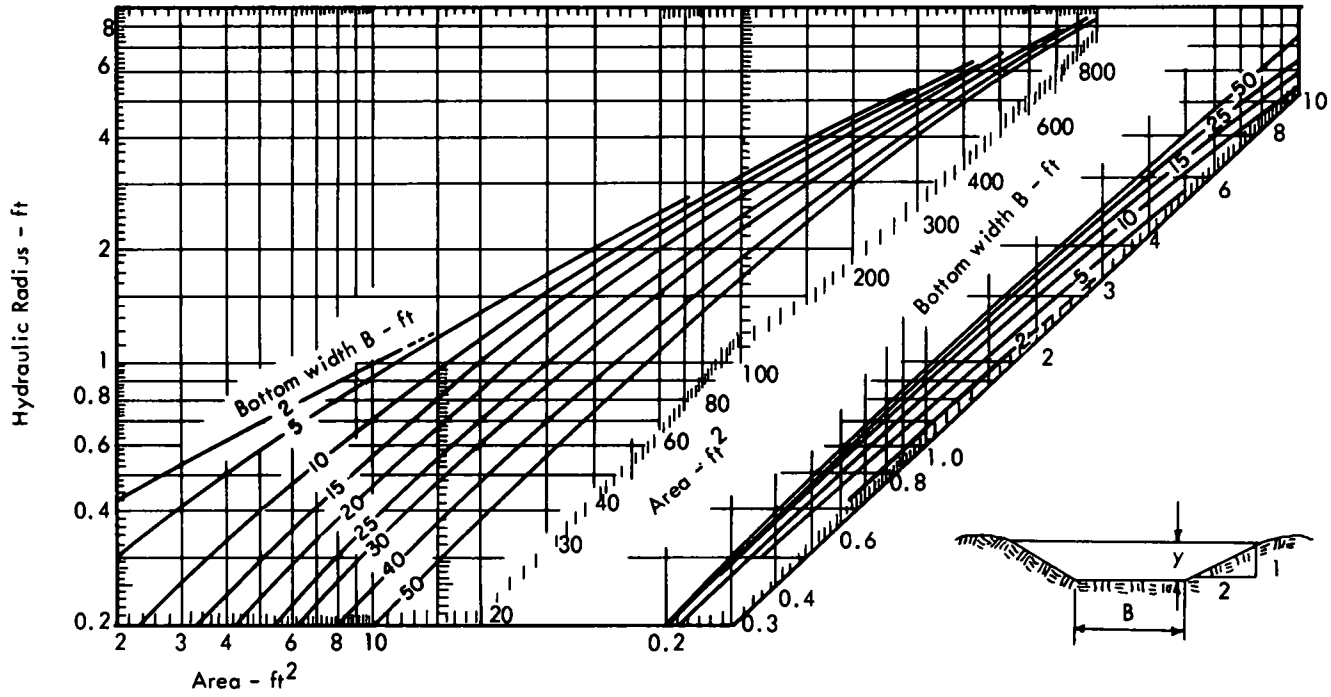

Figure 26b. Geometry of trapezoidal channels with 2:1 side slopes (3)

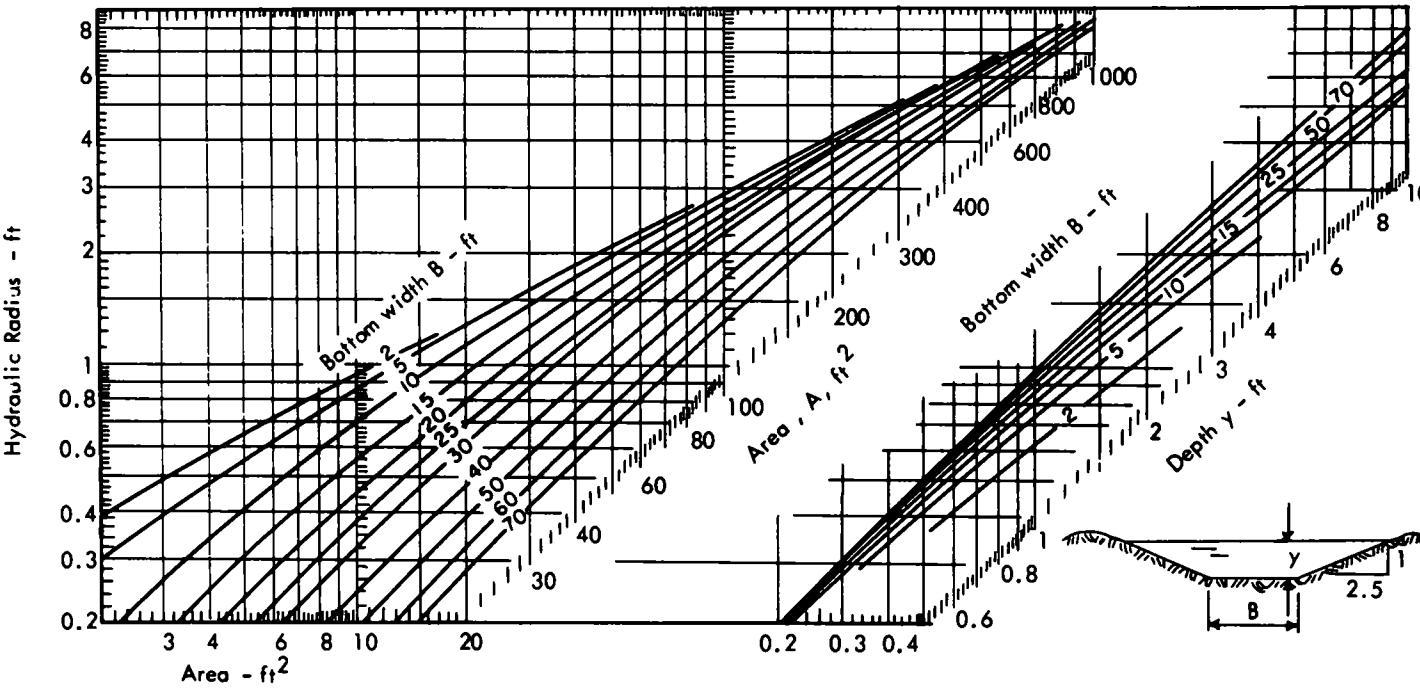

Figure 26c Geometry of trapezoidal channels with 2.5 1 side slopes (3)

The gradations of eight of these standard aggregates having a reasonably systematic change in mean size are given in Table 1 and are plotted in Figures A-1 through A-8 (Appendix A) to show the range of particle size distribution, the approximate minimum value of d_{50}, and the maximum and minimum standard deviation as obtained from the distribution curves. The standard deviation is a measure of the range of sizes present and indicates the effectiveness of the aggregate to provide a compact riprap layer. Although other standard aggregates are listed in the AASHO designa-

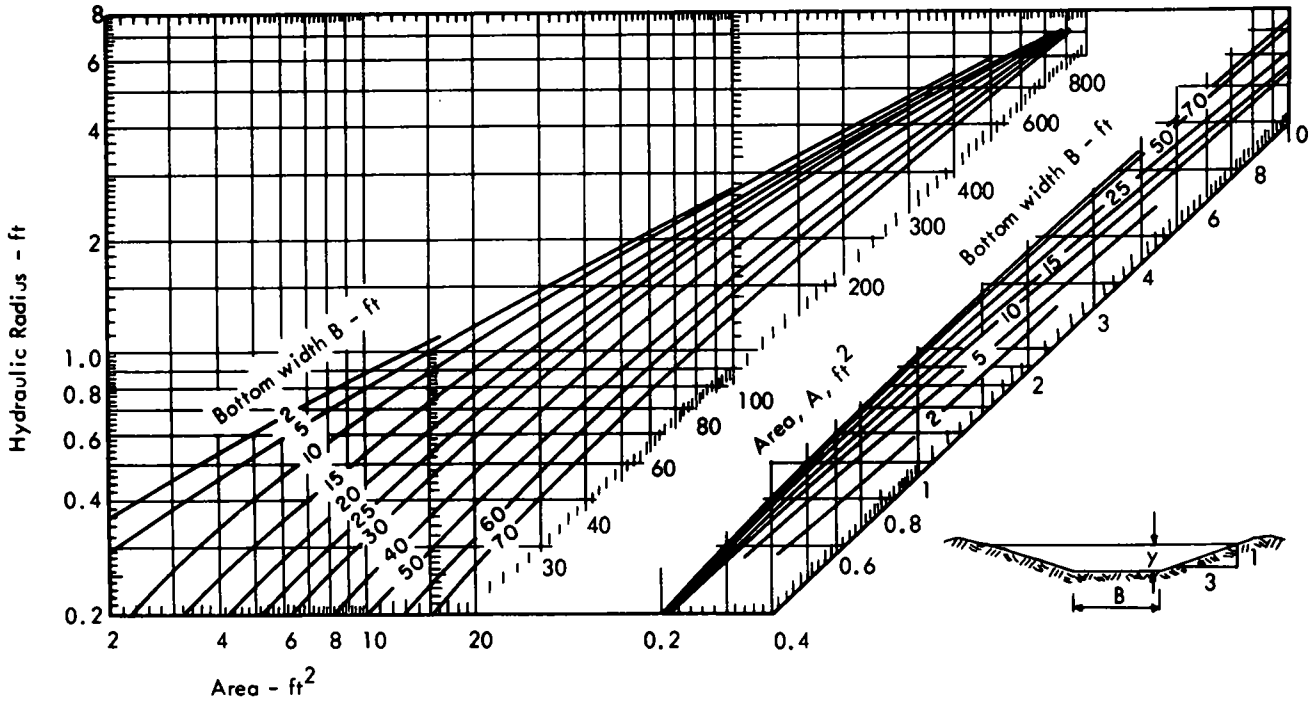

Figure 26d. Geometry of trapezoidal channels with 3·1 side slopes (3)

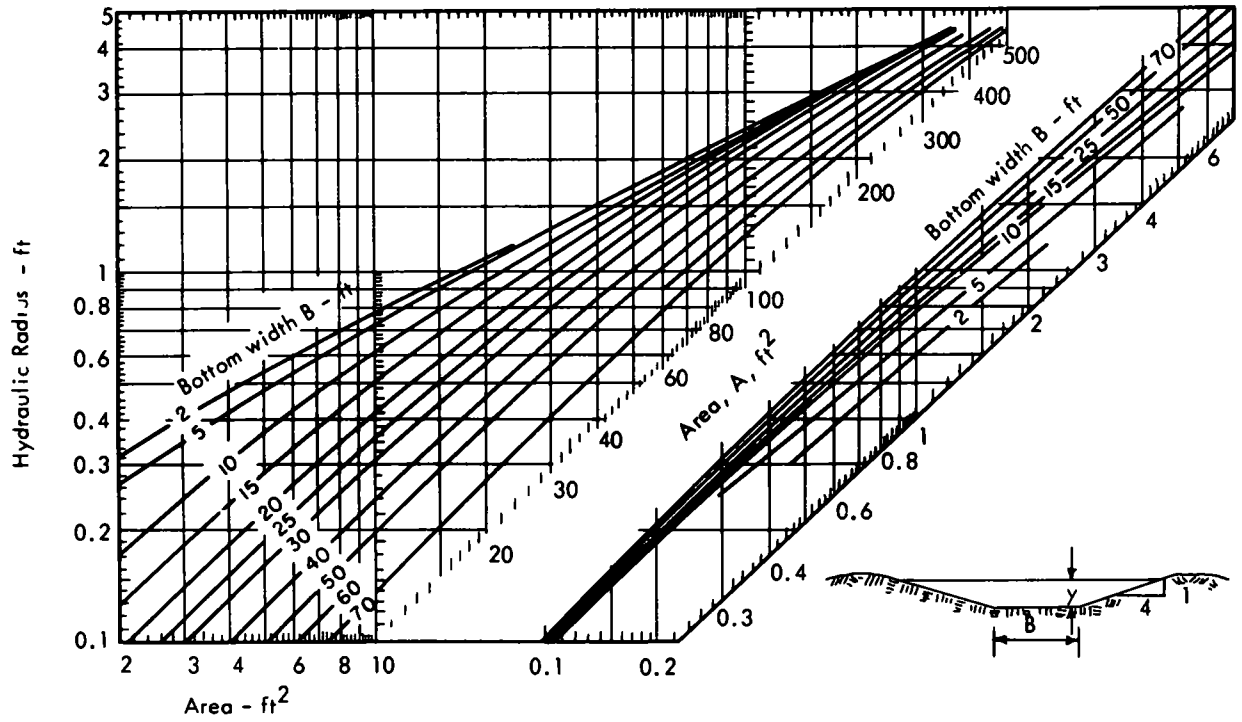

Figure 26e. Geometry of trapezoidal channels with 4 1 side slopes (3)

TABLE 1

GRADATIONS OF EIGHT STANDARD AGGREGATES

SIZE NO.	NOMINAL SIZE SQ OPEN.	PERCENT PASSING											
		4 IN.	3½ IN	3 IN.	2½ IN.	2 IN.	1½ IN.	1 IN.	¾ IN.	½ IN.	⅜ IN.	NO. 4	NO. 8	NO. 16
1	3½–1½ in	100	90–100		25–60		0–15		0–5					
2	2½–1½ in			100	90–100	35–70	0–15		0–5					
24	2½–¾ in.			100	90–100		25–60		0–10	0–5				
4	1½–¾ in.					100	90–100	20–55	0–15		0–5			
357	2 in –No 4				100	95–100		35–70		10–30		0–5		
467	1½ in -No 4					100	95–100		35–70		10–30	0–5		
57	1 in -No 4						100	90–100		25–60		0–10	0–5	
68	¾ in - No. 8							100	90–100		30–65	5–25	0–10	0–5

tion, it is believed that those selected provide an adequate range of riprap materials for small channels. It is anticipated that local aggregates having approximately the same gradation as those designated could be used

Provision also has been made to include side slopes ranging from 3.1 to 10 1 These include all side slopes that can reasonably be expected to be encountered in channels of this shape used for roadway drainage

As for trapezoidal channels, the basic equation relating the discharge to the channel properties is the Manning equation combined with the equation of continuity.

The application of the Manning equation depends on the conditions that govern the magnitude of the hydraulic radius and the roughness coefficient

The hydraulic radius is determined by the shape and size of the channel. For a triangular channel where the bed width is zero, the ratio P/R depends only on the side slope of the channel and can be expressed as

$$P/R = \frac{P^2}{A} = \frac{4(z^2+1)}{z} \tag{34}$$

in which z is the side slope

The hydraulic radius is also a function of the size of the riprap inasmuch as this governs the permissible velocity Eq 10 shows that the mean boundary shear is directly proportional to the hydraulic radius and the longitudinal slope of the channel However, because the boundary shear is not uniformly distributed, the maximum boundary shear stress must be evaluated. Figure 10 shows the maximum boundary shear stress on the side of the triangular channel defined as

$$\tau_{s(\max)} = C_{Rs}\,\gamma y S_b \tag{35}$$

Eq. 35 can be written as

$$\tau_{s(\max)} = C_{Rs}\,\gamma R S_b\,(y/R) = C_{Rs}C_z\,\gamma R S_b \tag{36a}$$

in which, from the geometry of triangular channels,

$$C_z = y/R = 2\,\frac{\sqrt{z^2+1}}{z} \tag{36b}$$

Because the critical shear stress on riprap on the sloping sides is less than what it would be on the bottom, Eq. 25 shows that

$$\tau_{cs} = K\tau_{cb} = K\tau_c \tag{37}$$

in which τ_c defined by Eq 22 is the critical shear stress for riprap lying on a channel bottom. Because for equilibrium $\tau_{cs} = \tau_{s(\max)}$,

$$\tau_c = \frac{C_{Rs}\cdot C_z}{K}\,\gamma R S_b = C\,\gamma R S_b \tag{38}$$

If it is assumed that the riprap will have an angle of repose, θ, of 30°, then K is a function of z alone, as are C_{Rs} and C_z (If θ is greater than 30° the factor of safety against failure is somewhat improved.) The value of C computed for values of z between 3 and 10 is given in Table 2. When the components of C are combined the value of C is very close to 2 over nearly the entire range of z, so that within the accuracy of its development Eq. 38 can be written as

$$\tau_c = 2\,\gamma R S_b \tag{39}$$

Combining Eq. 39 and Eq. 22, the hydraulic radius in terms of the size of riprap and the longitudinal slope becomes

$$R = \frac{4}{2\gamma}\,\frac{d_{50}}{S_b} = 0.032\,\frac{d_{50}}{S_b} \tag{40}$$

TABLE 2

COMPUTED VALUES OF C

z	K	C_z	C_{Rs}	C
3	0 78	2 11	0 77	2 08
4	0 88	2 06	0 84	1 97
5	0.92	2 04	0 89	1 97
6	0 94	2 03	0 93	2 01
7	0 96	2 02	0 96	2 02
8	0.97	2 02	0 98	2 02
9	0 98	2 01	0 99	2 03
10	0.98	2 01	0.99	2 03

Now, by substitution of Eq. 40 into Eq. 27, the mean velocity can also be written in terms of the size of riprap and longitudinal slope as

$$V = 3\,80\,\frac{d_{50}^{1/2}}{S_b^{1/6}} \tag{41}$$

By combining Eq. 40 with the relation

$$y/R = 2\,\frac{\sqrt{z^2+1}}{z} \tag{36b}$$

the depth, y, of the flow becomes

$$y = 0\,064\,\frac{d_{50}}{S_b}\,\frac{\sqrt{z^2+1}}{z} \tag{42}$$

Further, substituting Eq. 41, Eq 40, and Eq. 34 into the equation of continuity

$$Q = VA = VPR = VR^2\,P/R \tag{31}$$

the discharge can be written as

$$Q = \frac{1}{64\,4}\,\frac{d_{50}^{5/2}}{s_b^{13/6}}\,\frac{z^2+1}{z} \tag{43}$$

Eq. 43 is the final design equation relating the discharge, longitudinal slope, riprap size, and the side slope of the channel. Eq 43 is plotted in Figures 27 through 34 for prescribed values of the side slope, z, between 3 and 10. From these charts the size of riprap in the form of an AASHO gradation and the depth of flow can be determined for given discharge, longitudinal slope, and side slope. The chart corresponding to the given side slope is entered with the discharge and longitudinal slope, and the riprap classification is read off at their intersection. If, however, the intersection does not fall on a standard size, the next larger size of aggregate is chosen. The depth of flow, however, may be interpolated at the point of intersection.

For situations that lie beyond the scope of the charts, recourse may be had to the equations themselves, from which the properties may be computed.

It is sometimes convenient or desirable to modify the triangular channel described previously so that it will have a flat bottom to facilitate the movement of maintenance vehicles or to simplify construction. Such a modification can be made easily if the cross-sectional area—and therefore the mean velocity—remains the same and the revised channel has the same side slopes If the bottom of the given triangular channel is flattened, the elevation of the water surface will be somewhat increased to compensate for the cross-sectional area lost at the bottom. Figure 35 shows the original triangular cross section of side slopes, z, depth, y, and surface width, B_s. On this channel has been superimposed a shallow trapezoidal channel having the same side slopes, z, but with a bottom width, B_b', a new surface width, B_s', and a new depth, y'. From geometrical considerations based on the requirement that the cross-sectional area and the side slopes remain constant it can easily be shown that the ratio of the revised depth of the trapezoidal channel to the original depth of the triangular channel, y'/y, is

$$y'/y = [(B_b'/B_s)^2 + 1]^{1/2} - (B_b'/B_s) \tag{44}$$

in which B_b' is the new bottom width and B_s is the water surface width of the original triangular channel. Similarly, it can be shown that the ratio of the new surface width to the original surface width is

$$B_s'/B_s = [(B_b'/B_s)^2 + 1]^{1/2} \tag{45}$$

and that the change in water surface elevation, if the new channel is created by simply filling the bottom of the original triangular channel, is

$$\Delta y/y = [(B_b'/B_s)^2 + 1]^{1/2} - 1 \tag{46}$$

Eqs. 44, 45, and 46 are plotted on Figure 35 in terms of B_b'/B_s The chart shows the changes that may be expected if a flat bottom is introduced into a wide triangular channel.

For drainage channels located at the side of the roadway rather than in the median strip it is generally desirable to have a flat side slope adjacent to the roadway for vehicle safety and a relatively steep side slope on the opposite side in order to reduce the channel width and hence the necessary right-of-way. Such a nonsymmetrical triangular channel is characterized by two side slopes that are not equal and a depth, y. In such designs the discharge, Q, the longitudinal slope, S_b, and the two side slopes, z_1 and z_2, are given, the discharge is prescribed by hydrologic conditions and the longitudinal slope is prescribed by local topography.

The design procedure is similar to that developed for symmetrical channels in that the starting point is the continuity condition

$$Q = VA = VPR = VR^2(P/R) \tag{31}$$

in which V is the mean velocity, R is the hydraulic radius, and P is the wetted perimeter. For nonsymmetrical channels, the ratio P/R is a function of the side slopes only, just as it is for symmetrical channels, that is,

$$P/R = P^2/A = \frac{D^2(\sqrt{1+z_1^2} + \sqrt{1+z_2^2})^2}{(D^2/2)(z_1+z_2)} = \frac{2(\sqrt{1+z_1^2} + \sqrt{1+z_2^2})^2}{z_1+z_2} \tag{47}$$

By substituting Eqs 40, 41, and 47 into Eq. 31 an expression for Q involving the size of the riprap, the longitudinal slope, and the two side slopes can be written as follows:

$$Q = \frac{1}{128.8}\,\frac{d_{50}^{5/2}}{S_b^{13/6}}\left(\frac{(\sqrt{1+z_1^2} + \sqrt{1+z_2^2})^2}{z_1+z_2}\right) \tag{48}$$

Comparison of this equation with Eq. 43 suggests that an effective side slope, z_*, might be defined so that Eq. 48 would take the same form as Eq. 43 and hence involve the same type of computation. Eq. 48 may be written in parallel with Eq. 43, as follows:

$$Q = \frac{1}{64.4}\,\frac{d_{50}^{5/2}}{S_b^{13/6}}\,\frac{z_*^2+1}{z_*} \tag{49}$$

in which z_* is an "effective" side slope for an equivalent symmetrical channel. If such an effective side slope can be found that does not involve a different set of design charts and can be applied to some of those already prepared for symmetrical channels, the design can be simplified. In Table 3 the value of z_* is given for various combinations of values of z_1 and z_2 An examination of these values of

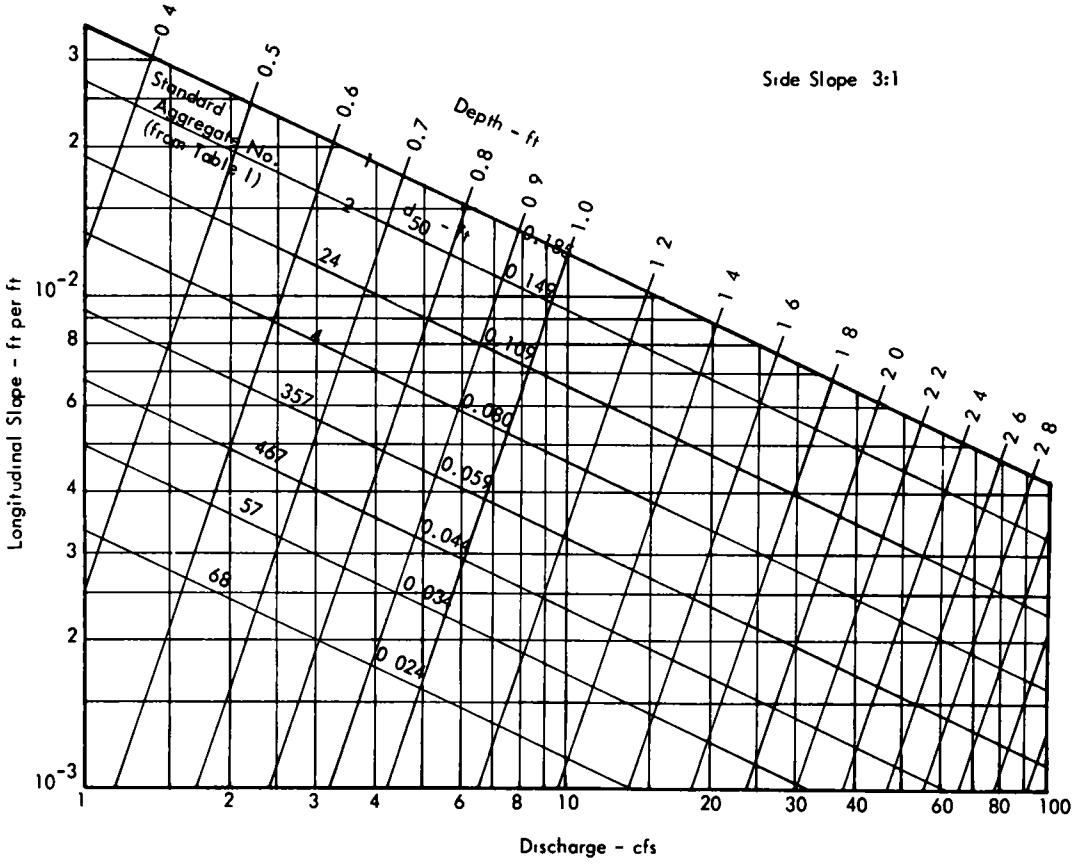

Figure 27. Depth of flow and size of standard aggregate for channel stability; side slope, 3 1

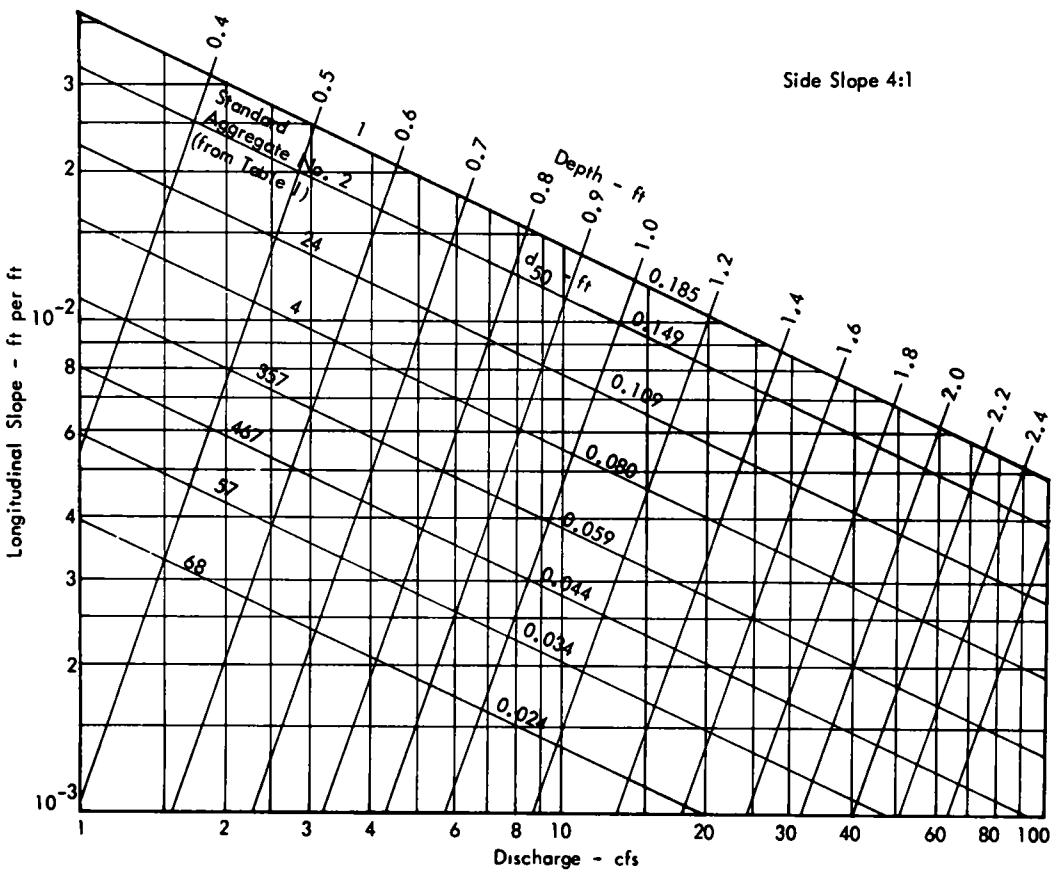

Figure 28 Depth of flow and size of standard aggregate for channel stability, side slope, 4.1.

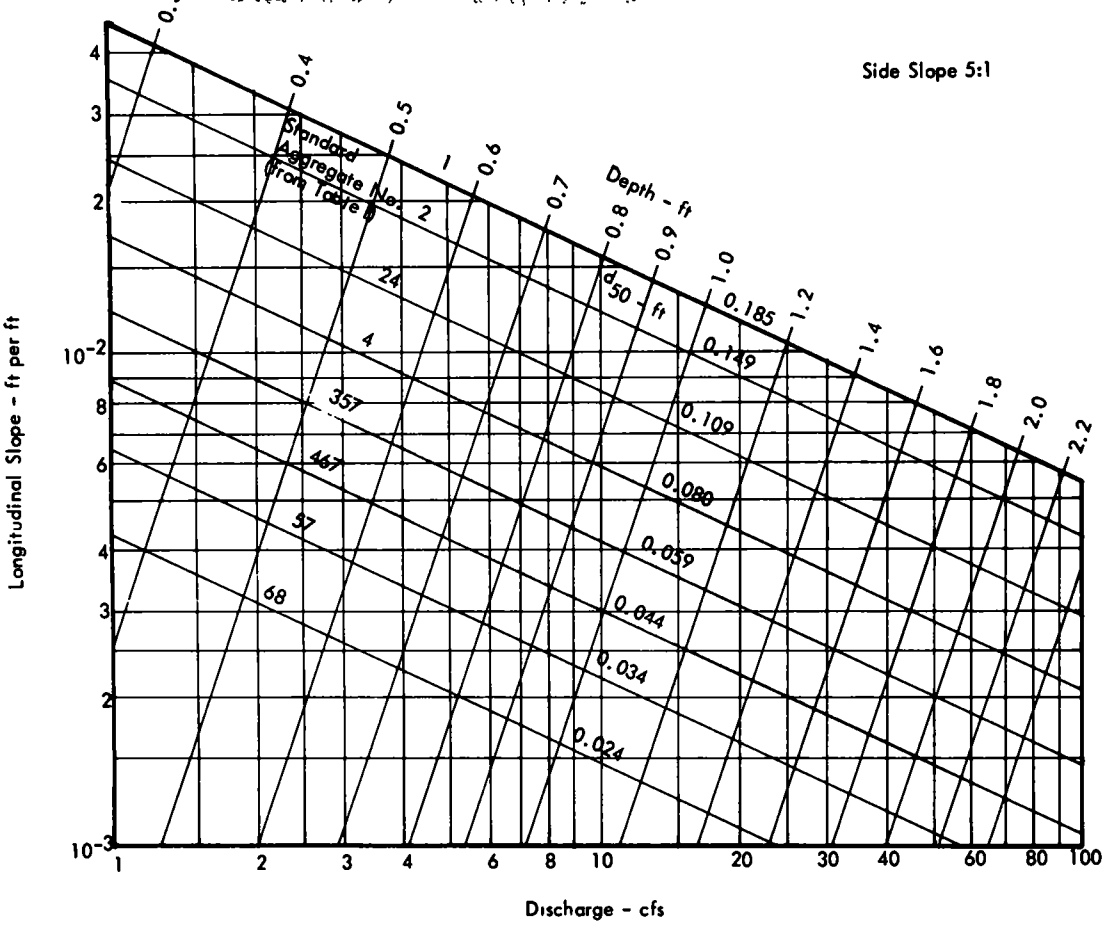

Figure 29 Depth of flow and size of standard aggregate for channel stability; side slope, 5.1.

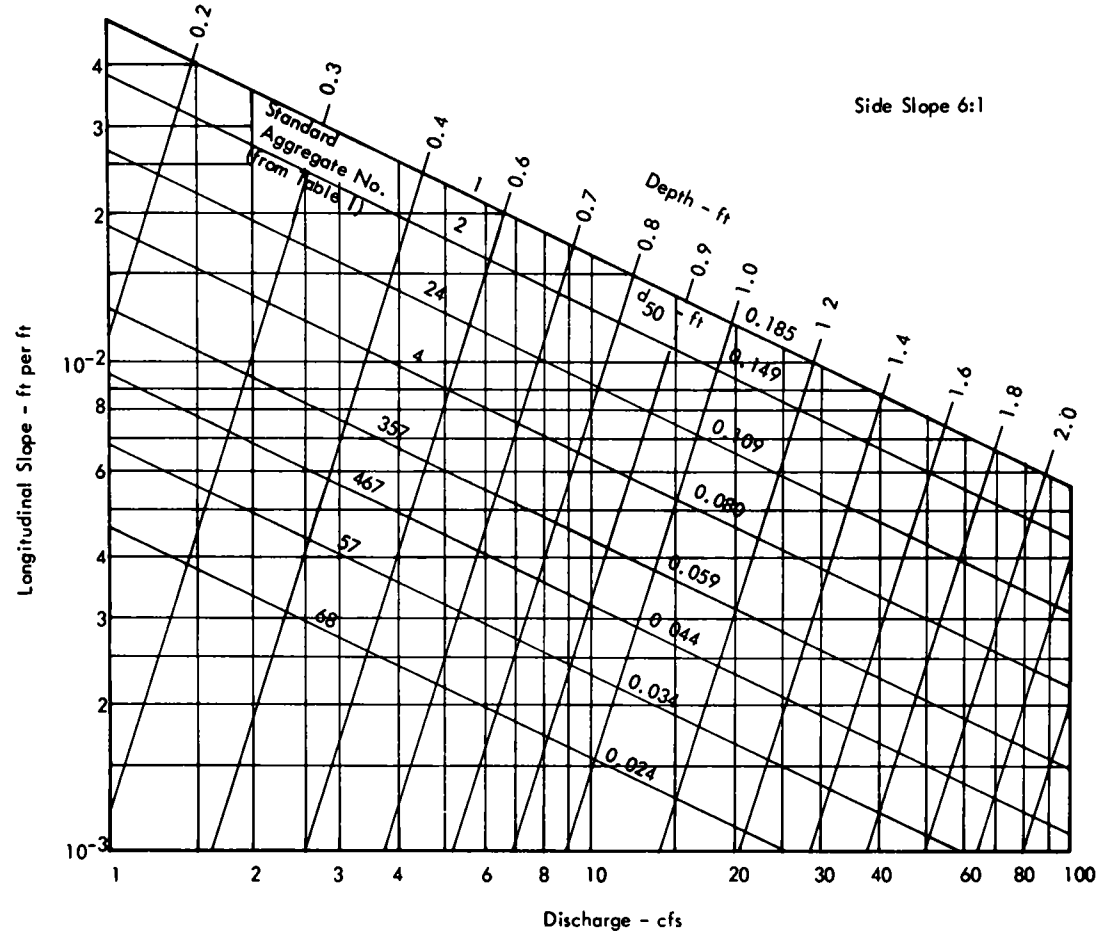

Figure 30. Depth of flow and size of standard aggregate for channel stability, side slope, 6:1.

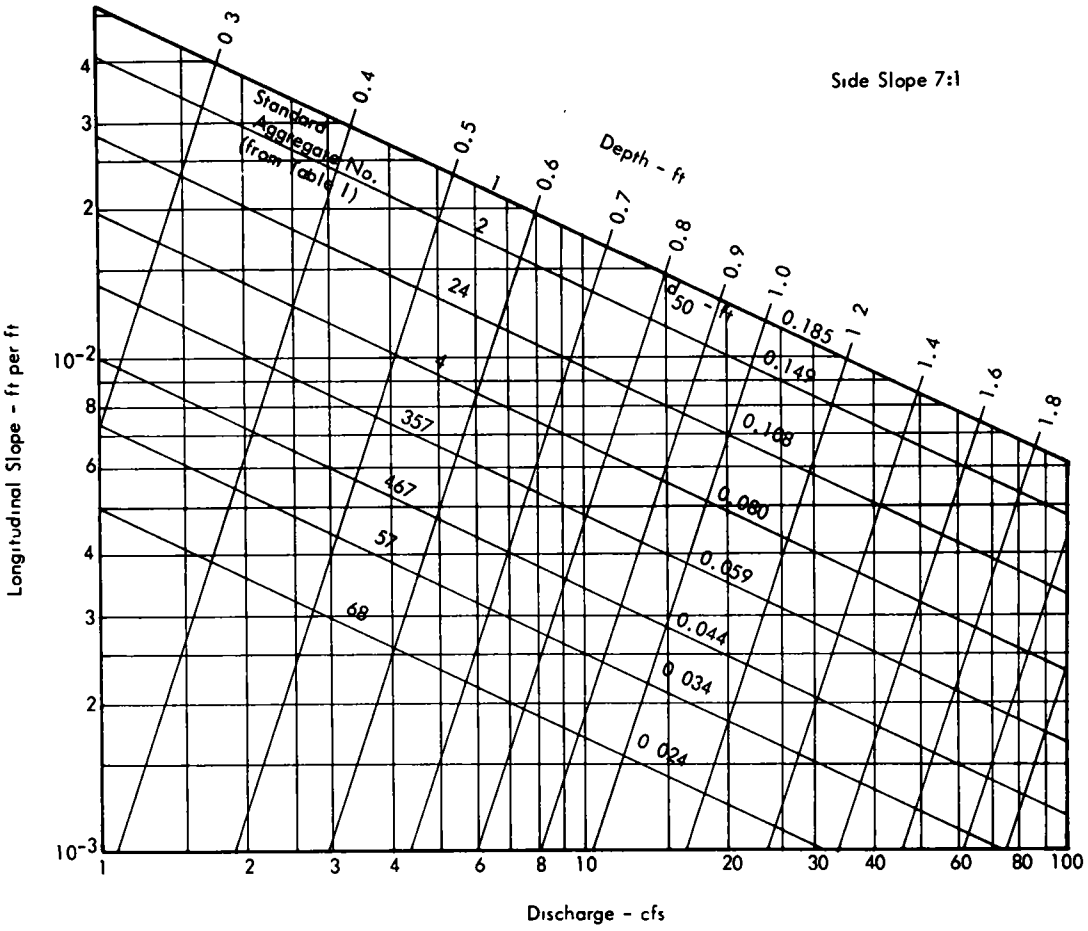

Figure 31. Depth of flow and size of standard aggregate for channel stability, side slope, 7 1

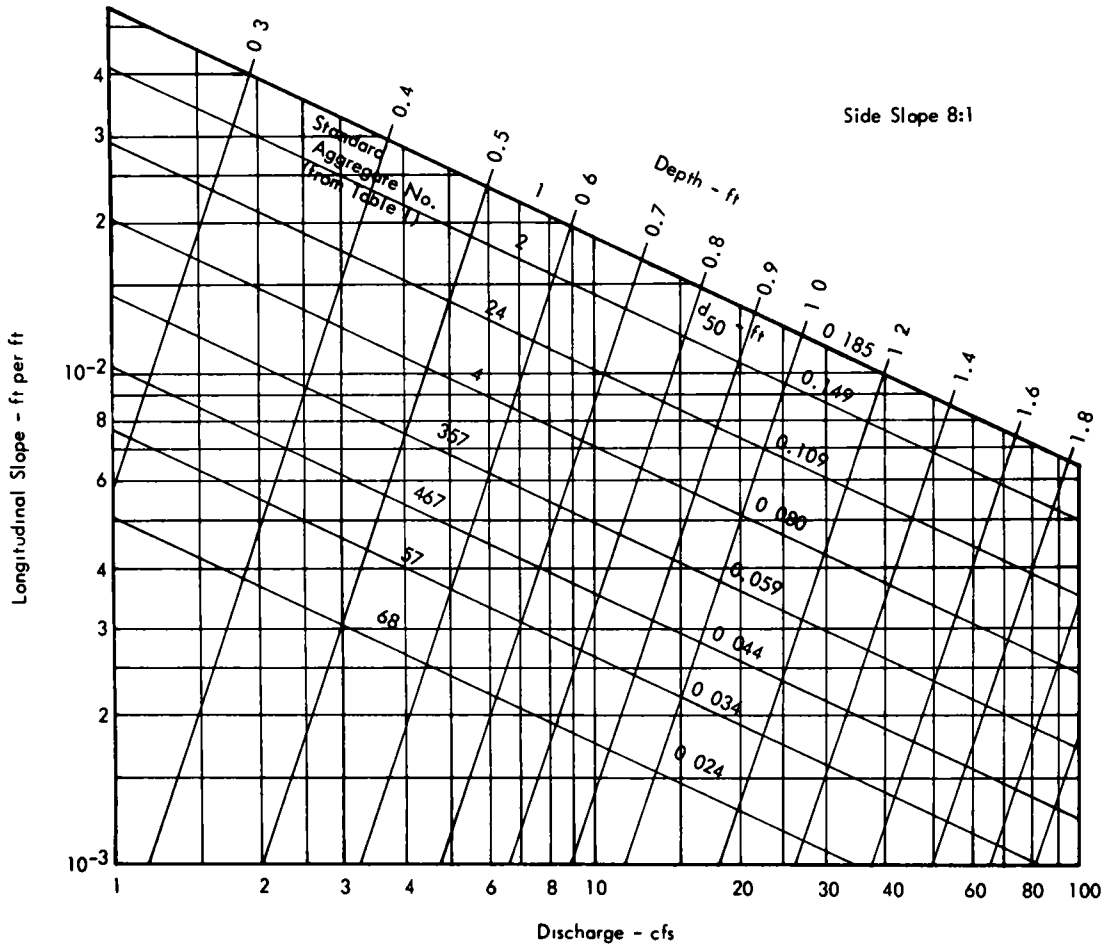

Figure 32. Depth of flow and size of standard aggregate for channel stability; side slope, 8 1

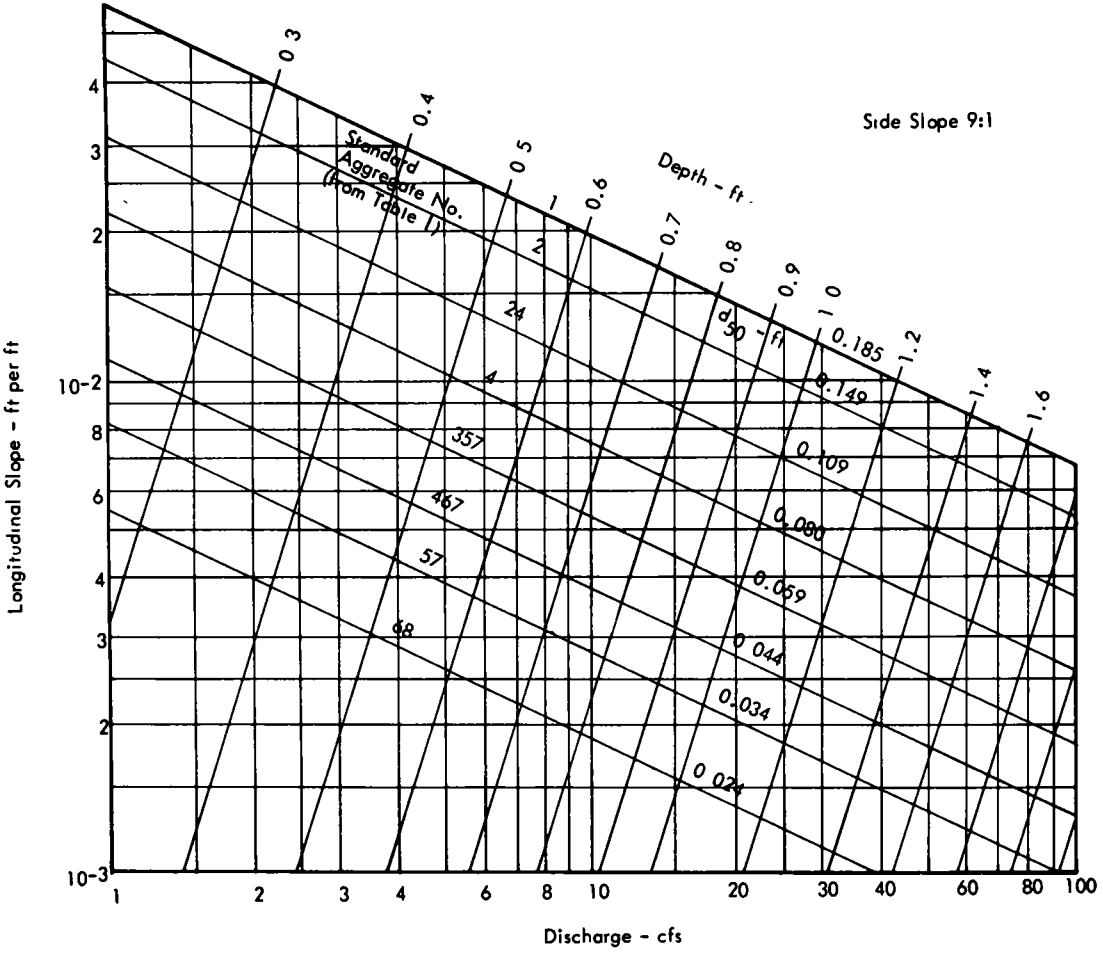

Figure 33 Depth of flow and size of standard aggregate for channel stability, side slope, 9 1

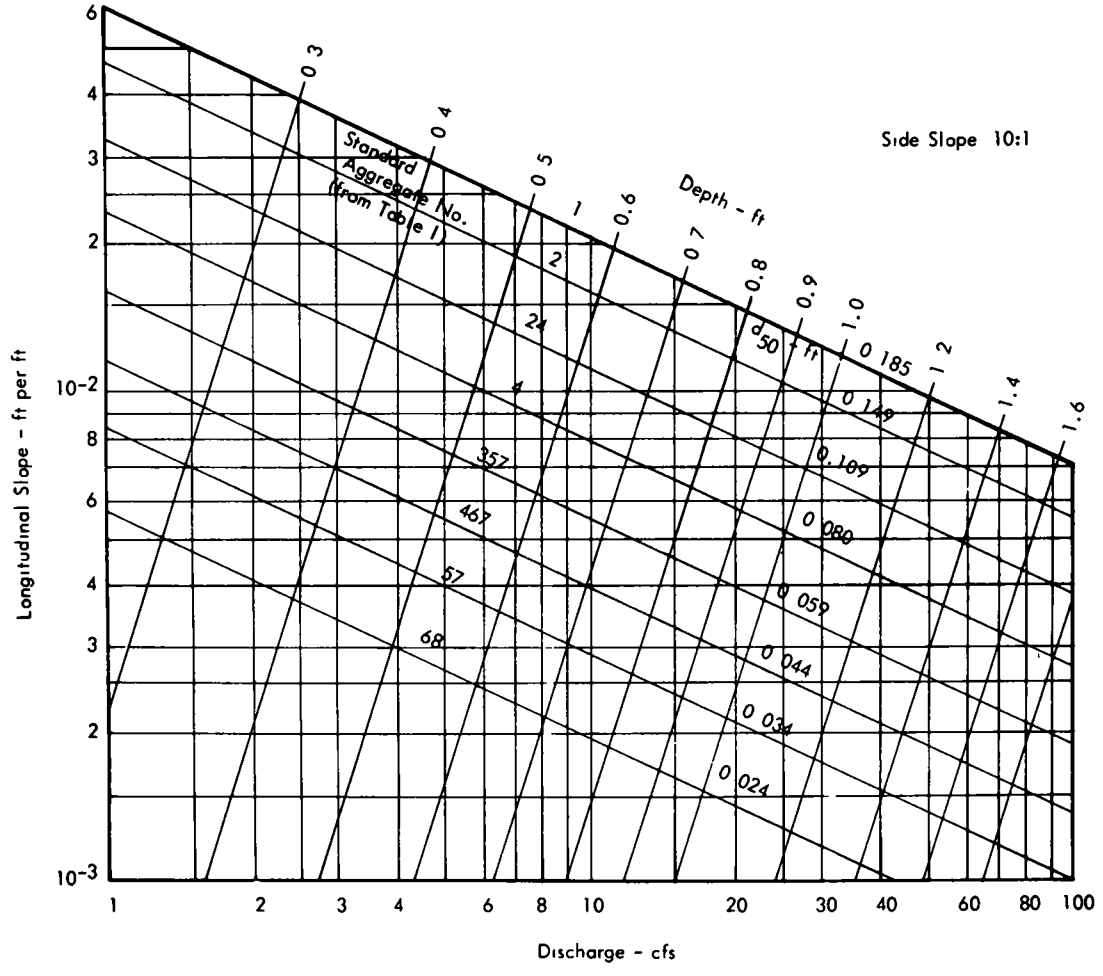

Figure 34 Depth of flow and size of standard aggregate for channel stability, side slope, 10 1

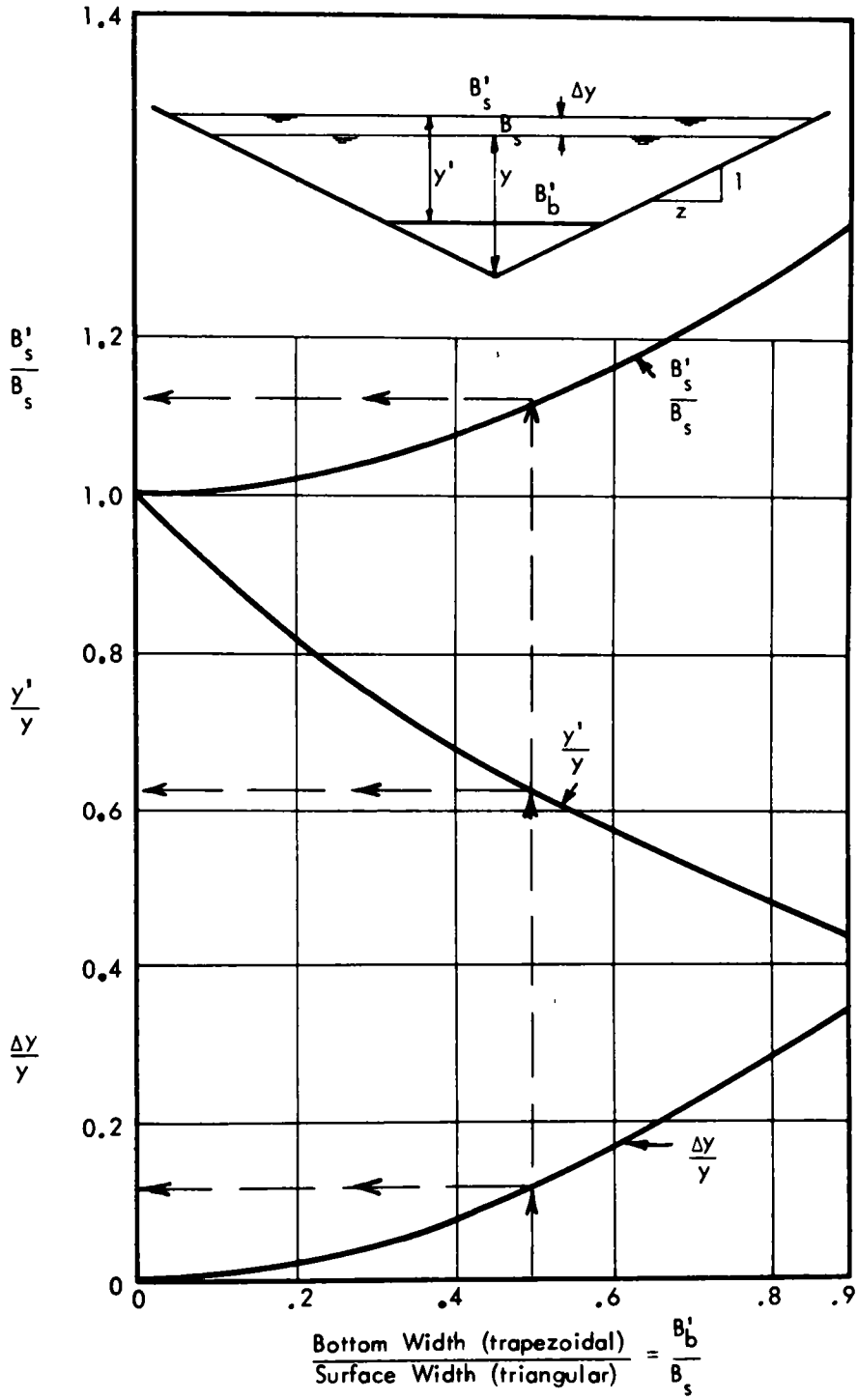

Figure 35. Variations in channel geometry for riprap-lined channel to transport 500 cfs at slope of 0.008

z_* shows immediately that they are approximately equal to the average of z_1 and z_2. To facilitate such a comparison, the next column in the table gives the average of the side slopes for each of the combinations for which z_* was computed. The last column of the table gives the ratio of z_* and $\bar{z} = (z_1 + z_2)/2$. It is apparent that z_* is always greater than $\bar{z}$, but differs from $\bar{z}$ by only 2 percent or less. This result indicates that the design charts already prepared for symmetrical triangular channels can also be used for non-symmetrical triangular channels when the average of the side slopes is used as the effective side slope

EXAMPLE 1. TRAPEZOIDAL CHANNEL

Suppose that it is necessary to design a riprap-lined channel to convey a peak discharge of 500 cfs, as prescribed by some previous hydrologic study. The topography of the area where the channel is to be constructed and the channel alignment indicate that the longitudinal slope of the resulting channel will be $S_b = 0\ 008\ (8 \times 10^{-3})$.

Then, given $Q = 500$ cfs, $S_b = 8 \times 10^{-3}$.

In Figure 19 ($P/R = 13.3$) enter the ordinate and abscissa with Q and S_b, respectively, and read

$$d_{50} = 140 \text{ mm } (0.46 \text{ ft}, 5\frac{1}{2} \text{ in.})$$

The size, $d_{50} = 140$ mm, is that size that will be stable in a trapezoidal channel for which $P/R = 13.3$. Such a channel will be relatively narrow and deep.

From Figure 20 ($P/R = 30$) the same process will yield $d_{50} = 100$ mm (0.33 ft, 4 in.). This size will be stable in a wide, shallow channel. It appears from this that any size between the foregoing two limits will result in a suitable channel geometry.

With $d_{50} = 140$ mm (0.46 ft), the following flow parameters and channel geometric properties are determined·

Figure 21	$V = 6.8$ fps
Figure 22	$R = 2.4$ ft
Figure 23	$A = 74$ sq ft
Figure 24 (crushed rock)	$\theta = 42°$
Figure 25 (side slope)	$\phi = 2.5{:}1$
Figure 26c	$B = 10$ ft $y = 3.8$ ft

On the other hand, if the riprap is chosen with $d = 100$ mm (0.33 ft), the following flow conditions and channel geometry are obtained:

Figure 21	$V = 6.0$ fps
Figure 22	$R = 1.75$ ft
Figure 23	$A = 84$ sq ft
Figure 24 (crushed rock)	$\theta = 42°$
Figure 25 (side slope)	$\phi = 2.5{:}1$
Figure 26c	$B = 35$ ft $y = 2.1$ ft

These two channels represent the two extremes of channels that will just be stable. The first is rather narrow, the second is quite wide. It may be desirable to consider an intermediate size. For this purpose it is assumed that the riprap should have an effective size of 130 mm (0.425 ft) Then, the charts provide the following information for $d = 130$ mm:

Figure 21	$V = 6.7$ fps
Figure 22	$R = 2.3$ ft
Figure 23	$A = 76$ sq ft
Figure 24 (crushed rock)	$\theta = 42°$
Figure 25 (side slope)	$\phi = 2.5.1$
Figure 26c	$B = 15$ ft $y = 3.3$ ft

TABLE 3

COMPUTATION OF EFFECTIVE SIDE SLOPE FOR UNSYMMETRIICAL TRIANGULAR CHANNELS

$$\frac{1}{2}\frac{(\sqrt{1+z_1^2}+\sqrt{1+z_2^2})^2}{z_1+z_2} = \frac{z_e^2+1}{z_e}$$

z_1	z_2	z_e	$\bar{z}=(z_1+z_2)/2$	$z_e/\bar{z}$
2	2	2 00	2	1.00
	4	3.04	3	1.01
	6	4 08	4	1 02
	8	5.10	5	1 02
	10	6.125	6	1.02
3	4	3 50	3 5	1.00
	6	4.53	4.5	1.01
	8	5.55	5.5	1 01
	10	6 55	6.5	1.01
4	4	4.00	4	1.00
	6	5.01	5	1.00
	8	6 02	6	1.00
	10	7.04	7	1.00
6	6	6 00	6	1.00
	8	7.01	7	1.00
	10	8.00	8	1.00
8	8	8 00	8	1.00
	10	9 00	9	1.00

These three channels lined with riprap of the size specified to safely transport 500 cfs at a slope of 0.008 are shown in Figure 36. The variations in channel shape indicate the flexibility that is provided in the design procedures if at the same time there is complete freedom to choose the effective size (d_{50}) of the riprap. The foregoing computations suggest that for each channel geometry there is a certain effective size of riprap that must be used. In fact, however, the riprap size as determined from the charts represents minimum size. After the channel dimensions have been determined, any coarser riprap can be used in its construction. Suppose that in this particular instance a specific size of crushed rock larger than that indicated by these computations is available for use or is for other reasons desirable to use as the riprap material. The effect of the larger riprap will be to decrease the mean velocity and consequently increase the cross-sectional area. This means that the larger riprap will be somewhat more stable than necessary Under these circumstances the charts cannot be used directly to determine if changes in geometry are needed, because they were designed to provide a channel geometry at the lower limit of stability and to define the minimum size of riprap to be used. Eq. 15 indicates that the roughness coefficient will be increased slightly with an increase in the effective size of the riprap. If one specifies that the hydraulic radius of the channel and the slope are to remain constant, then Eq 13, applied to both the basic design and the new design with larger riprap, can be used to determine the velocity to be expected in the new channel; that is,

$$V' = V(d_{50}/d_{50}')^{1/6} \qquad (50)$$

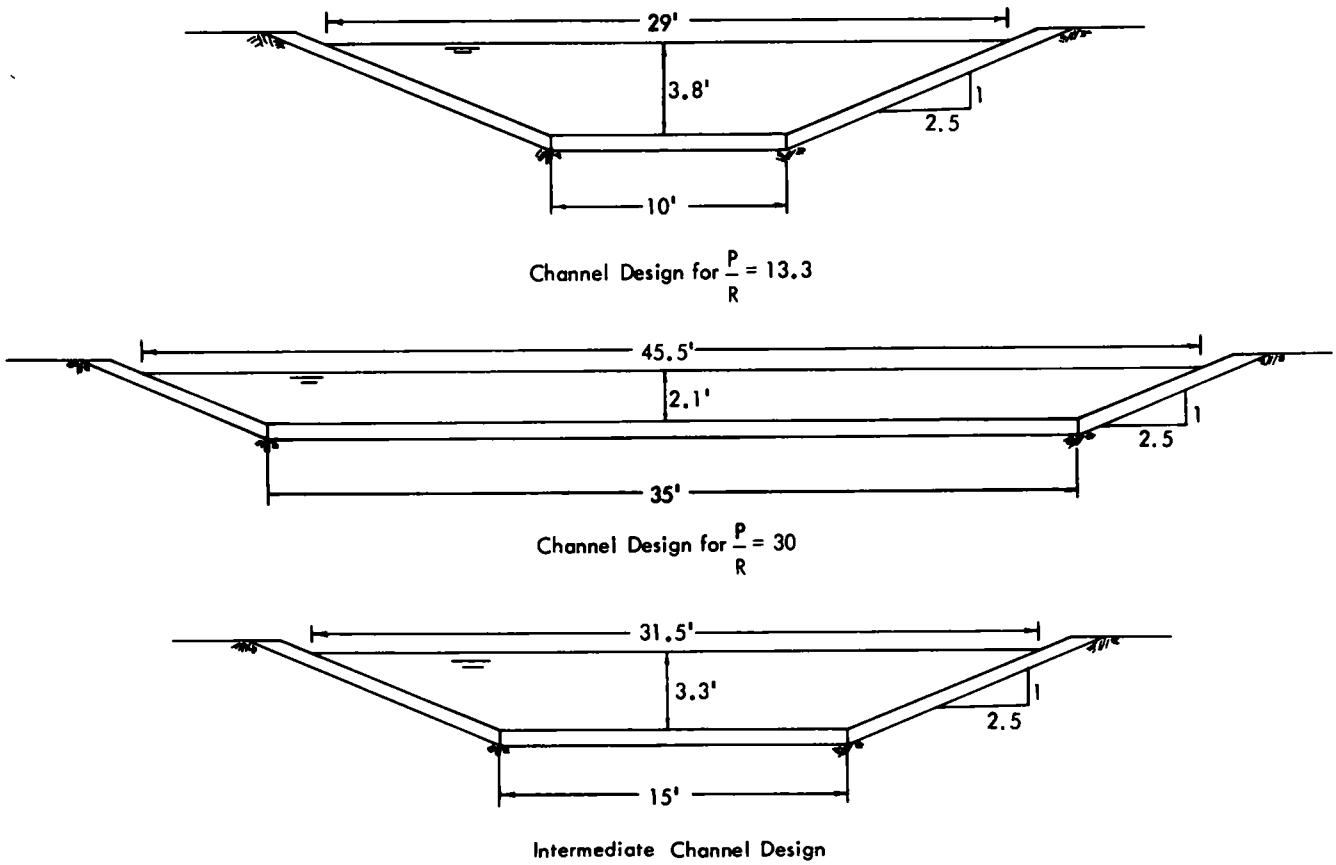

Figure 36 Variations in channel geometry for riprap-lined channel to transport 500 cfs at slope of 0 008.

in which V' is the velocity in the channel having the larger riprap and d_{50}' is the effective size of the proposed new riprap. Having the new velocity, the required area is

$$A' = Q/V' \tag{51}$$

Then, with the area and the hydraulic radius, which is unchanged, Figure 26c can be used as before to determine the new bottom width and the new depth.

Based on design procedure and the charts it was found that a suitable channel geometry would be obtained using a riprap having an effective size of 0 425 ft (130 mm). This resulted in a channel having a bottom width of 15 ft and a depth of 3.3 ft Suppose that riprap material having a mean size of 0 65 ft (198 mm) were available for use and it were proposed that this be used to line the channel. Using Eq. 50 the velocity to be expected in the revised channel would be

$$V' = V\left(\frac{d_{50}}{d_{50}'}\right)^{1/6} = 6.7\left(\frac{0.425}{0\ 65}\right)^{1/6} = 6.25 \text{ fps}$$

and

$$A = \frac{500}{6.25} = 80 \text{ sq ft}$$

$$R = 2.3 \text{ ft}$$

From Figure 26c the new bottom width, B, is 14 ft and the depth, y, is 3.5 ft. With the larger riprap the bottom width is reduced from 15 ft to 14 ft and the depth of flow is increased from 3.3 ft to 3 5 ft. It is worth noting that although the size of riprap was increased by 50 percent, the mean velocity was reduced by only 7 percent. For this reason there is relatively little change in the cross-sectional shape of the channel because of the increased size of the riprap material.

Occasionally in the design of a drainage channel it is necessary to incorporate a bend into the alignment Figure 17 shows that the shear stress may be increased locally due to the secondary currents that are generated and that the amount increases with the ratio B_s/R_0 It may therefore be necessary to use a larger riprap in this section of the channel to counteract the local increase in boundary shear. Eqs 22 and 23 relate the critical boundary shear to the size of the riprap and the channel geometry, so that for stability (Eq 28) in a straight channel

$$1\ 5\gamma RS_b = 4d_{50} \tag{52}$$

Figure 17 gives the relative increase in shear due to the channel curvature, so that, again for stability,

$$(\tau_0/\bar{\tau}_0)_{max}\gamma RS_b = 4d_{50}' \tag{53}$$

Here, τ_0 is the maximum local boundary shear in the bend, $\bar{\tau}_0$ is the mean shear in a corresponding straight channel,

and d_{50}' is the size of riprap needed for the bend. If one again specifies that the hydraulic radius and the slope are to remain constant, then

$$d_{50}' = d_{50} \frac{(\tau_o/\bar{\tau}_o)_{max}}{1.5} \quad (54)$$

Because of the increase in riprap sizes the velocity will be reduced as described by Eq. 50 and the area will be increased as shown by Eq. 51. With these data the appropriate Figure 26 can be used to determine the channel geometry.

In this example it might be supposed that the channel being designed includes a bend having a center-line radius, R_o, of 60 ft. This radius is probably much smaller than any found in practice, but it was chosen to illustrate the effect of curvature on the riprap size. The surface width of the chosen channel is 31 5 ft (see Fig 36) and the effective size of riprap required is 0.425 ft (130 mm). The relative curvature of the bend is then

$$B_s/R_o = \frac{31\,5}{60} = 0.525$$

and Figure 17 shows

$$(\tau_o/\bar{\tau}_o)_{max} = 1.82$$

The required size of the riprap (Eq 54) is

$$d_{50}' = 0.425 \frac{1\,82}{1\,50} = 0.515 \text{ ft (157 mm)}$$

and the mean velocity to be expected (Eq. 50) is

$$V' = 6\,7 \left(\frac{0\,425}{0\,515}\right)^{1/6} = 6.5 \text{ fps},$$

$$A = \frac{500}{6\,5} = 77 \text{ sq ft, and}$$

$$R = 2\,3 \text{ ft (specified as being constant)}$$

Under these conditions the remaining geometric properties are as follows·

Figure 24 (crushed rock)	$\theta = 42°$
Figure 25 (side slope)	$\phi = 2.5{:}1$
Figure 26c	$B = 15$ ft
	$y = 3\,3$ ft

The scale of Figure 26c precludes a more exact delineation of the channel geometry, and so although larger riprap (0 515 ft) is required to stabilize the bend, the channel cross-sectional geometry will not be appreciably changed. It also appears from Figure 17 that for bends for which the radius is more than four times the channel width no provision for added protection is needed This procedure for computing the increased size of riprap in a bend is, of course, independent of the actual velocity that exists in the channel and would be appropriate for much larger velocities than that used in this example This is because the size of the riprap needed is governed by the local shear and Figure 8 shows that the magnitude of the critical shear stress is proportional to the size of the riprap throughout the range of experimental data.

The riprap that is prescribed for the bend by such an analysis as that given previously should be applied throughout the bend and a portion of the straight channel upstream of the bend so that a good transition will be made. Aside from the special computation, other considerations such as filter blankets, thickness of riprap layer, rolling and compacting of the riprap, or steeper side slopes apply to the bend in the same way as to the straight section

The channel dimensions computed previously represent the finished geometry Provision must also be made in the excavation for both the riprap layer and the filter blanket, if one should be necessary For purposes of this example it is supposed that the drainage channel is to be constructed in a region where the base material is a gravelly mixture having an effective size, d_{50}, of 5 mm. Assuming that the shape of the gradation curves for both the base material and the riprap are similar, the criterion

$$\frac{d_{50}\ \text{Riprap}}{d_{50}\ \text{Base}} = \frac{130}{5} = 26 < 40$$

indicates that a filter blanket will not be needed. The thickness of the riprap in this case should be between two and three times the effective size of the riprap, that is, between 0 95 and 1 27 ft Because the base material is relatively coarse, a riprap thickness of 1 ft is appropriate. It is obvious that the effectiveness of the riprap lining will be influenced by the uniformity of the blanket Care must be taken in placing the riprap so that it will be homogeneous and of relatively uniform thickness.

Provision must also be made in the channel design for a minimum freeboard to accommodate any ordinary irregularities of the water surface and to provide a factor of safety in the channel design. The recommended freeboard is given in Figure 18. For a discharge of 500 cfs the riprap lining should be carried 1 ft above the computed water surface and the top of the channel should be approximately 2 ft above the design water surface.

EXAMPLE 2. TRAPEZOIDAL CHANNEL

This second example involves a large discharge on a relatively flat slope. It is necessary to convey 1,000 cfs in a channel constructed in sandy soil at a slope of 0.0005 (5×10^{-4}) In this case Figure 19 indicates that a riprap having an effective size of 16 mm will be sufficient. On the other hand, Figure 20, for a wide channel, indicates that $d_{50} = 12$ mm would be sufficient. Using $d_{50} = 16$ mm (0.053 ft), the following channel dimensions are required

Figure 21	$V = 3\,75$ fps
Figure 22	$R = 4.5$ ft
Figure 23	$A = 270$ sq ft
Figure 24 (crushed rock)	$\theta = 40°$
Figure 25 (side slope)	$\phi = 2\,5{:}1$
Figure 26c	$B = 25$ ft
	$y = 6.5$ ft

On the other hand, if $P/R = 30$ and $d_{50} = 12$ mm, these channel dimensions apply

Figure 21	$V = 3.1$ fps
Figure 22	$R = 3.1$ ft

Figure 23	$A = 310$ sq ft
Figure 24 (crushed rock)	$\theta = 39.5°$
Figure 25 (side slope)	$\phi = 2.5:1$
Figure 26c	$B = 85$ ft $y = 3.3$ ft

In this instance a change in riprap size of 4 mm resulted in a drastic change in channel dimensions, from 25 ft to 85 ft in bottom width and from 6.5 ft to 3.3 ft in depth. This indicates that any intermediate channel of appropriate dimensions based on the charts and using riprap having an effective size between 12 and 16 mm would be suitable. In this specific case any channel of side slope 2.5:1 having its bottom width between 25 and 85 ft along with an appropriate depth between 3 3 and 6.5 ft would work effectively with riprap having an effective size of between 12 and 16 mm.

In this problem it is assumed that the base material and the riprap material have the following composition:

BASE MATERIAL	RIPRAP MATERIAL
$d_{50} = 0.75$ mm	$d_{50} = 12$ mm
$\sigma = 2$	$\sigma = 2$
$d_{85} = 1.5$ mm	$d_{85} = 24$ mm
$d_{15} = 0.38$ mm	$d_{15} = 6$ mm

Then

$$\frac{d_{15}\ \text{Riprap}}{d_{85}\ \text{Base}} = \frac{6}{1.5} = 4 < 5$$

$$5 < \frac{d_{15}\ \text{Riprap}}{d_{15}\ \text{Base}} = \frac{6}{0.38} = 16 < 40$$

$$\frac{d_{50}\ \text{Riprap}}{d_{50}\ \text{Base}} = \frac{12}{0\ 75} = 16 < 40$$

These ratios indicate that a filter layer is not required between the riprap and the base material, and the riprap lining can be placed directly on the base material. If a layer three diameters thick ($d_{50} = 16$ mm) were used, the thickness would be only about 2 in. Further, because d_{85} of the riprap is approximately 24 mm, a thickness of 2 in. would also satisfy the criterion that the thickness should be two times the maximum size. In this case, however, construction techniques should determine the thickness of the riprap layer in order that the final result will be of uniform thickness and homogeneous in character In view of the magnitude of the discharge and the size of the channel it is recommended that a riprap layer at least 6 in. thick be placed and carefully spread by mechanical equipment in order to assure a layer of constant thickness. In addition, the stability of the riprap and channel will be improved by rolling the riprap to increase its density, because the riprap material is rather small. In this discussion it has been assumed that the base material was a noncohesive mixture of sand particles. In many instances, however, the soil will contain varying amounts of silts and clays that will provide a certain degree of cohesiveness to the base material through which the channel is being excavated. This condition may be further enhanced by pre-treatment or compacting before the riprap layer is placed. If this is done, a filter layer may be dispensed with, even though the criteria indicate its use. The absence of the filter can be further compensated for by increasing the thickness of the riprap blanket to three grain diameters or more. There are essentially no applicable data or experience to relate the resistance to erosion to the properties of a cohesive soil mixture These estimates must be based on experience as to the resistivity of broad classes of cohesive materials.

A minimum amount of freeboard must be provided for this channel because the velocities are relatively small compared to the depth and discharge. The Froude number is 0.3 or less, which means that the flow will be relatively smooth and quiet. Disturbances will be minimal, and the freeboard is needed primarily as a factor of safety in recognition of the uncertainties in the computation.

In this example the required riprap was less than 1 in. in size, so that instead of crushed rock the riprap might be a well-rounded gravel from some nearby sources. If this were so, the angle of repose, θ, would be less than 30°. Consequently, the side slopes would have to be flattened to 4:1, according to Figure 25. The bottom width and depth would then be determined from Figure 26e as $B =$ 65 ft and $y = 3\ 8$ ft. The first channel design ($P/R = 13.3$) could not be used, because with side slopes of 4:1 the minimum would be $P/R = 17$. Comparisons could be made, however, for any intermediate channel that might be designed. By way of comparison with the widest channel ($P/R = 30$), when well-rounded gravel is used instead of crushed rock the side slopes are flattened to 4.1 from 2 5.1, the bottom width is reduced to 65 ft from 85 ft, and the depth is increased to 3.8 ft from 3 3 ft. Not including any freeboard, the surface width of the revised channel using gravel is 95 ft, as compared to 102 ft for the crushed rock.

EXAMPLE 3. TRAPEZOIDAL CHANNEL

In this example the same discharge (1,000 cfs) is to be conveyed in a much steeper channel, one having a slope of 0 01 (10^{-2}). From Figures 19 and 20 the range of minimum sizes of riprap material that can be used for protection is between $d_{50} = 225$ mm (0.74 ft) ($P/R = 13.3$) and $d_{50} = 162$ mm (0 53 ft) ($P/R = 30$). The first channel would tend to be relatively small, with the largest velocity. The second channel would be somewhat larger, with a somewhat lower velocity. The channel properties for the two sizes of riprap are compared as follows:

$d_{50} = 225$ MM	$d_{50} = 162$ MM
$V = 8.5$ fps	$V = 7.0$ fps
$R = 3.0$ ft	$R = 2.2$ ft
$A = 120$ sq ft	$A = 145$ sq ft
$\theta = 41.5°$	$\theta = 41.3°$
$\phi = 2.5.1$	$\phi = 2.5:1$
$B = 17$ ft	$B = 55$ ft
$y = 4\ 4$ ft	$y = 2\ 4$ ft

Allowing a freeboard of 1.5 ft in both cases, minimum width requirements for these channels are 46.5 ft for the first and 74.5 ft for the second. Normally the right-of-way would be sufficient for the construction of any appropriate channel, but, if it were limited in this instance to 50 ft, then the first channel would be the only appropriate one. A third channel that would satisfy the requirement for conveying 1,000 cfs on a slope of 0.01 and having a $d_{50} =$ 200 mm (0.66 ft) is as follows.

$d_{50} = 200$ MM (0.66 FT)
$V = 8.0$ fps
$R = 2.75$ ft
$A = 130$ sq ft
$\theta = 41.5°$
$\phi = 2.5{:}1$
$B = 30$ ft
$y = 3.4$ ft

The total width, including 1.5 ft of freeboard, is 54.5 ft.

With these channel shapes, consideration might be given to increasing the side slope of the channel in order to make it narrower and reduce the total width required. If the side slope of 1.5:1 is chosen for the third channel, then the size of the riprap required on the steeper side can be determined using Eq. 33, where the values of K (Fig. 15) are determined for the original and the steeper side slope. For a slope of 1.5:1 with $\theta = 41.5°$, $K' = 0.48$; for a 2 5·1 slope at the same angle of repose, $K = 0.85$. Therefore, according to Eq. 33, riprap material having an effective size of $d_{50} = 350$ mm (1.16 ft) will be required. Assuming that the cross-sectional area and the hydraulic radius will remain the same, Figure 26a for the steeper side slope gives bottom width, $B = 35$ ft, and depth, $y = 3.4$ ft. By using the steeper side slopes and including 1.5 ft for freeboard, the total width is reduced from 54.5 ft to 49 7 ft. Care must be taken that the increase in side slope does not exceed the angle of repose of the riprap material. As this value is approached, K' in Eq. 33 approaches zero, with a consequently rapid increase in the required size of riprap for the new slope. The larger the angle of repose of the riprap material for a given slope, the smaller will be the necessary increase in riprap size.

It is now assumed that the channel will be constructed in a base material having the following characteristics:

$$d_{50} = 0.5 \text{ mm}$$
$$\sigma = 3$$
$$d_{85} = 1.5 \text{ mm}$$
$$d_{15} = 0.167 \text{ mm}$$

The riprap properties are assumed to be

$$d_{50} = 200 \text{ mm}$$
$$\sigma = 2$$
$$d_{85} = 400 \text{ mm}$$
$$d_{15} = 100 \text{ mm}$$

These two gradation curves are shown in Figure 37. The application of the filter criteria to these gradations shows that

$$\frac{d_{15}\ \text{Riprap}}{d_{85}\ \text{Base}} = \frac{100}{1.5} = 66.7 \not< 5$$

$$\frac{d_{15}\ \text{Riprap}}{d_{15}\ \text{Base}} = \frac{100}{0.167} = 600 \not< 40$$

and thus indicates that a filter layer is required for stability of the channel. The properties of the filter can be determined as follows:

$$\frac{d_{50}\ \text{Filter}}{d_{50}\ \text{Base}} < 40, \text{ so } d_{50}\ \text{Filter} < 40 \times 0.5 = 20 \text{ mm}$$

$$\frac{d_{15}\ \text{Filter}}{d_{15}\ \text{Base}} < 40, \text{ so } d_{15}\ \text{Filter} < 40 \times 0.167 = 6\ 67 \text{ mm}$$

$$\frac{d_{15}\ \text{Filter}}{d_{85}\ \text{Base}} < 5, \text{ so } d_{15}\ \text{Filter} < 5 \times 1.5 = 7.5 \text{ mm}$$

$$\frac{d_{15}\ \text{Filter}}{d_{15}\ \text{Base}} > 5, \text{ so } d_{15}\ \text{Filter} > 5 \times 0.167 = 0.83 \text{ mm}$$

Therefore, with respect to the base material, the filter must satisfy 0.83 mm $< d_{15}$ Filter < 6.67 mm and d_{50} Filter < 20 mm.

Now, considering the riprap and a filter, the properties of the filter must satisfy

$$\frac{d_{50}\ \text{Riprap}}{d_{50}\ \text{Filter}} < 40, \text{ so } d_{50}\ \text{Filter} > \frac{200}{40} = 5 \text{ mm}$$

$$\frac{d_{15}\ \text{Riprap}}{d_{15}\ \text{Filter}} < 40, \text{ so } d_{15}\ \text{Filter} > \frac{100}{40} = 2.5 \text{ mm}$$

$$\frac{d_{15}\ \text{Riprap}}{d_{85}\ \text{Filter}} < 5, \text{ so } d_{85}\ \text{Filter} > \frac{100}{5} = 20 \text{ mm}$$

$$\frac{d_{15}\ \text{Riprap}}{d_{15}\ \text{Filter}} > 5, \text{ so } d_{15}\ \text{Filter} < \frac{100}{5} = 20 \text{ mm}$$

Therefore, with respect to the riprap, the filter must satisfy $2.5 < d_{15}$ Filter < 20 mm, d_{50} Filter > 5 mm, and d_{85} Filter > 20 mm The limits of filter material with respect to the riprap and the base material are plotted in Figure 37, where the curves have been extrapolated somewhat arbitrarily beyond the computed points. The ranges of suitable filter for both the riprap and the base have been cross-hatched, any filter material that falls within the region where the cross-hatching overlaps will meet the criteria of both the riprap and the base material and will thus be suitable for the filter blanket.

With the use of the filter blanket as described previously the riprap layer can be placed with a minimum thickness This thickness for the 1.5.1 side slopes should be approximately 2 ft. This corresponds to approximately two times the effective size. The usual provision for freeboard and height of riprap layer above the water surface as given in Figure 18 should be incorporated.

EXAMPLE 4. TRIANGULAR CHANNEL

For triangular channels the shape and dimensions of the channel are fixed whenever the side slopes are prescribed. There is then, for a given discharge and longitudinal slope, only one channel that will satisfy these conditions. The dis-

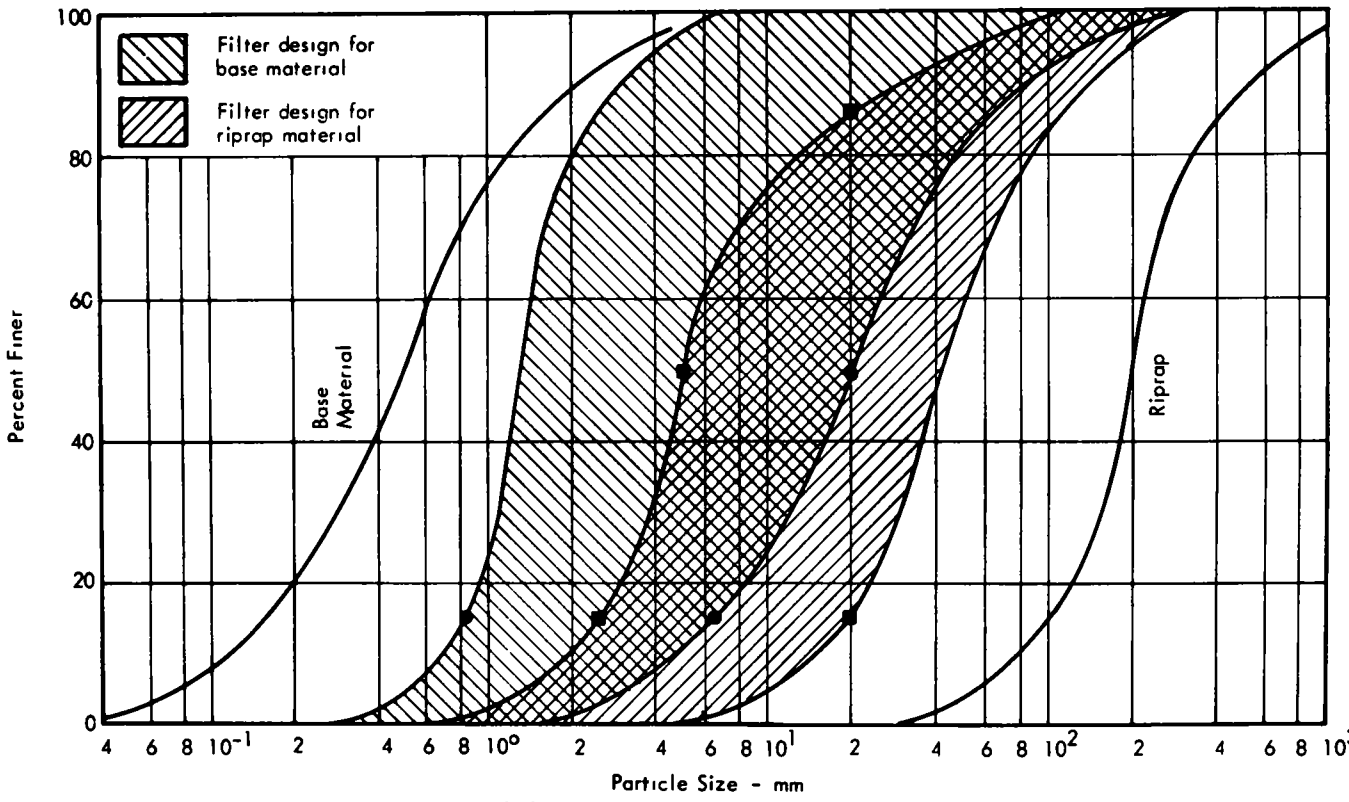

Figure 37 Gradations of filter blanket for Example 3

charge and the slope are, as before, the independent variables, and are usually established by a hydrologic study and highway grade. The choice of the side slope is generally determined according to nonhydraulic considerations.

In this example it is presumed that the discharge is 35 cfs, the longitudinal slope is 0.005, and the side slope has been fixed at 6.1. By entering a discharge of 35 cfs and a slope of 5×10^{-3} on Figure 30, for $z = 6$, one determines directly the depth of flow and the standard aggregate classification. The intersection of the coordinates indicates a d_{50} size of 0.109 ft (33.2 mm), which corresponds to Standard Aggregate No. 24 The depth of flow for this discharge will be 1.41 ft. These dimensions represent the finished construction, and provision must also be made in the excavation for a riprap layer and a filter layer, if one is required. The usual procedure should be followed in establishing the need for a filter blanket. The thickness of the riprap layer for channels of this kind is usually determined by problems of construction The minimum thickness of the riprap layer should be the equivalent of three diameters of the effective size, d_{50}, or the minimum thickness for effective placement, whichever is greater. In no case should it be less than 4 in , and it should be uniformly spread and homogeneous in character. To provide a more dense riprap layer it is also recommended that the layer be rolled to compact the blanket and provide greater resistance to the flow and less likelihood of damage by vehicles.

It might be desirable for the channel to have a flat bottom in order to provide for movement of equipment A bottom width of 8.5 ft would normally be sufficient for this purpose. Because the surface width of the triangular channel is $B_s = 2zy = 17$ ft, the ratio $B_b'/B_s = 8.5/17 = 0.5$. If this value is entered on the abscissa of Figure 35 the following changes in the geometry of the channel are indicated:

$$B_s'/B_s = 1.12, \text{ so } B_s' = 1.12 \times 17 = 19 \text{ ft}$$

$$y'/y = 0\ 62, \text{ so } y' = 0.62 \times 1.41 = 0.87 \text{ ft}$$

$$\Delta y/y = 0.12, \text{ so } \Delta y = 0\ 12 \times 1.41 = 0.17 \text{ ft}$$

The new trapezoidal channel of equivalent capacity will have a surface width $B_s' = 19$ ft, a bottom width $B_b' = 8.5$ ft, and a depth $y' = 0.87$ ft, and its water surface will be 0.17 ft higher than originally planned. The required freeboard will be the same as that previously determined.

If, on the other hand, it had been proposed to construct an asymmetrical channel along the side of the roadway to handle the same discharge on the same slope but with side slopes that were $z_2 = 2$ for the far side slope and $z_2 = 6$ for the roadway side slope, the revision could be accomplished by using the design charts directly The average of the side slopes would be

$$\bar{z} = z_* = \frac{z_1 + z_2}{2} = 4$$

Entering $Q = 35$ cfs and $S_b = 0\ 005$ on Figure 28 it is found that the required depth would be 1.7 ft and the

required riprap size would be between $d_{50} = 0.109$ ft and $d_{50} = 0.149$ ft. Because these grades are standard gradations, the coarser riprap, $d_{50} = 0.149$ ft (Standard Aggregate No. 2), would be chosen for channel protection. This computation gives the required depth, but a check should be made on the size of riprap needed on the steeper slope, $z = 2$. This can be done by assuming a symmetrical triangular channel with that side slope and using the appropriate chart. In this case there is no chart for $z = 2$, but the required size can be computed from Eq. 43, on which the charts are based:

$$Q = \frac{1}{64.4} \frac{d_{50}^{5/2}}{S_b^{19/6}} \frac{z^2 + 1}{z} \qquad (43)$$

Substituting the discharge, the longitudinal slope, S_b, and the side slope, $z = 2$, into Eq. 43 results in $d_{50} = 0.156$ ft. This is nearly equal to the size prescribed by the charts, so no further modification is needed. From these computations it appears that a drainage channel having side slopes of 2:1 and 6:1 and protected with gravel riprap having a mean size of 0.149 ft (Standard Aggregate No. 2) would be suitable for transporting 35 cfs on a slope of 0.005 at a depth of 1.7 ft.

EXPERIMENTAL VERIFICATION OF DESIGN PROCEDURES

Aside from the basic equations of open channel flow, the procedure for designing riprap-lined channels is based on experimental data defining the critical shear stress and the resistance of the riprap material. Hence, there are two factors that have a bearing on the validity of these procedures for prototype drainage channels. These are the manipulation of theoretical equations to develop useful design criteria and the adequacy of experimental data. Once a design procedure has been established, the resulting design should be tested to determine the efficacy of the design procedure from the standpoints of stability, factor of safety and convenience, and verification, insofar as it is possible, of the empirical constants that are involved. Ideally, such testing should be done in prototype channels, but such testing would depend on the occurrence of design discharges and the opportunity to carry out the necessary observations and measurements. On the other hand, laboratory experiments on a model scale can provide much useful information regarding the basic mechanics of movement, but the extrapolation of such quantitative results to the prototype scale introduces a degree of uncertainty. These experiments represent a compromise between the desirable prototype tests and the efficiency and convenience of laboratory experiments. It was proposed to design a small trapezoidal channel based on these design procedures and to test separately several longitudinal segments of it in a laboratory flume. Because the entire channel could not be duplicated in the laboratory it was proposed that a segment in the central portion of the cross section and one incorporating the side slope be successively fitted into the flume and tested with proportionate discharges and the design slope. The experiments have provided information as to the adequacy of the design, the magnitude of the critical shear stress, and the flow resistance of the riprap material. Subsidiary information has corroborated the empirical curves for the critical shear stress and roughness coefficients used in setting up the design procedures.

DESIGN OF THE PROTOTYPE DRAINAGE CHANNEL

The prototype channel was designed according to the tentative design procedure. For this purpose and in order to stay within the capacity of the available laboratory channels, a design discharge of 9 cfs was chosen. The longitudinal slope was taken as 0.0089 so that the Froude number of the resulting flow would be in the neighborhood of unity. Then from

Figure 19 ($P/R = 13.3$) $d_{50} = 30$ mm

Figure 20 ($P/R = 30$) $d_{50} = 21$ mm

These values of d_{50} give the upper and lower limits of riprap size that will be stable in the proposed channel. In order that standard sieves could be used the d_{50} selected for the experiment was 22.2 mm (0.875 in.), the average of the 0.75-in. and 1.0-in. sieves. Then from

Figure 21 $V = 2.73$ fps

Figure 22 $R = 0.35$ ft

Figure 23 $A = 3.3$ sq ft

Figure 24 $\theta = 30°$

Figure 25 $\phi = 4.1$

Figure 26e $B = 5.75$ ft
$y = 0.44$ ft

The central 3 ft of this section could be duplicated in a laboratory channel 3 ft wide and of sufficient length to establish uniform flow. The discharge, slope, and depth for this portion of the channel cross section were duplicated in the laboratory flume. The test discharge in the laboratory flume corresponding to the design discharge was 4.6 cfs and was determined on the basis of equal bed shear intensity in the prototype and laboratory channels. In the same way, a portion of the 4:1 side slope was duplicated in the channel. For this condition the test discharge was 1.18 cfs, determined on the basis of equal shear in the model and the prototype. The experiments on the flat bed were designated Series I; those for which the side slope was installed were designated Series II.

In the design procedure the riprap material is characterized by its geometric mean size, d_{50}, without regard to its gradation. In practice it might be expected that riprap materials of a prescribed effective size, d_{50}, might have gradations covering a rather wide range. In these experiments it was proposed to use riprap material of three gradations, all having the same effective size. Relatively uniform material was obtained by separating a mixture of gravel between the 0.75-in. and the 1.0-in. sieves. This material had a standard deviation, $\sigma = 1.07$. Another typical gradation was obtained through the judicious removal of the fine and very coarse particles from the gravel mixture. This gave a gradation having the same mean size but a standard deviation, $\sigma = 1.50$. The third gradation was obtained from the same mixture, but had a standard deviation, $\sigma = 2.7$. The mean size of the riprap material was $d_{50} = 22.3$ mm

(0.073 ft). The size distribution curves of these riprap materials are shown in Figure 38. The base material representing the original soil under the riprap consisted of sand having a mean size, d_{50}, of 0 42 mm (0.00138 ft) and a standard deviation, $\sigma = 1.26$ (Fig. 39).

Apparatus and Method of Measurement

The laboratory representation of the design channel was a painted steel flume 3 ft wide, 50 ft long, and 15 in. deep (Figs. 40 and 41). The Manning roughness coefficient, n, for the steel surface was found to be 0.0092, so that when the hydraulically rough riprap was in place the surface of the side walls had only a small effect on the flow pattern generated by the riprap bed. The side wall effect was eliminated for the computations to determine the effective shear. The channel could be tilted to various slopes, and provision was made for trapping particles transported from the channel. The discharge from the Mississippi River came through the laboratory system and was measured by means of a calibrated Pitot cylinder mounted in the inlet conduit. The water surface and bed profiles before and after each run were measured at 1-ft intervals along the channel center line by means of a movable point gauge that could be read to 0 001 ft. Measurements of the bed elevation were obtained by attaching an equivalent 2-in. circular plate to the point gauge The entrance and exit regions of the channel were eliminated from consideration, and only the central portion of the bed, which assumed a fairly uniform slope and depth, was selected as the test reach. The water surface and bed profiles for the design discharge are shown in Figure 42 for the Series I experiments and in Figure 43 for the Series II experiments. The energy gradient, S_e, was calculated using

$$S_e = S_w - Fr^2 (S_w - S_b) \qquad (55)$$

in which S_w and S_b are the water surface and bed slopes, respectively, and Fr is the Froude number $[V/(gy)^{1/2}]$.

Velocity profiles were taken at different sections along the channel using a Pitot tube and micromanometer. The vertical and transverse profiles for the design flow in the Series I experiments are shown in Figure 44; the equivalent profiles for Series II are shown in Figure 45.

Transverse velocity profiles for the Series II experiments were measured at a section 26 ft from the inlet for various discharges in addition to the design discharge. These are shown in Figure 46. The reason for the characteristic shape of these profiles is not readily apparent, but it may be due to secondary currents generated in the lower corner of the channel It is not clear whether such currents occur in the complete prototype channel as well.

In the case of the flat bed—Series I—the base material was placed in the channel prior to the experiments to a depth of 3.0 to 3 5 in. and screeded to the slope of the channel For the Series II experiments the base material was placed so that the transverse slope was 4:1 and the longitudinal slope was equal to that of the channel Over this the riprap material was placed at a predetermined amount per square foot of bed area Because the riprap material had a bulk specific weight of 96 pcf, a riprap layer the equivalent of one grain diameter of 0.073 ft required 7 lb per square foot of bed area. For a layer two particle diameters thick the amount was doubled. Other equivalent thicknesses were obtained in the same fashion.

The bedload transported in the model was collected in the trap at the downstream end of the flume, and after each run the mechanical composition of the transported riprap material was determined by sieve analysis.

For the first experiment in a series the flume was run at a discharge less than the design discharge of the channel. The design discharge was defined as that discharge that would produce the same boundary shear stress (maximum) as would exist in the prototype channel. The design slope and the depth of flow are approximately equal in the prototype and the model.

The experiment was run for more than 2 hr in each case, and bed elevations were determined before and after each test. The water surface was measured after the flow had become fully established. At the end of the test, if no changes had occurred in the riprap layer over the base material, the experiment was repeated at a higher discharge. Additional experiments were made at successively higher discharges until failure of the riprap layer occurred. Failure, in this sense, was defined as the occurrence of either of the following events: (1) appreciable transport of the riprap material occurred, so that the riprap layer was unstable, or (2) an appreciable amount of sand was leached out of the interstices of the riprap. In the first instance the rate of riprap transport was determined from the amount trapped at the end of the channel. For the second, the occurrence of appreciable leaching was determined as the difference in bed levels computed from the bed profiles before and after the test. The total lowering of the bed during the test is a measure of the removal of the base material.

The experimental program for Series I tests on the flat portion of the designed channel consisted of 34 runs grouped into seven series according to the nature of the riprap material and its thickness, those performed on the sloping sides of the designed channel (Series II) consisted of 36 runs grouped into six series. The results are given in Tables 4 and 5, respectively.

Discussion of Experimental Results

This discussion of the results of the experiments deals with the nature of the riprap function and the differences between layers of uniform material and layers of material having two considerably different gradations. Along with the gradation curves in Figure 38, the photos of the riprap material in place before and after the test show the great difference between types of riprap material. Uniform material, so called because of its narrow grading, is shown in Figures 47 and 48. Because the material is so uniform it is clear that a thickness of several grain diameters is necessary to prevent the flow from penetrating to the bed Figures 49 through 52 show riprap layers made up of material of the same effective size as the uniform riprap but having standard deviations of 1.5. In Figures 49 and 50 the layer is one grain diameter thick. Figure 49 shows the surface before a test and Figure 50 shows the surface after the test. The extensive leaching that has occurred is apparent. In layers of one grain thickness the particles are not suffi-

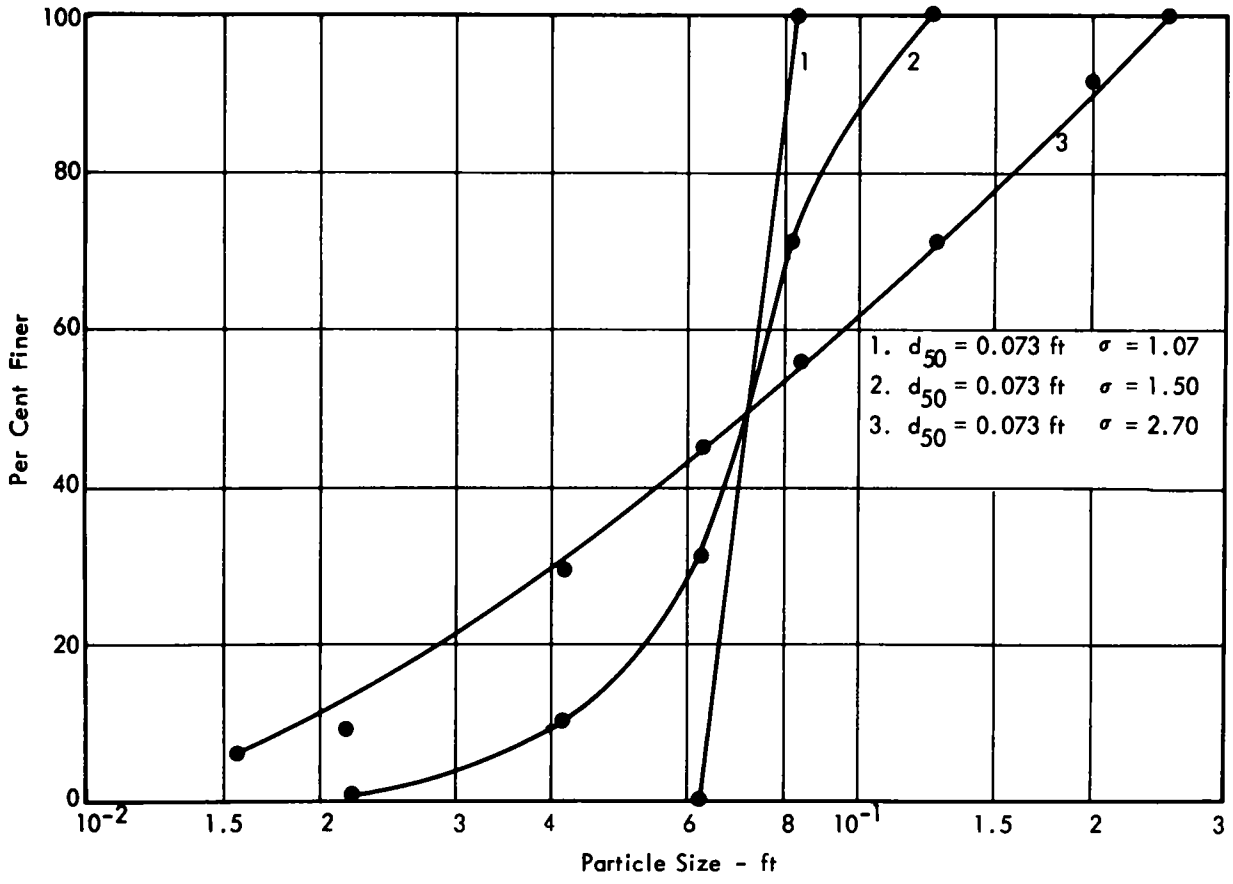

Figure 38. Size distribution of gradations used in channel stability experiments.

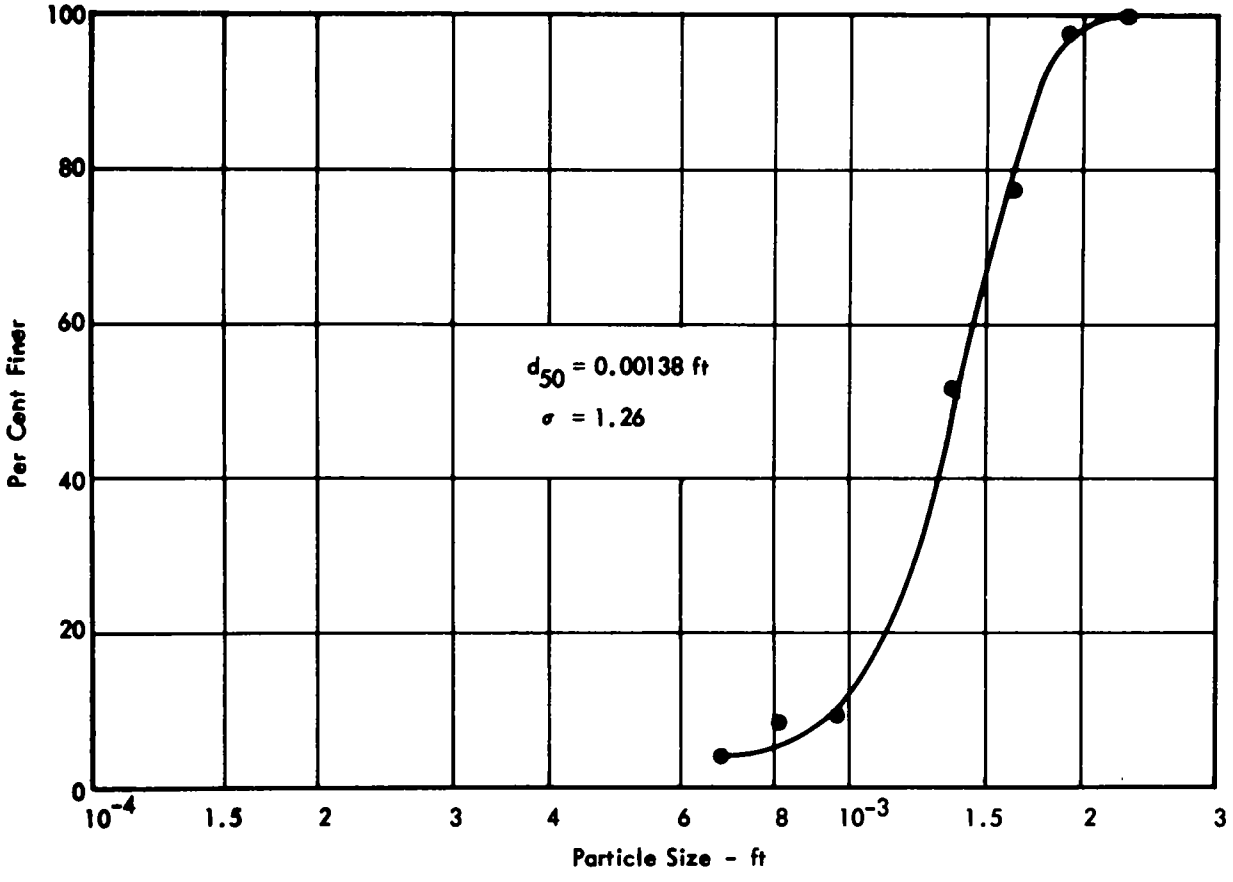

Figure 39 Size distribution of base material used in channel stability experiments

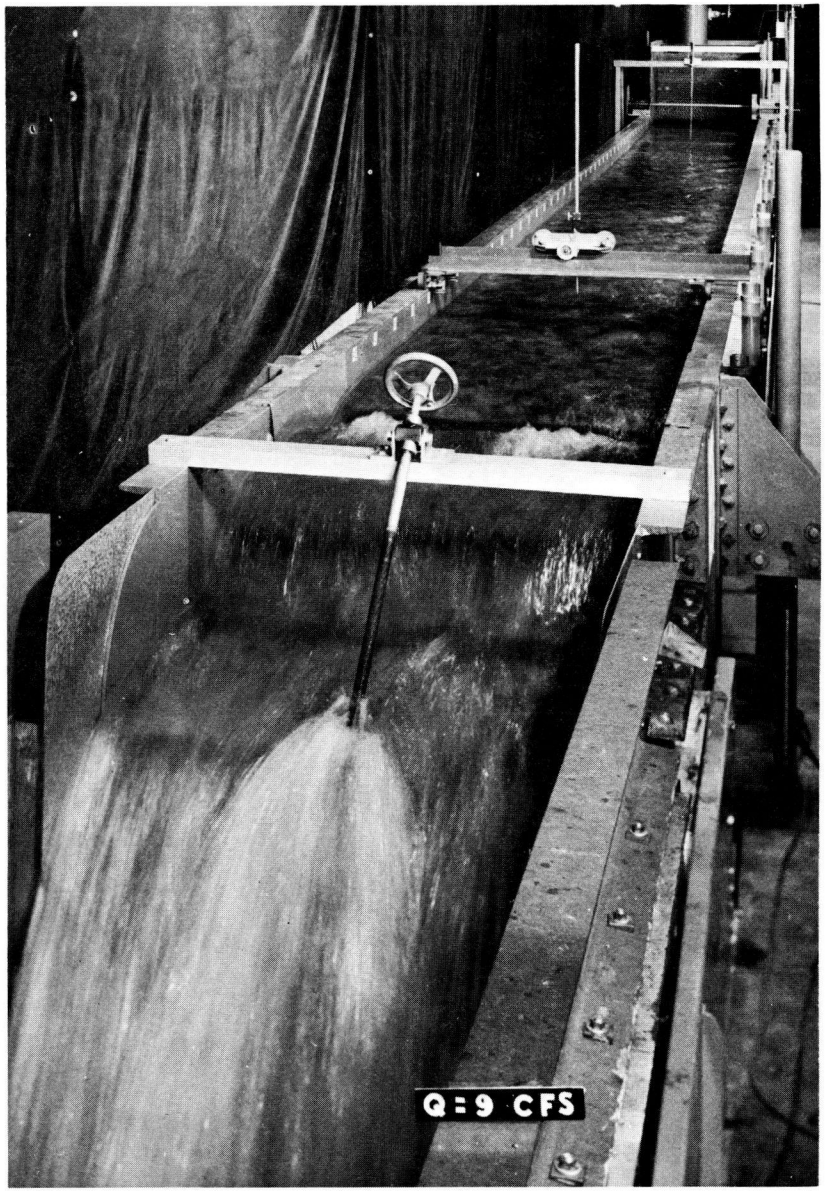

Figure 40. The flume inlet, tailwater control, and the point gauges used for measuring water surface elevations, bed elevations, and velocity profiles. This 3-ft-wide and 50-ft-long flume represents the central portion of a channel designed to convey 9 cfs at a slope of 0.0089 using riprap with $d_{50}=0.073$ ft. The flow occurring in this channel had the same depth, velocity, and boundary shear as would occur in the prototype channel. It is presumed that inasmuch as the same size of riprap and proportionate discharge were used in this channel, the flow is the same as it will be in the central portion of the prototype channel.

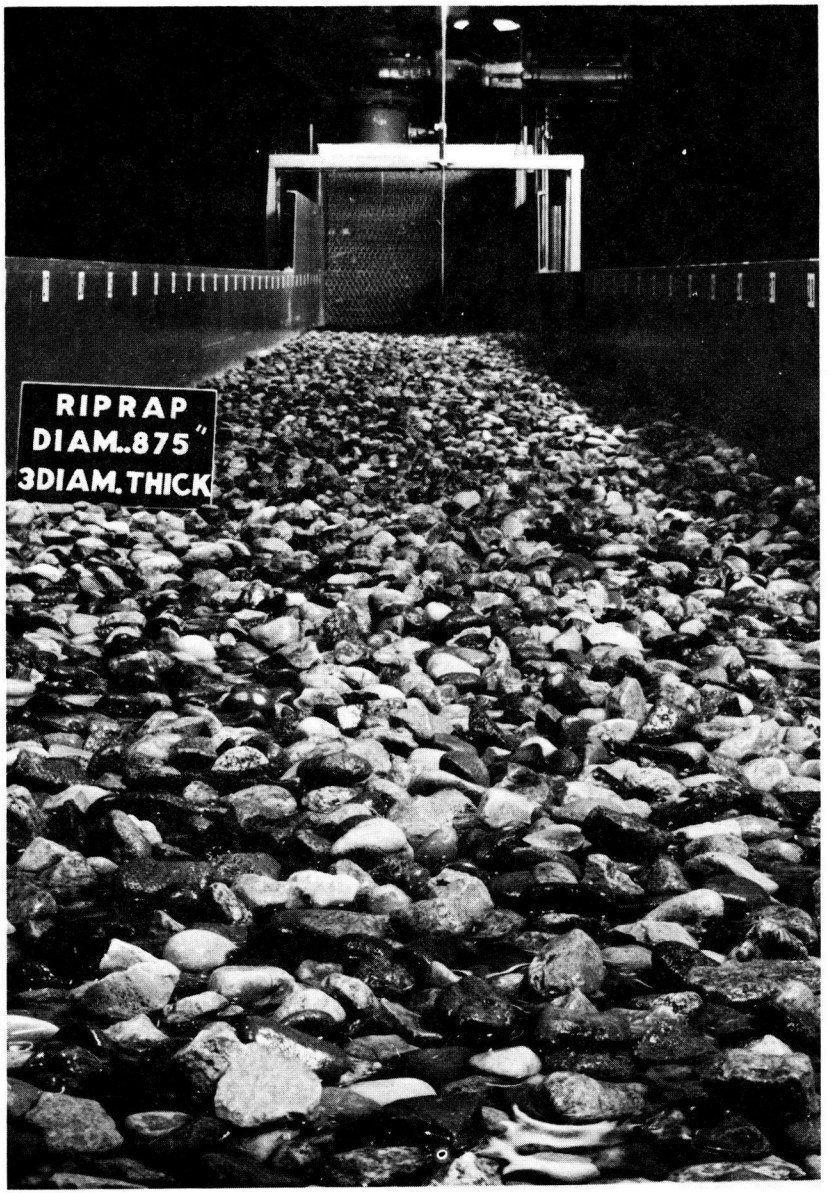

Figure 41. Characteristic roughness of a riprap layer. A uniform riprap material, effective size 0.875 in., has been placed three diameters thick on a smooth sand base.

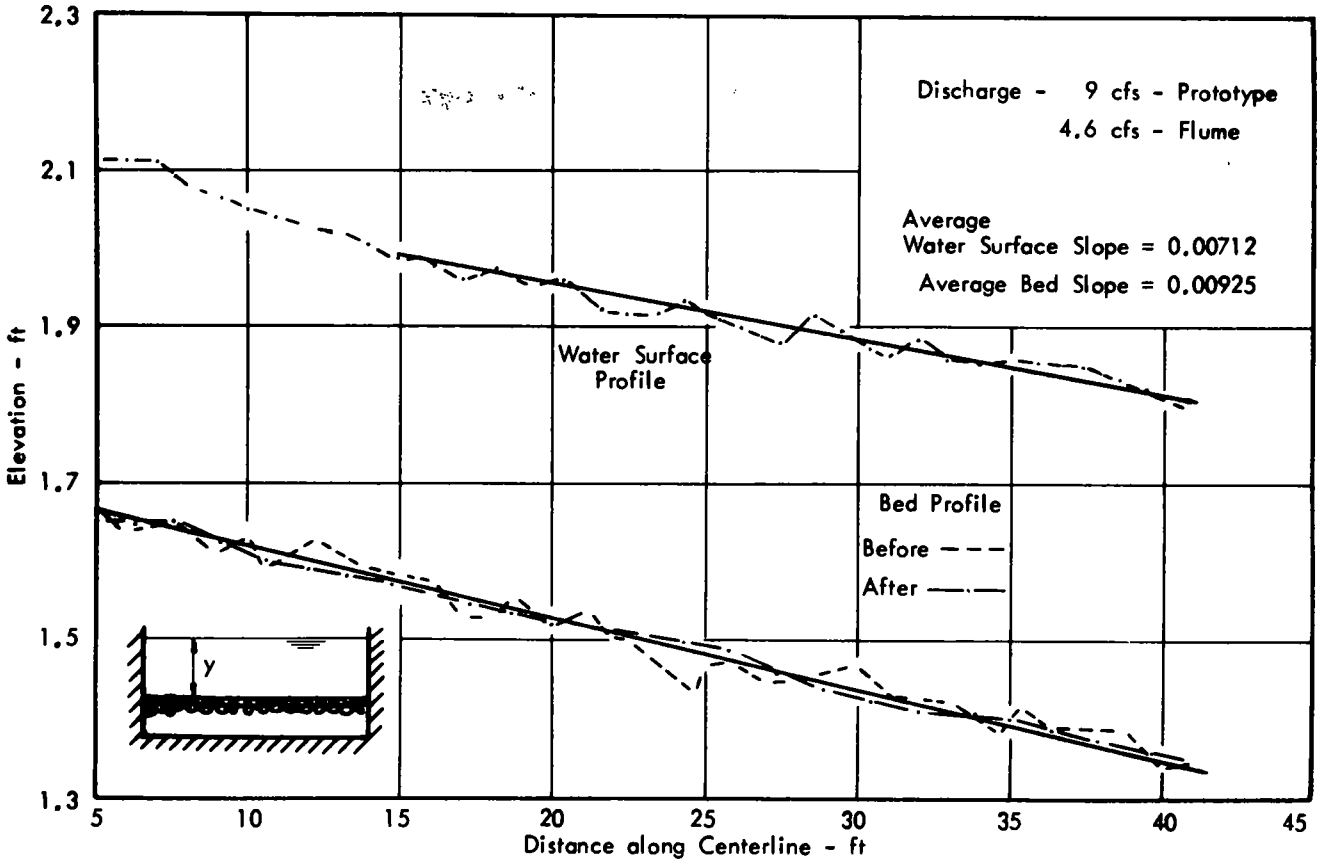

Figure 42 Water surface and bed profiles for design discharge, bottom experiments—Series I

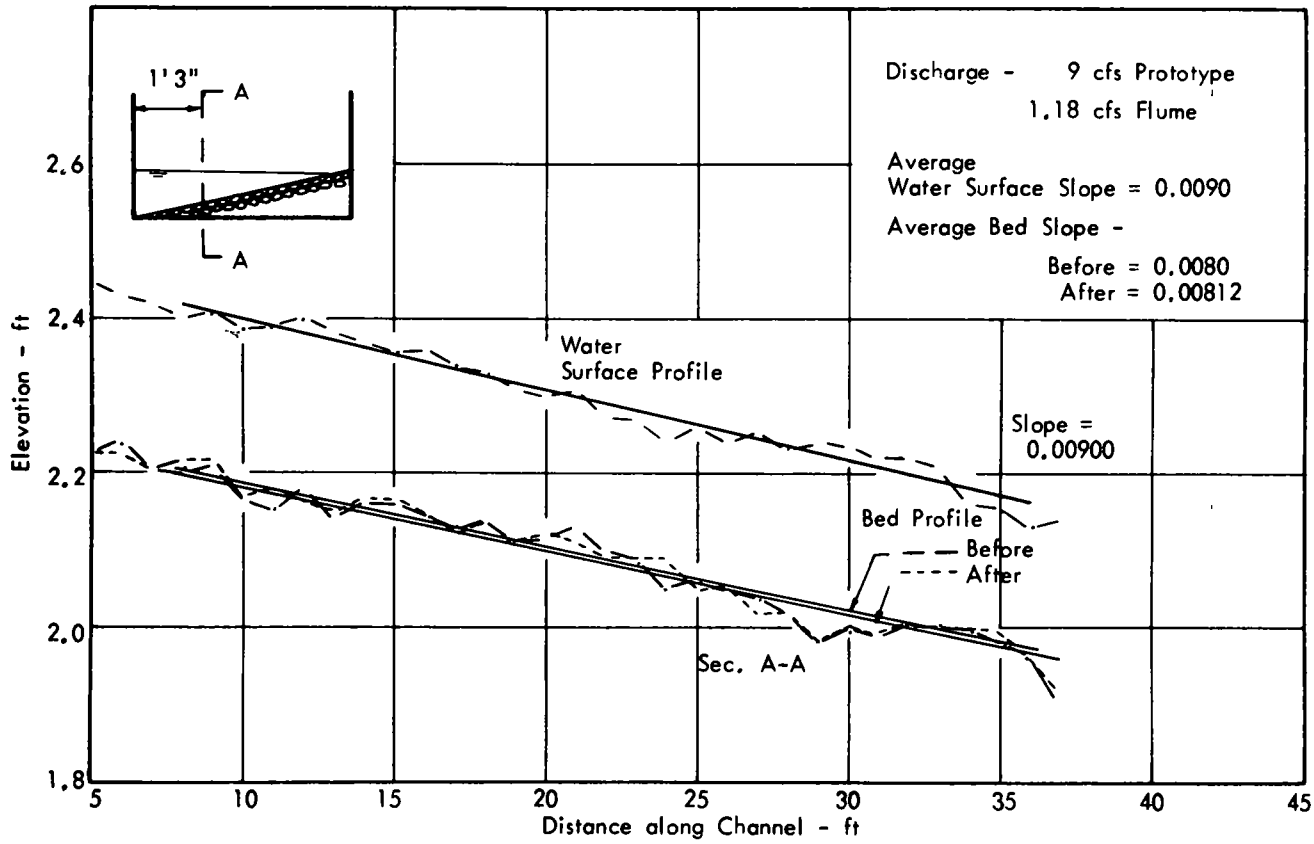

Figure 43. Water surface and bed profiles for design discharge, side slope experiments—Series II.

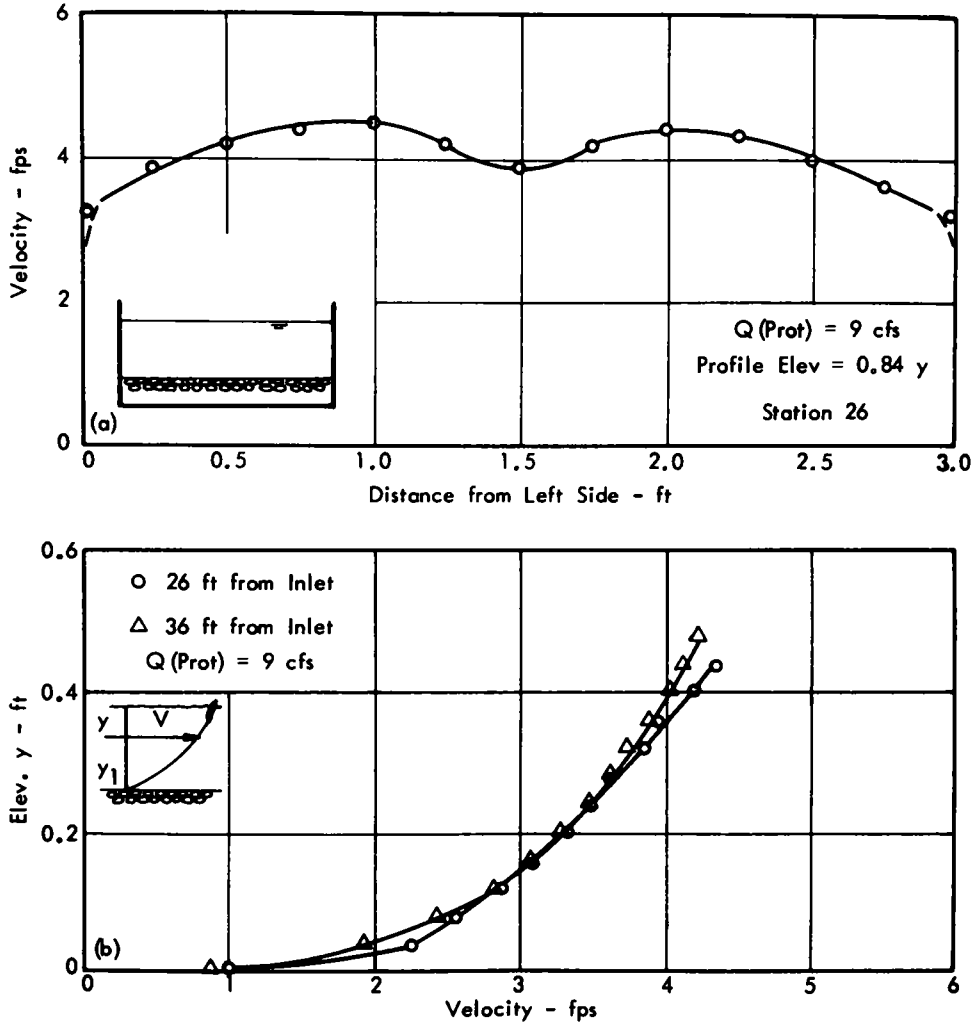

Figure 44. Velocity profiles for design flow, Series I experiments transverse velocity profile (upper); vertical velocity profiles (lower).

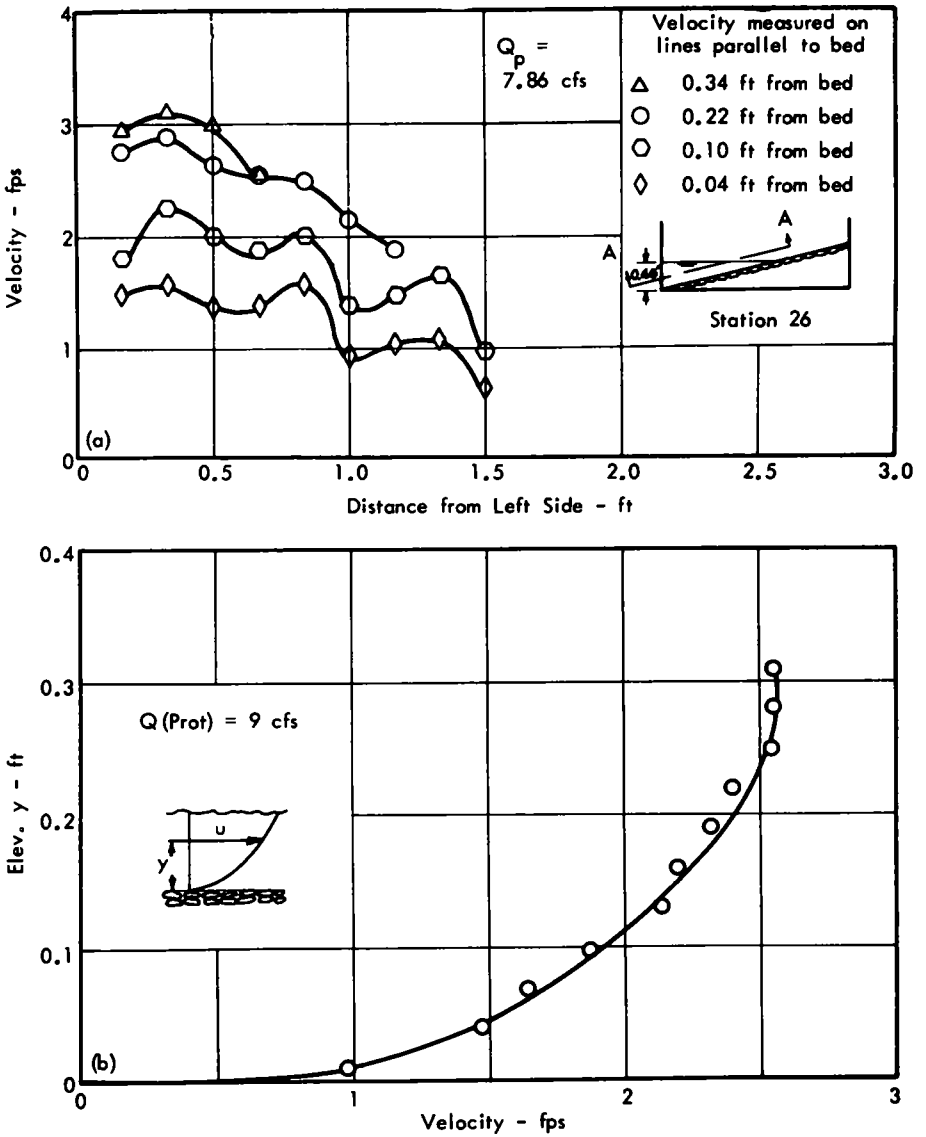

Figure 45. Velocity profiles for design flow, Series II experiments transverse velocity profiles (upper); vertical velocity profile (lower).

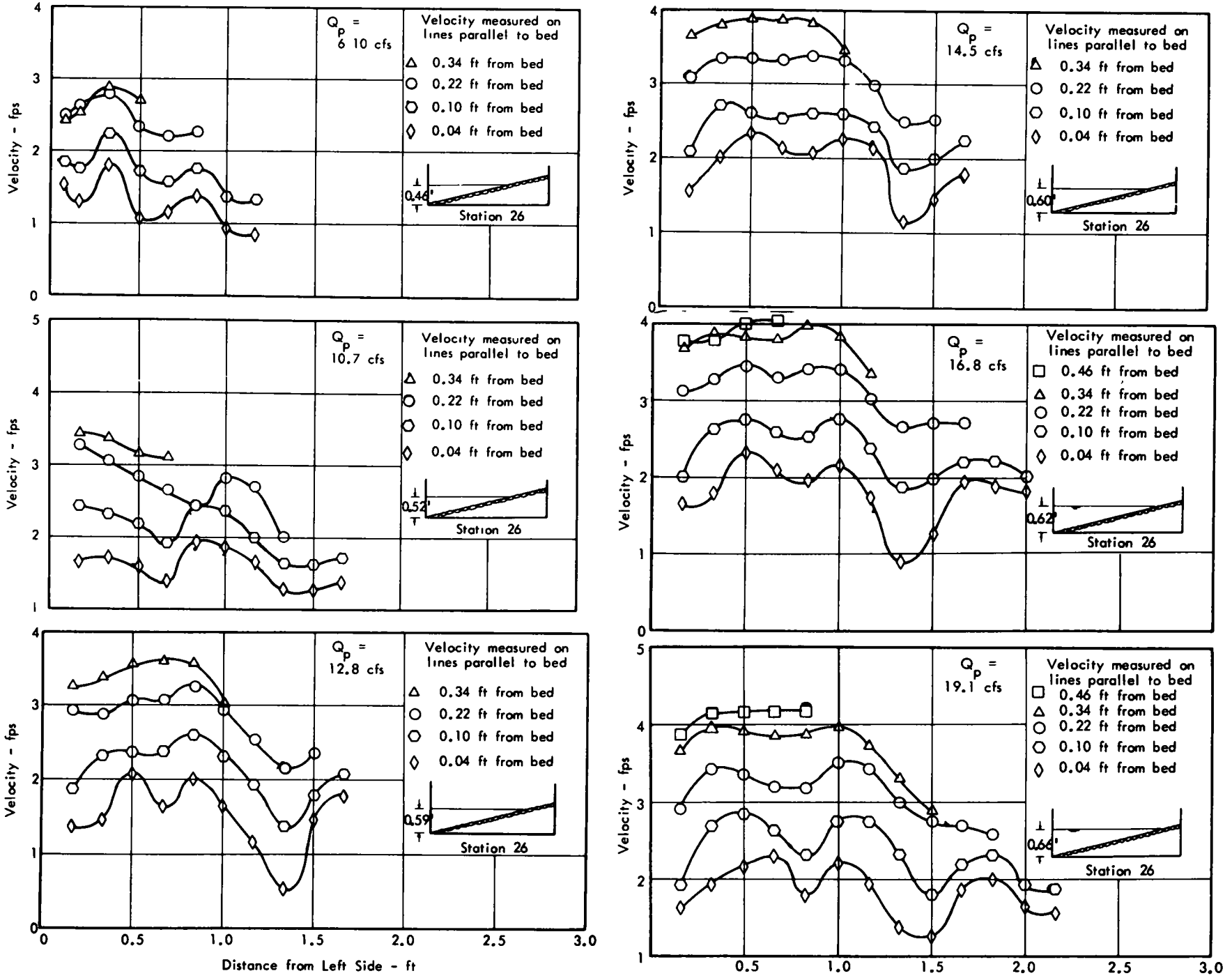

Figure 46. Transverse velocity profiles—Series II.

TABLE 4

SUMMARY OF TEST OBSERVATIONS ON STABILITY AND LEACHING CHARACTERISTICS OF RIPRAP ON FLAT PORTION OF CHANNEL

Mean diameter of sand bed material = 0.415 mm — Mean diameter of gravel riprap = 22.2 mm

Run	Riprap thickness (diameter)	σ	Q (Model) cfs	y ft	V ft/sec	Fr	S_b	S_w	S_e	τ_b lbs/ft^2	n_b	Rate of degradation ft/hour	Riprap transport rate lbs/ft/hr
A-1	3	1.07	2.5	0.315	2.65	0.82	0.00925	0.00675	0.00846	0.158	0.023	0	0.0133
A-2			3.0	0.345	2.905	0.87	0.00925	0.0074	0.0088	0.1785	0.0226	0	0.0167
A-3			3.5	0.375	3.110	0.88	0.00925	0.007	0.00874	0.195	0.0198	0	0.0103
A-4			3.9	0.41	3.18	0.885	0.00925	0.00725	0.00882	0.211	0.023	0	0.0086
A-5			4.6	0.433	3.42	0.918	0.00925	0.00712	0.00891	0.225	0.0224	0	0.0041
A-6			5.0	0.481	3.48	0.883	0.00925	0.0070	0.00875	0.244	0.0231	0	0.0218
A-7			5.5	0.49	3.73	0.938	0.00925	0.0070	0.00887	0.251	0.0222	0	0.064
A-8			6.0	0.52	3.85	0.941	0.00925	0.00725	0.00901	0.271	0.0224	0	0.077
A-9			6.5	0.535	4.06	0.976	0.00925	0.00700	0.00914	0.278	0.0217	0	0.193
A-10			7.0	0.560	4.16	0.98	0.00925	0.0067	0.00915	0.29	0.0217	0	0.196
A-11			7.6	0.60	4.22	0.96	0.00925	0.0065	0.00905	0.303	0.0222	0.00041	0.36
A-12			8.0	0.612	4.35	0.976	0.00925	0.00675	0.00912	0.309	0.0219	0.0008	0.423
A-13			9.0	0.665	4.52	0.976	0.00925	0.0065	0.00912	0.333	0.0219	0.0022	1.06[1]
B-1	1	1.5	4.6	0.48	3.2	0.812	0.00825	0.00625	0.00757	0.198	0.0226	0.16	2.88[1]
C-1	2	1.5	4.7	0.47	3.33	0.855	0.01	0.0105	0.0103	0.28	0.0264	0	0.31
C-2			4.5	0.47	3.2	0.82	0.00825	0.00925	0.0086	0.238	0.025	0	0.34
C-3			5.5	0.52	3.53	0.864	0.00825	0.00930	0.0086	0.259	0.024	0	0.5
C-4			6.5	0.54	3.55	0.85	0.009	0.01	0.00925	0.29	0.0252	0	0.557
C-5			7.6	0.605	4.17	0.945	0.009	0.0095	0.0091	0.307	0.0224	0.0025	1.23[1]
C-6			8.5	0.655	4.32	0.942	0.009	0.01	0.0091	0.323	0.0091	0.0091	2.25[1]
D-1	3	1.5	4.6	0.47	3.26	0.838	0.0095	0.00825	0.0088	0.241	0.0248	0	0.58
D-2			6.5	0.575	3.76	0.874	0.00925	0.01	0.00943	0.313	0.0223	0	4.38
D-3			8.5	0.63	4.5	1.0	0.00950	0.012	0.0095	0.342	0.0222	0	16[2]
E-1	1	2.7	4.6	0.495	3.09	0.775	0.00875	0.007	0.00805	0.233	0.0257	0.059	7.68[1]
F-1	2	2.7	3.8	0.455	2.78	0.728	0.0085	0.00725	0.0079	0.216	0.0252	0	0.51
F-2			4.76	0.515	3.08	0.755	0.0095	0.008	0.00885	0.264	0.0275	0	0.6
F-3			5.6	0.575	3.25	0.755	0.009	0.0085	0.00878	0.295	0.029	0	2.0
F-4			6.7	0.61	3.67	0.83	0.0085	0.008	0.00833	0.291	0.025	0.004	0.98[1]
F-5			7.7	0.66	3.90	0.845	0.009	0.0075	0.00856	0.322	0.025	0.004	3.9[1]
F-6			8.2	0.70	3.90	0.822	0.00875	0.00775	0.00825	0.332	0.0257	0.01	13.1[3]
G-1	3	2.7	3.6	0.43	2.79	0.75	0.00825	0.0105	0.00949	0.243	0.0286	0	1.7
G-2			4.6	0.51	3.0	0.738	0.0090	0.009	0.0090	0.270	0.0288	0	3.6
G-3			5.5	0.56	3.27	0.77	0.0090	0.01	0.00941	0.307	0.0286	0	5.1
G-4			7.6	0.62	4.08	0.915	0.01	0.01	0.01	0.352	0.025	0.02	20[2]

[1]Failure by leaching [2]Failure by riprap movement [3]Failure by leaching and riprap movement

TABLE 5

SUMMARY OF TEST OBSERVATIONS ON STABILITY AND LEACHING CHARACTERISTICS OF RIPRAP ON SIDE SLOPES OF CHANNEL

Mean diameter of sand bed material = 0.415 mm													Mean diameter of gravel riprap = 22.2 mm
Run	Riprap thickness (diameter)	σ	Q (Model) cfs	y ft	V ft/sec	Fr	S_b	S_w	S_e	τ_b lbs/ft^2	n_b	Rate of degradation ft/hour	Riprap transport rate lbs/ft/hr
H-2	3	1.07	0.346	0.330	1.58	0.485	0.009	0.0085	0.00867	0.0741	0.023	0	0
H-3			0.584	0.375	2.08	0.597	0.009	0.0088	0.00887	0.0931	0.0206	0	0
H-4			0.800	0.420	2.28	0.621	0.009	0.00875	0.00885	0.1038	0.0202	0.00000637	0.0253
H-5			1.03	0.460	2.42	0.630	0.009	0.0090	0.009	0.1165	0.0204	0	0
H-6			1.40	0.520	2.60	0.638	0.00875	0.0095	0.0092	0.1340	0.0208	0	0
H-7			1.68	0.590	2.72	0.625	0.00875	0.0095	0.0092	0.1528	0.0216	0	0
H-8			1.90	0.600	2.64	0.600	0.00875	0.0095	0.00923	0.1565	0.0238	0	0
H-9			2.20	0.620	2.86	0.641	0.00825	0.00975	0.00913	0.1590	0.0217	0.0000112	0.0444
H-10			2.50	0.660	2.88	0.625	0.0085	0.0105	0.01072	0.2020	0.0239	0	0
I-1	1	1.5	0.960	0.450	2.37	0.620	0.0095	0.00975	0.00965	0.1228	0.0246	0	0
J-1	2	1.5	0.606	0.410	1.81	0.499	0.00925	0.00925	0.00925	0.1140	0.0260	0	0
J-2			0.800	0.441	2.06	0.549	0.00875	0.00875	0.00875	0.1097	0.0231	0	0
J-3			1.00	0.480	2.17	0.554	0.0085	0.0085	0.0085	0.1160	0.0228	0	0
J-4			1.20	0.512	2.29	0.565	0.0080	0.0090	0.0087	0.1265	0.0228	0	0
J-5			1.05	0.509	2.03	0.503	0.0086	0.0086	0.0086	0.1255	0.0257	0	0
J-6			1.32	0.532	2.32	0.560		0.0088				0	0
J-7			1.515	0.564	2.39	0.559	0.0089	0.0096	0.0094	0.1466	0.0243	0	0
K-1	3	1.5	0.210	0.310	1.09	0.347	0.0090	0.0070	0.00724	0.0650	0.0321	0	0
K-2			0.275	0.330	1.26	0.388	0.0090	0.0084	0.00929	0.0396	0.0326	0	0
K-3			0.450	0.383	1.53	0.436	0.00894	0.00842	0.00852	0.0950	0.0284	0	0
K-4			0.560	0.427	1.54	0.417	0.0090	0.00896	0.00897	0.0705	0.0228	0	0
K-5			0.907	0.490	1.895	0.479	0.0096	0.00974	0.0097	0.1375	0.0288	0	0
K-6			1.12	0.525	2.04	0.496	0.00934	0.0095	0.0095	0.1430	0.0275	0	0
K-7			1.35	0.551	2.22	0.526	0.00920	0.0105	0.0104	0.1520	0.0275	0	0
M-1	1	2.7	0.065				0.00974	0.00788				0	0
M-2			0.168				0.00990	0.00812				0	0
M-3			0.258				0.00974	0.00728				0	0
M-4			0.436	0.350	1.78	0.530	0.01060	0.00764	0.008471	0.0340	0.0227	0.000046	0.182
M-5			0.525	0.3825	1.80	0.513	0.00954	0.00752	0.008053	0.0376	0.0242	0	0
M-6			0.620	0.400	1.94	0.540	0.00979	0.00778	0.008365	0.0952	0.0225	0	0
M-7			0.990	0.480	2.15	0.547	0.0106	0.00800	0.00878	0.1205	0.0238	0	0
M-8			1.24	0.570	1.91	0.445	0.0100	0.00728	0.007819	0.1070	0.0250	0	0
N-1	2	2.7	0.870	0.450	2.15	0.564	0.0089	0.00863	0.003719	0.1111	0.0224	0.0000129	0.0509
N-2			1.175	0.500	2.35	0.585	0.00905	0.0074	0.007962	0.1121	0.0209	0.000042	0.167
N-3			1.380	0.544	2.33	0.556	0.00912	0.00770	0.008140	0.1380	0.0242	0	0
N-4			1.730	0.585	2.53	0.583	0.00936	0.0085	0.008690	0.1442	0.0227	0	0

Figure 47. Uniform riprap material, showing size and shape of particles that have passed a 1-in. mesh sieve and have been retained on a ¾-in. mesh sieve.

Figure 48. Uniform riprap material as placed on the channel bed and subjected to the design flow. The effective diameter, d_{50}, equals 0.073 ft (0.875 in.). The standard deviation of this material based on the sieve limits is 1.07. The thickness of this riprap layer is equivalent to three times the effective diameter.

Figure 49. Riprap material having an effective size, d_{50}, equal to 0.073 ft but a standard deviation of 1.5. The standard deviation is a measure of the spread of the particle gradation, and the larger the standard deviation, the wider is the range of particle sizes. This is apparent by comparing Figure 49 with Figure 48. Here the layer of riprap material is only one diameter thick, so base material is exposed at various points through the interstices of the riprap.

Figure 50. Riprap bed after an experiment during which the design discharge flowed over the bed for a period of ½ hr. Because the riprap layer is so thin the sand forming the base may be rather easily picked up through the interstices and transported over the riprap layer. This results in a gradual degradation of the bed.

ciently numerous to provide protection from leaching. Figures 51 and 52 are corresponding photos taken before and after a test on a riprap layer two grains thick. The particles are more densely distributed and are relatively effective in preventing leaching, because the bed in Figure 52 is relatively free of sand

Riprap material having a standard deviation of 2.7 is shown in Figures 53 through 56 This material is characterized by a very wide range of sizes Figures 53 and 54 show the bed before and after an experiment with a riprap layer one grain diameter thick; Figures 55 and 56 are corresponding views of a riprap layer three grain diameters thick.

Figures 57 and 58 show the experimental arrangement for the Series II experiments. The portion shown represents the prototype channel side slope from the junction with the flat bottom up the 4 1 side slope beyond the free water surface In Figure 57 the riprap was the uniform grading ($d_{50} = 0\ 073$ ft) placed on the side slope to a thickness equivalent to three grain diameters. Figure 58 shows water flowing over the riprap at a discharge corresponding to the design discharge

Figures 59 and 60 show the riprap surface before and after a prototype discharge of 22 cfs (nearly 2.5 times the design discharge) had flowed through the channel It is immediately apparent from a comparison of Figures 59 and 60 that no movement of riprap particles took place and that the blanket was quite stable. Figures 61 and 62 are before and after views of the bed on which riprap of standard deviation 1.5 was placed two grains thick and which was then subjected to a flow of 9 cfs (the design discharge) for 2 hr A comparison of these photographs shows that essentially no movement took place during this test

Behavior of Uniform Riprap Material

A riprap blanket three grain diameters thick consisting of uniform material is shown in Figures 47 and 48 prior to an experiment on the flat bed. The flow was progressively increased until observable motion of the riprap material occurred. Occasional particles were observed to move at flow rates below the design discharge, for which the bed shear stress was approximately half the design shear stress. As the discharge was progressively increased, the number of particles put into motion also increased. At the discharge that produced the same shear stress as would exist in the prototype channel, the transport rate was 0 013 lb per hour. At a discharge of 9 cfs (21 cfs prototype) the transport of riprap material reached 3 16 lb per hour. In those experiments below the design discharge the mean boundary shear stress was less than the critical shear stress, so that the local shear rarely approached or exceeded the critical Because of momentary increases in local shear, transport took place even at very low mean shear values. The frequency of local excess shear increased with increasing mean shear

When an appreciable amount of riprap had been moved, the bed was exposed here and there between the interstices of the particles. This permitted the base material to be scoured from the bed and between the armoring particles by the flow or by turbulent pulsations At a discharge of 9 cfs (21 cfs prototype) the rate of degradation was 0.0022 ft per hour. At all discharges less than 9 cfs the rate of bed lowering was insignificant

In these experiments it appears that a discharge approximately twice the design discharge could be reached before failure of the riprap blanket occurred.

Behavior of Graded Riprap Material

A factor of considerable importance in the design of riprap-lined channels is the effect of the riprap gradation on the stability of the riprap blanket and its effectiveness in the prevention of leaching of the base material. Because of the average shape of the particles a layer equivalent to one grain diameter does not completely cover the whole bed. The particles on the average touch each other, but the bed is exposed through the interstices between the particles (Figs 49 and 53). In the case of the graded mixture the particles are separated from each other by a lesser distance than for uniform material As the thickness of the layer is increased, the interstices of the larger particles are filled by the smaller particles, and when the layer is greater than one diameter the particles tend to overlap and to close the interstitial spaces through which the bed may have been exposed With the increase of either thickness or standard deviation of the riprap the number of direct paths to the bed is reduced and the region of relatively high velocity is moved farther and farther from the easily eroded base material. Leaching may occur either through direct attack on the base material by the flow turbulence in which small masses of high velocity fluid may penetrate to the bed or through the development of a pressure difference between the static pressure of fluid within the bed and the lower wake pressure behind the particle As the thickness is increased these interstices are cut off, or the paths to the bed are lengthened, so that the possibility of direct attack by the flow is reduced In the case of graded riprap, because the smaller particles tend to fill the interstices between the larger particles, the thickness required to prevent the attack on the base material tends to be appreciably less than for uniform riprap material. When the boundary shear stress due to the flow over the riprap is less than the critical shear of the smaller particles in the riprap blanket, the leaching is greatly reduced. Where the shear stress on the riprap is of the order of the critical shear stress some of the riprap material that is smaller than the effective size may be transported from around the larger riprap particles, thus locally exposing the bed at many points. In such cases failure may first take place through movement of the riprap material, which in turn leads to failure by leaching. In most cases, however, the larger particles of the riprap material provide shelter for the smaller ones, and hence no movement of the base material takes place.

Transport of Riprap Material

When the material constituting the riprap blanket begins to move it is classified as bedload, and its transport at low shear stresses can be broken down into four different groups (*14*)

Figure 51. Similar to Figure 49, except that the thickness of the riprap layer is the equivalent of two diameters. It has the same effective size ($d_{50}=0.073$ ft) and standard deviation ($\sigma=1.5$). Because the layer is twice as thick, the riprap material rather effectively closes the interstices and covers the bed more completely.

Figure 52. The bed in Figure 51, after the design discharge had been flowing over it for 9 hr. Because of the increased thickness, very little sand from the base has been removed and the bed is quite stable.

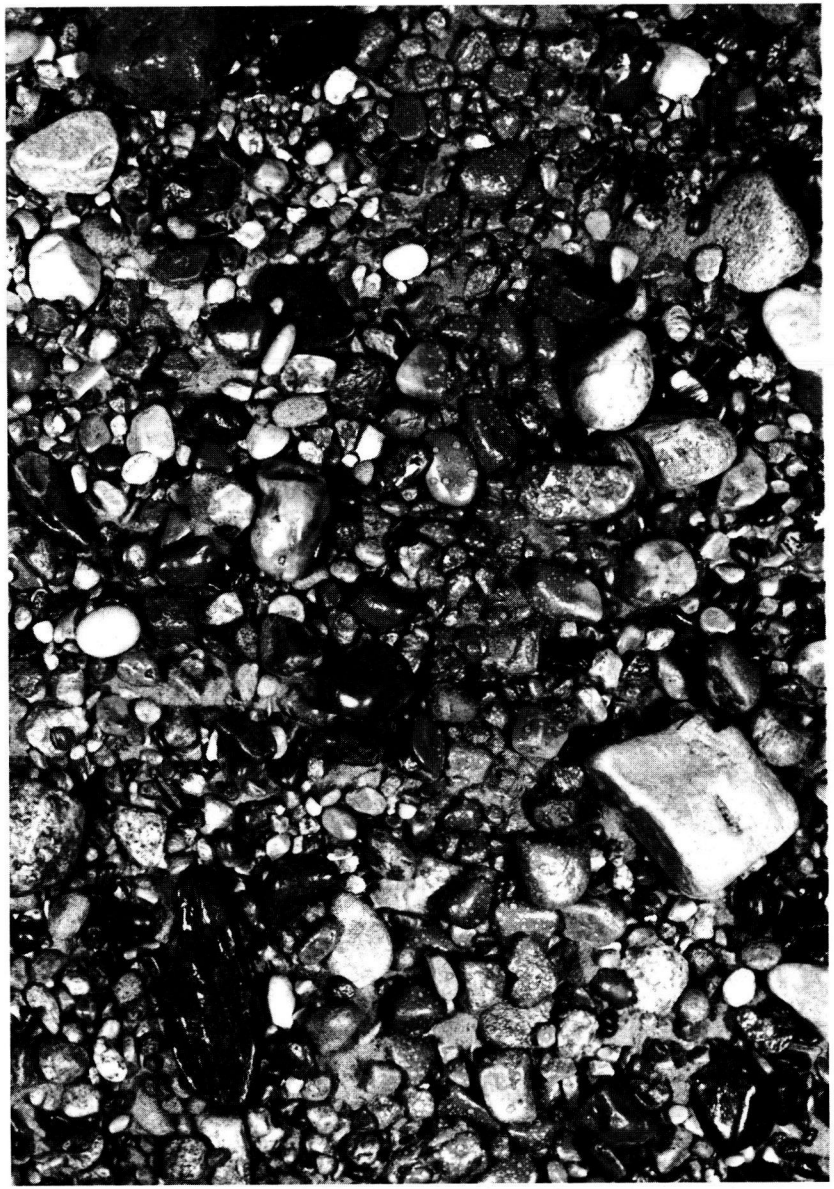

Figure 53. The bed when a riprap having the same effective size as the previous photos (0.073 ft), but with a standard deviation, σ, of 2.7, is placed on the bed prior to the test. The extreme range of sizes found in this mixture is characteristic of material with a high standard deviation. In this test the riprap layer was only one diameter thick; again, base material can be seen between the interstices at various points on the bed.

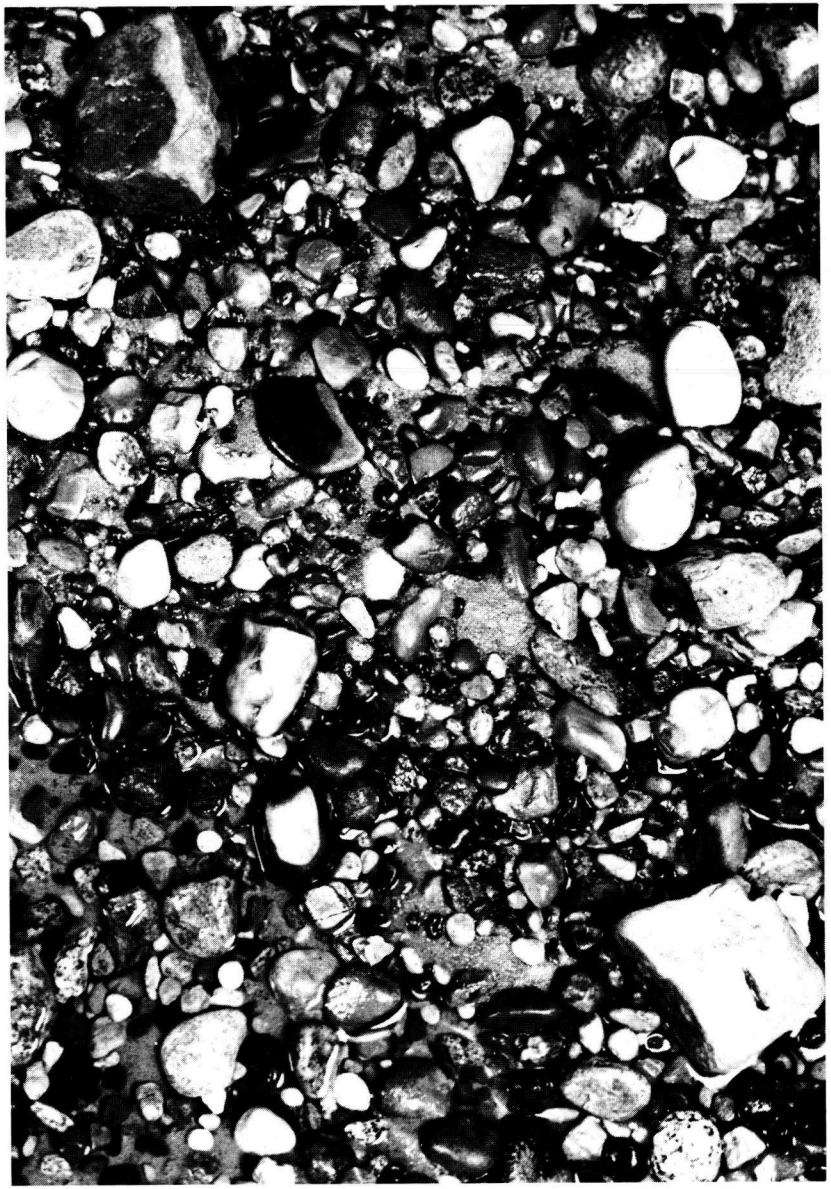

Figure 54. The area in Figure 53, but after an experiment of 51-min duration at the design flow. The larger particles appear to be undisturbed, but considerable movement of intermediate and smaller particles has taken place. The leaching of sand through the interstices by the flow is also apparent from the sand deposits on the riprap surface.

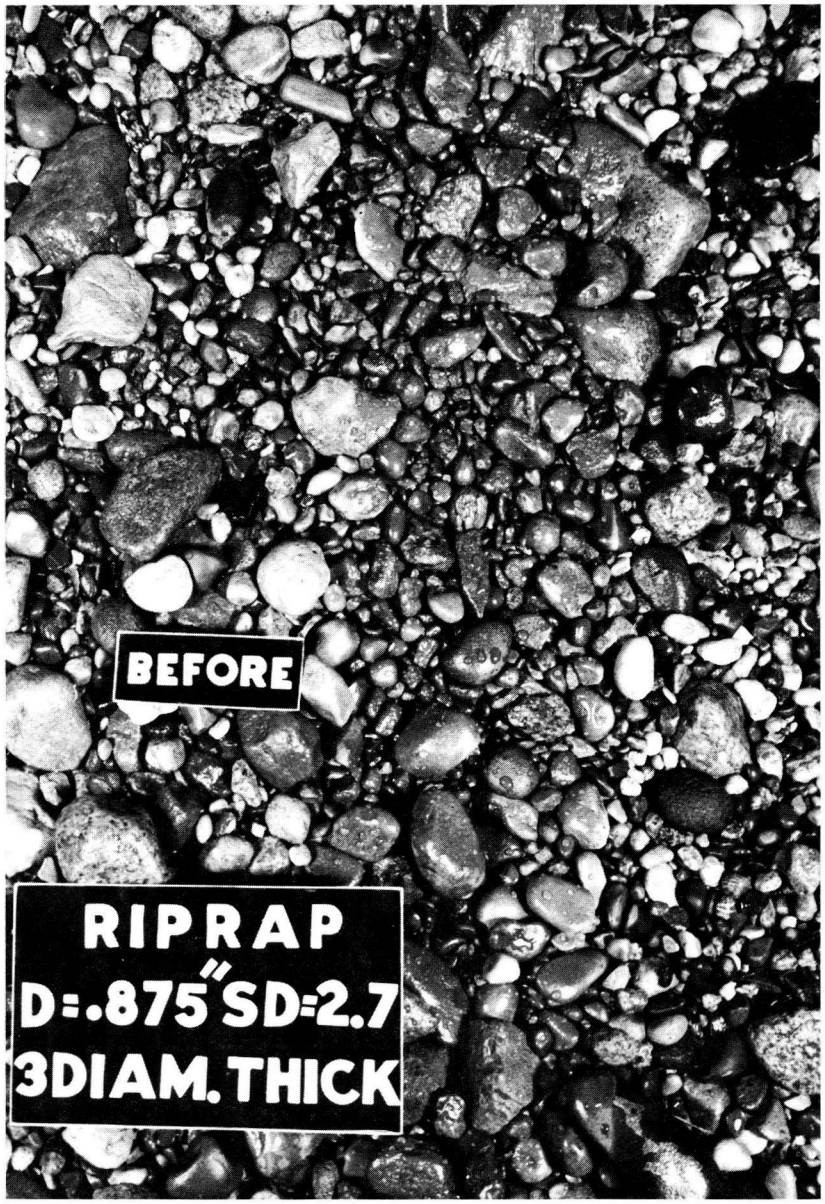

Figure 55. When the same riprap material as in Figure 53 is placed on the bed to a thickness of approximately three diameters, the bed is more thoroughly covered and all the interstices appear to be closed.

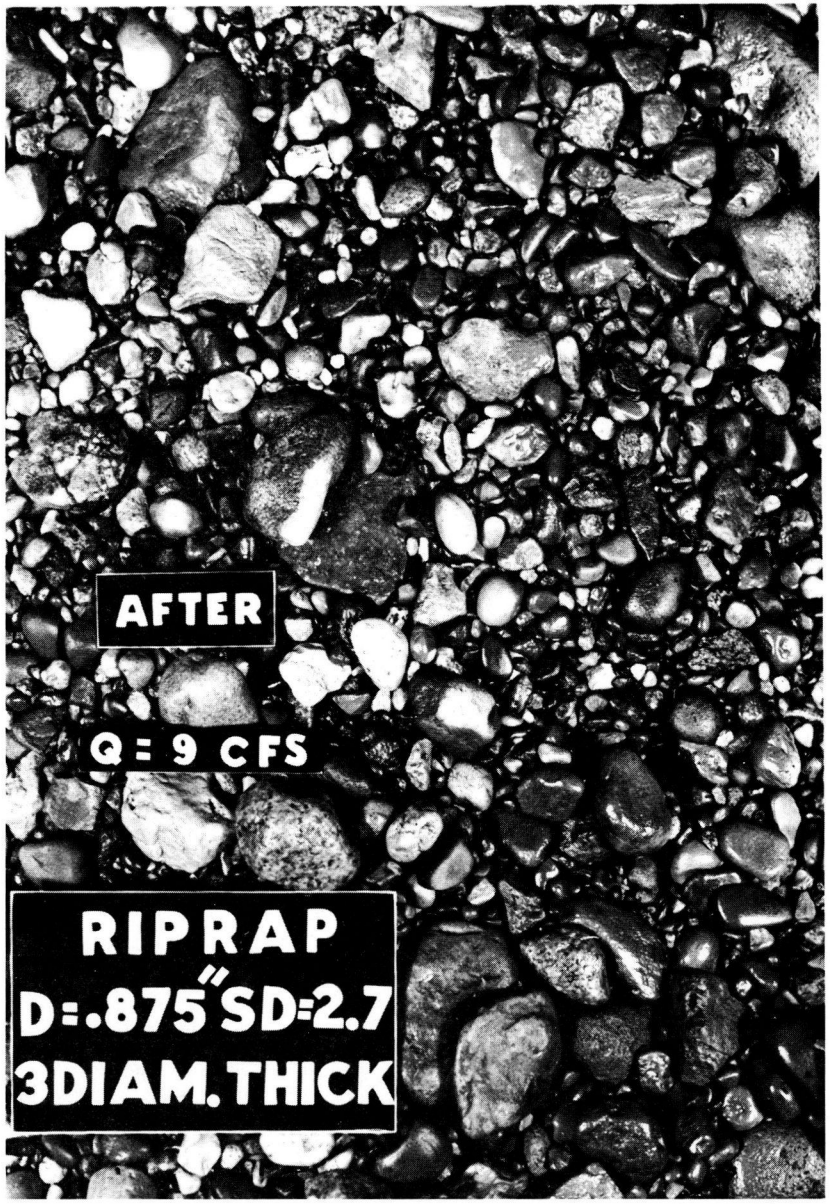

Figure 56. After an experiment of 3 hr at the design discharge, the larger particles of the riprap layer are relatively undisturbed. This thickness of protective blanket is effective in the reduction of leaching and appears to provide a stable riprap layer.

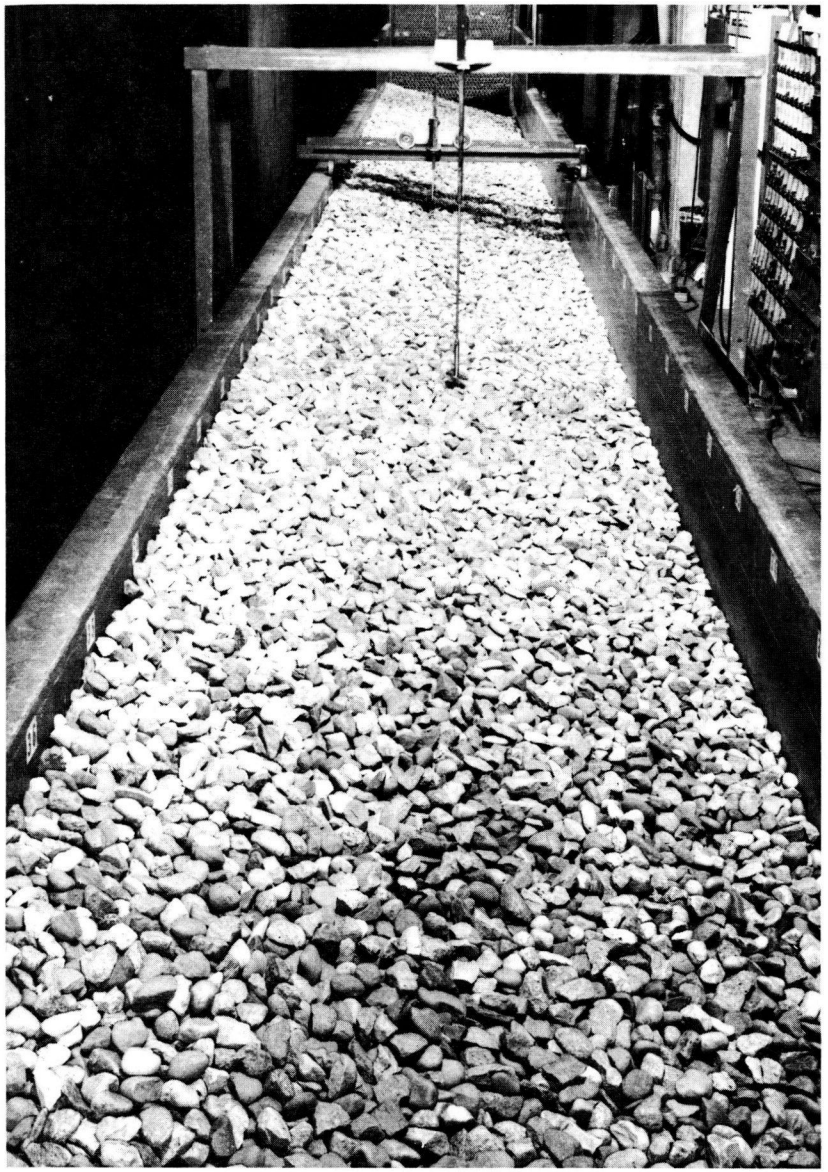

Figure 57. The downstream end of the channel, showing riprap placed on the side slope. The deepest point in the channel represents the junction with the horizontal central portion of the channel.

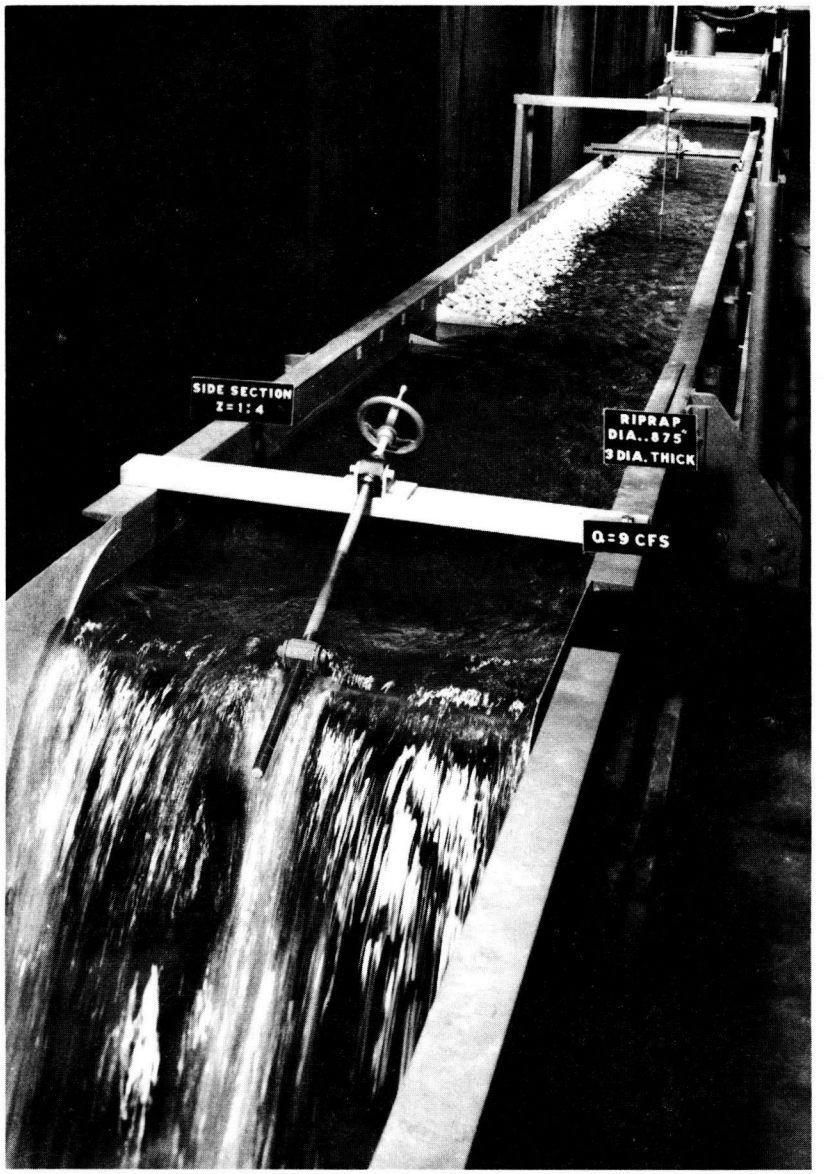

Figure 58. The flow in the channel represents that occurring over the sloping sides of the trapezoidal channel. The appropriate discharge was taken as that which provided maximum shear on the side slope equal to that which would occur in the prototype.

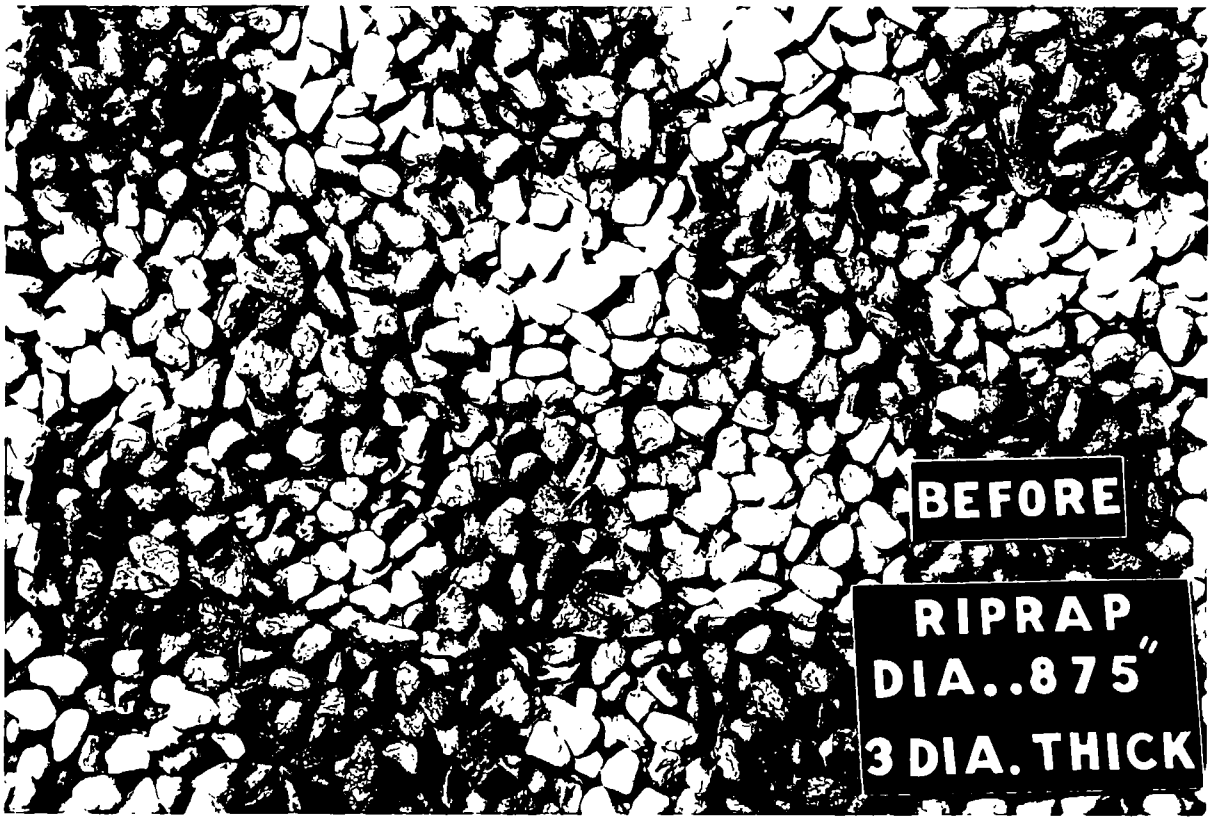

Figure 59. The layer of riprap on the 4 1 side slope is the equivalent of three grain diameters thick. With such placement the base material is apparently well protected and safe from turbulent eddies that seek to penetrate the riprap. The surface was sprayed with paint in the form of a grid to assist in locating the same point after the experiment

Figure 60 Even when the channel has been subjected to an excessive discharge there does not seem to have been any movement of individual particles on the surface.

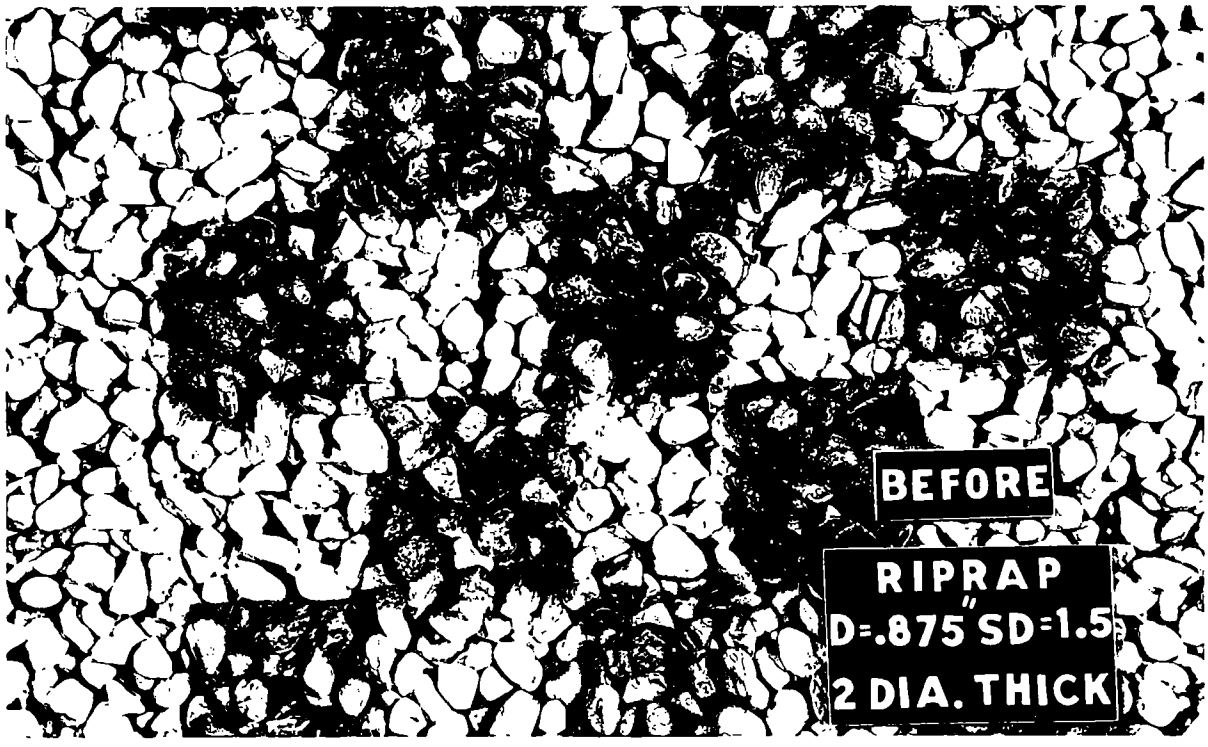

Figure 61 The bed, when the riprap is less uniformly graded before the test as the design discharge

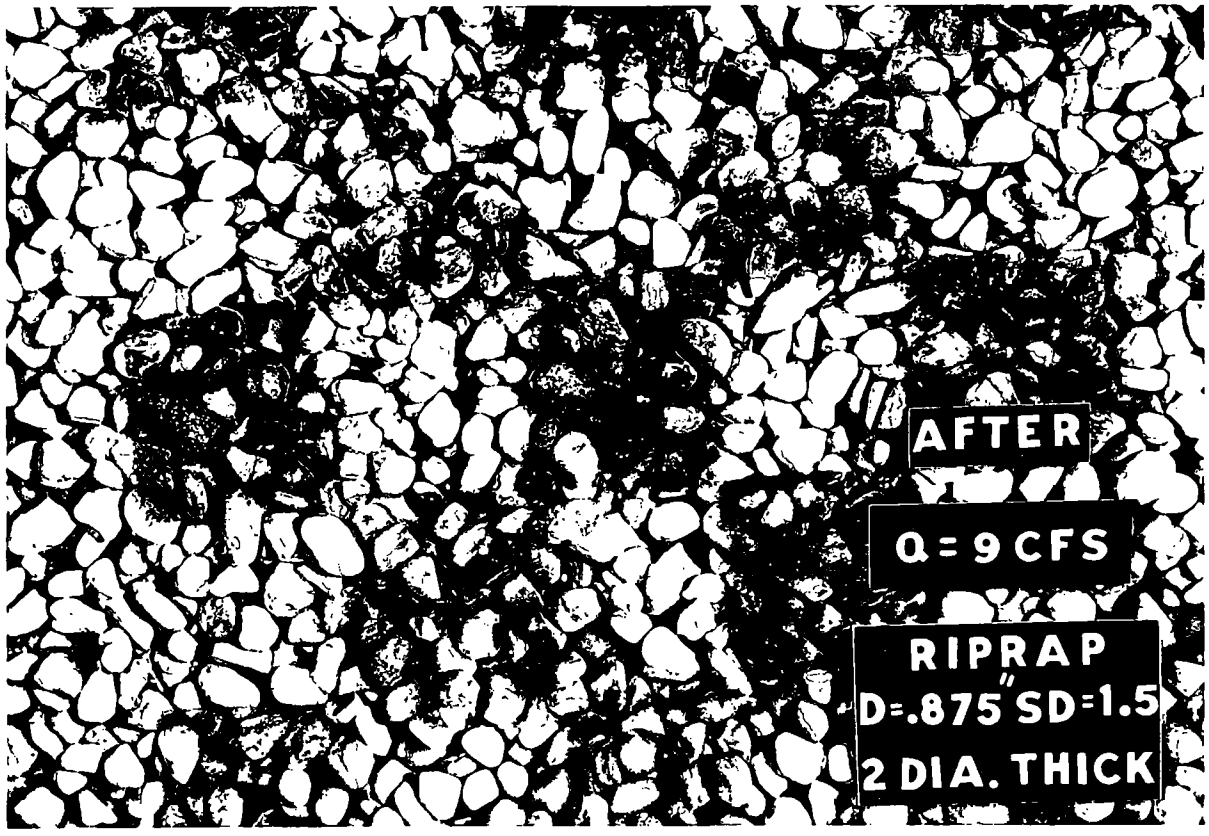

Figure 62. After the test there is no readily apparent movement, because many of the individual particles can be identified in both photos.

1. "None" refers to that condition in which absolutely no sediment particles are in motion.

2. "Weak" movement indicates that a few or several of the smallest sand particles are in motion in isolated spots in countable numbers. Countable means that by confining the field of observation the particles in motion can be counted by the observer

3. "Medium" movement is used for the condition in which grains of medium size are in motion in numbers too large to be counted. Such movement is no longer local in character but is not yet strong enough to affect the configuration of the bed and does not result in transportation of an appreciable amount of sediment

4 "General" means that condition in which sediment up to and including the largest is in motion The movement is also general in character. It is sufficiently vigorous to change the bed configuration, and an appreciable amount of sediment is transported.

Critical shear stress has been defined as that stress that brings about general movement of the bedload mixture; hence, the most important factor in the design of drainage channels is the limiting boundary shear stress to which the particles will be subjected. The values of the limiting shear to be used in channel design and critical shear stress should not be equal. In the absence of any specific experimental information it was proposed that for purposes of channel design the limiting shear stress be 80 percent of the critical shear stress. When a channel designed according to this method was tested it was found that some movement took place at shear stresses less than the critical shear stress Such bedload movement was slight and did not belong in the "general movement" category A definition of general movement proposed by the Waterways Experiment Station (*9*) in connection with hydraulic model studies where relatively fine sands were used is that rate of movement (at critical boundary shear) equal to 1 lb per hour per foot width or more This definition, however, cannot be used for gravel or crushed rock mixtures because the movement of only a few isolated particles might be sufficient to satisfy this requirement, even if the movement were not general in character In these experiments the transport rate at critical shear stress for the type of materials tested was defined as general movement when the following two conditions were satisfied (1) the material in transport was reasonably similar in composition to the material composing the bed, and (2) the rate of movement was equal to or in excess of 10 lb per hour per foot width This meant that about 3 percent of the top particles would move per hour at the so-called critical shear stress. The flow rate for which bedload transport exceeded 3 percent of the top particles of the riprap layer every hour (equivalent to 10 lb per foot per hour) was considered to be the maximum discharge for which the channel could function effectively.

Figure 63 shows the transport rate of riprap material as a function of the dimensionless shear stress, τ_*, for various thicknesses and gradations of the riprap where $\tau_* = \frac{\gamma R_b S_e}{(\gamma_s - \gamma) d_{50}}$ (see Eqs. 19 and 10). A more clearly defined relationship between transport rate and stability appears in Figure 64, which shows that riprap transport rate in terms of the prototype discharge.

Size Distribution of the Transported Material

The size gradation of riprap trapped at the downstream end of the flume is shown in Figures 65 through 70 for Series I and in Figure 71 for Series II. In each figure the gradation curve for the original material is plotted The curves show that for the riprap material for which $\sigma = 1.5$ (Figs 65, 66, and 67) the trapped material consisted almost entirely of the coarser particles of the riprap. On the other hand, the transported portion of the riprap blanket for which $\sigma = 2.7$ (Figs. 68, 69, and 70) had more of the finer particles than were present in the original riprap material. This was clearly the case for the Series II experiments (Fig 71) also. It appears that at the point at which the movement of the riprap was observed the material in motion was not representative of the mixture that was originally placed on the bed. For the riprap material for which $\sigma = 1\ 5$ it was noticed that in every instance the first particles to move were the larger ones and that as the depth was increased more of the smaller particles were put into motion. It is believed that the larger particles that protrude a small distance above the general level of the bed are acted on by a greater velocity than are the fine particles that fill the interstices and lie in between the larger particles Although this vertical distance is very small, the change in velocity near the bottom is very rapid, and a small difference in particle location causes a relatively larger difference in transporting force At greater depth, however, which is to say at greater boundary shear stress, the increase in velocity at the bottom aided by the increased turbulence of the flow appears to be sufficient to remove the finer particles of riprap

If the standard deviation of bed material is above a certain value, more of the smaller particles will be in the top layer of the riprap, in addition to those in the interstices between the larger particles. Because the majority of these smaller particles will thus not be protected against movement by the larger particles, they can be moved independently in relatively large numbers At the same time, the very large particles that are present do not move first because of their size The reason may be that the resistance to motion of a particle varies as the cube of its diameter, whereas the distance the particle protrudes above the bed and the velocity generating the forces on the particle vary as a much smaller power, probably less than unity. Hence, there must be a limiting size of particle at which the larger ones no longer move first and above which the finer particles are the first to be put into motion It may be that this critical standard deviation lies between those of the mixtures tested (1.5 and 2.7)

Manning's Roughness Coefficient, n

The Manning coefficient was determined for all the experiments The data obtained in these experiments are plotted in Figure 72, taken from Figure 5 The laboratory results show very good agreement with the curve that had been fitted to the data in Figure 5. The relationship given in Figure 77 leads to the interesting conclusion that Man-

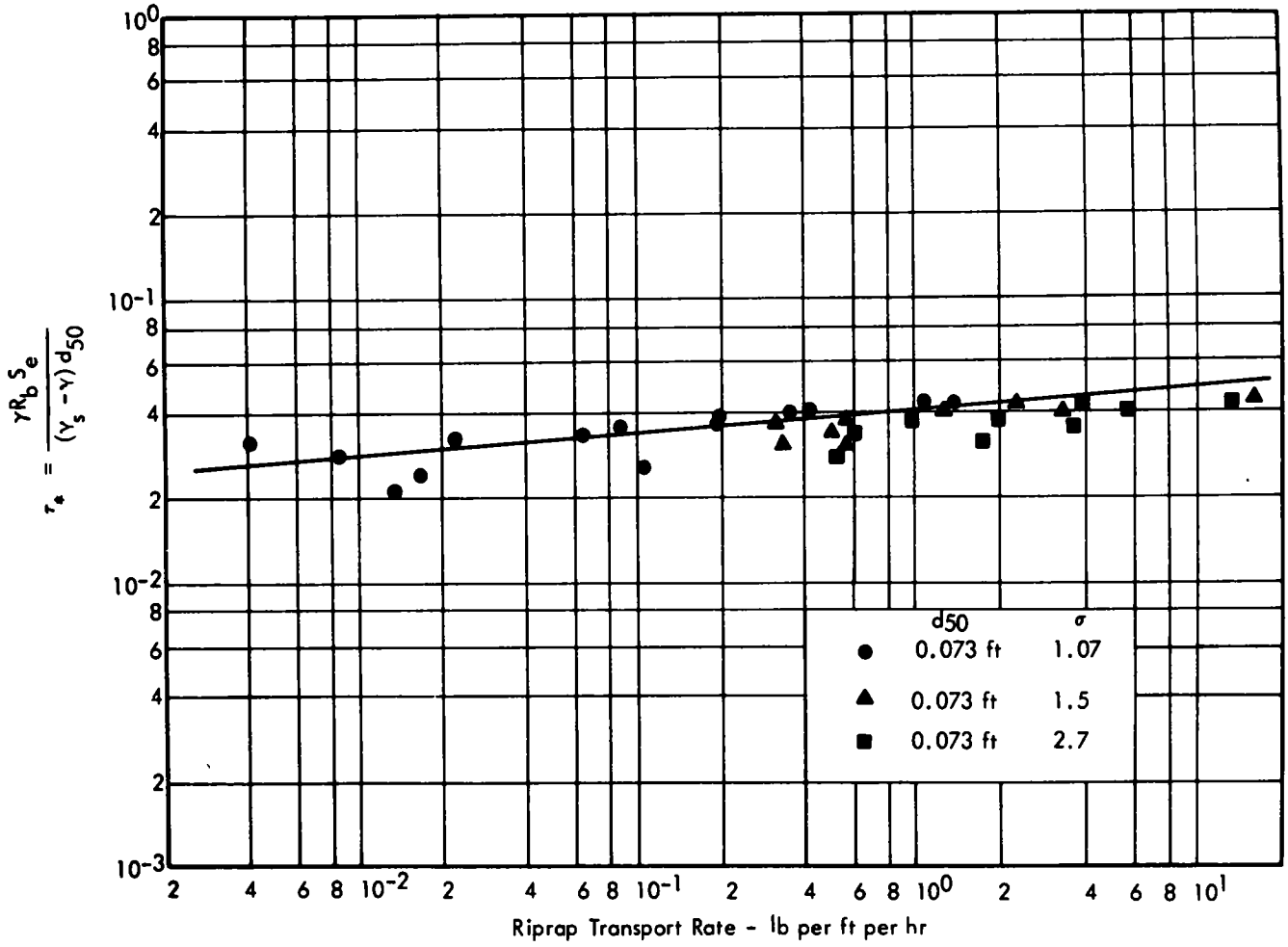

Figure 63. Riprap transport rate as a function of dimensionless shear, τ_*.

ning's n varies with the ⅙ power of the particle size (that is, $n = 0.0395\ d_{50}^{1/6}$). This means that a thousandfold change in linear measurement of the roughness height results in about a threefold increase in Manning's roughness coefficient. This relationship is shown in Figure 73, which is taken from Figure 6 and shows again a very good agreement with the original curve.

CONCLUSIONS

The results of these experiments on the stability of riprap blankets designed in accordance with the proposed design procedures suggest the following conclusions:

1. The drainage channel designed on the basis of the tentative design procedures described in this report was found to be stable with respect to leaching and riprap movement at the design discharge. For the uniform riprap material, failure occurred at a discharge approximately twice the design discharge. For the graded riprap material, failure occurred when the discharge exceeded 1 5 times the design discharge.

2. The riprap consisting of the graded mixtures has been found to be as effective as riprap consisting of uniform material. It is even more effective in the prevention of leaching, but is somewhat less stable than the uniform material with regard to movement of individual particles.

3. It appears that a layer of riprap whose thickness is the equivalent of three grain diameters is adequate to prevent leaching of sand through the riprap. The uniform and the graded riprap materials were equally effective in this regard.

4. The experiment substantiated the experimental data used in the design procedure in that the measured critical boundary shear at general movement corresponded with the data shown graphically in Chapter One.

5. The Manning roughness coefficient as measured in the experiment agreed very well with the experimental data used in developing the design procedure.

EXPERIMENTS ON THE LEACHING OF BASE MATERIAL

In the experiments on the stability of the riprap layer over which the discharge flowed, the measurement of the leaching of base material through the riprap layer was inciden-

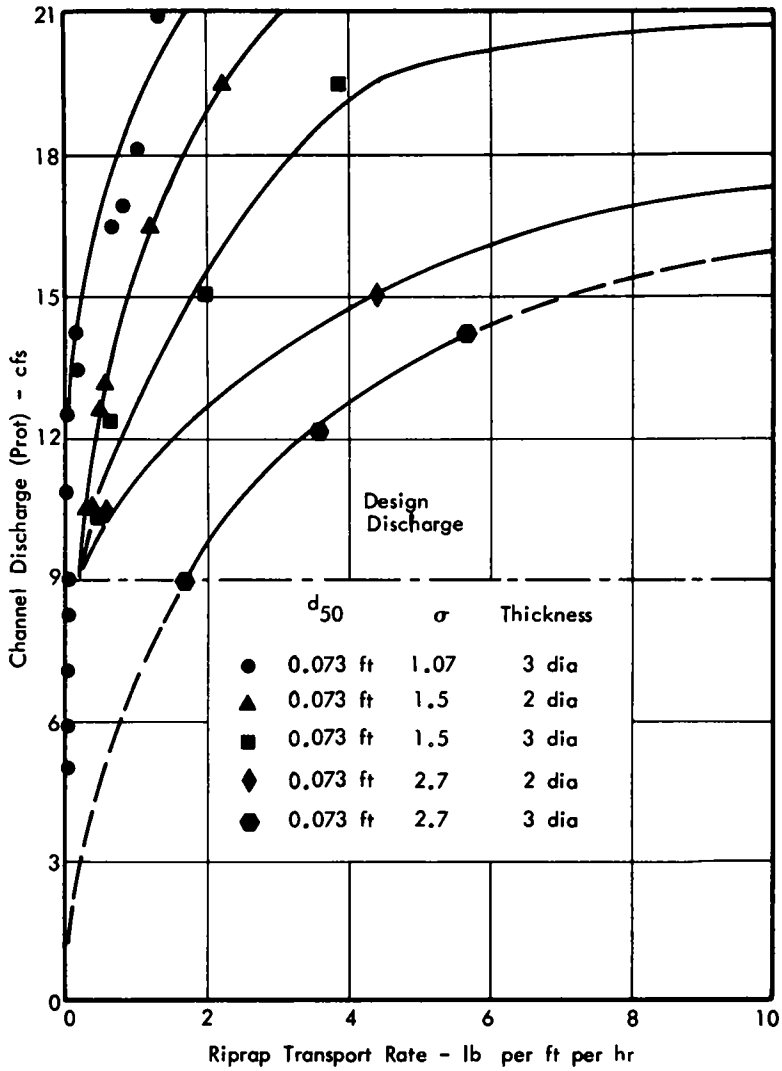

Figure 64. Rate of riprap transport in terms of channel discharge—Series I

tal to the primary study of stability. A special study was undertaken to relate the properties of the riprap layer to the rate at which base material was removed from the bed.

A riprap or protective layer may be formed on a sand bed by selective erosion that exposes coarse particles in the bed mixture, or by the actual placement of sufficiently large particles on the bed to cover and protect the sand. The formation of a protective layer by selective erosion hinges on the presence of a sufficient number of coarse particles in the bed mixture, so that as the bed is degraded these coarser particles will form the nonerodible layer (*37*) (*38*). The position of the final protective layer will depend on the equilibrium between the sediment complex and the concentration of the nonerodible particles in the bed mixture. If the final or equilibrium level is prescribed, however, as in the case of drainage channels, then it is necessary to artificially place the riprap layer of sufficient thickness on the bed so that it will be stable and leaching will be prevented.

These experiments deal with the leaching through riprap blankets of various compositions placed on the surface of the base material.

Experimental Apparatus and Measurements

These experiments were conducted in a glass-sided flume 1 ft wide, 2 ft deep, and 30 ft long. The flume was equipped with apparatus for measuring rates of transport, the discharge of water, and the water surface and bed elevations.

The base material consisted of a relatively fine sand for which $d_{50} = 0.5$ mm and the riprap layer was represented by gravel for which $d_{50} = 5.2$ mm (Fig. 74). The bed of the flume was covered by a layer of the sand base material to a thickness of about 2.5 in. The surface of the sand was carefully smoothed to the channel slope of 0.001 by means of a metal screed mounted on the measuring carriage. The riprap layer was formed by uniformly covering the sand bed with gravel. The relative thickness of the layer in terms of the effective size of the riprap could be varied by pre-

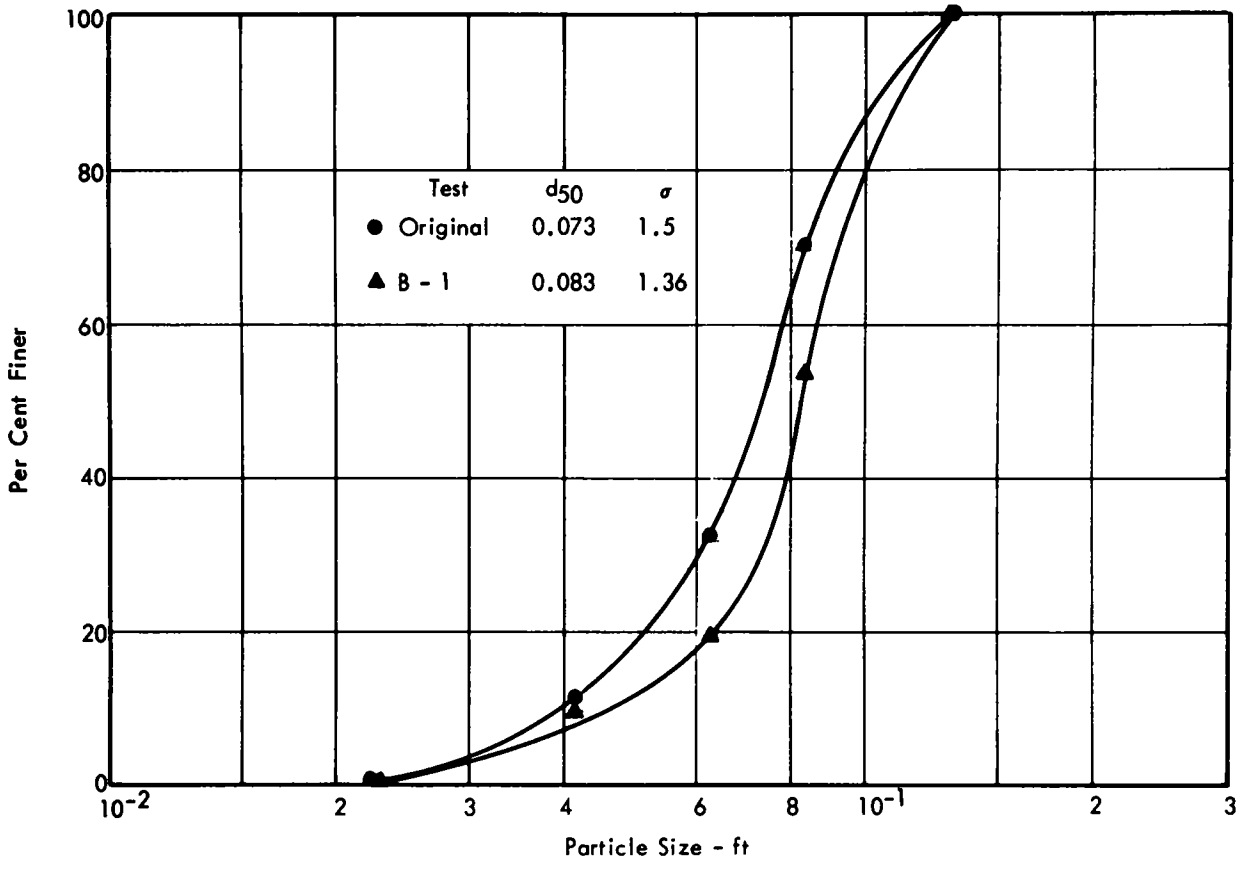

Figure 65. Size distribution of transported riprap (B series—Series I)

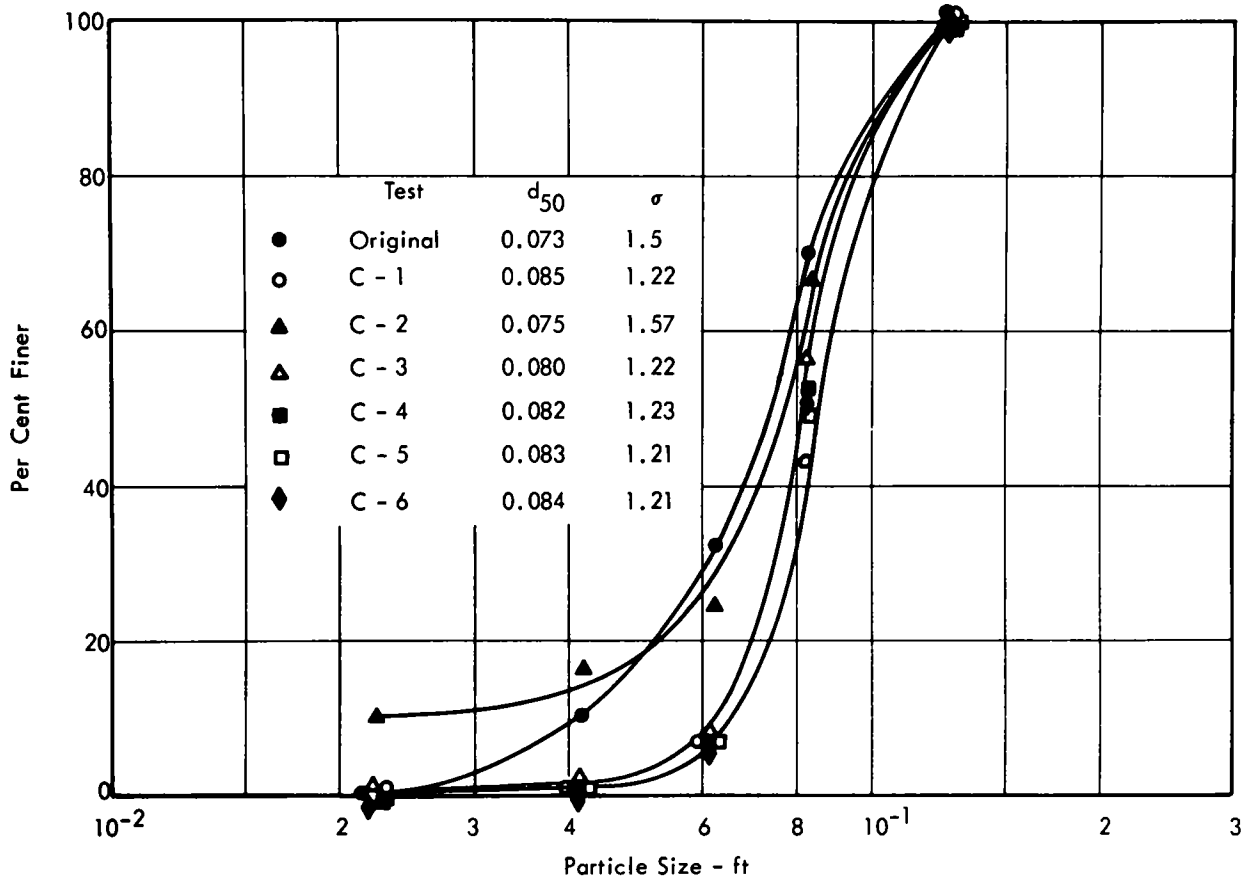

Figure 66. Size distribution of transported riprap (C Series—Series I).

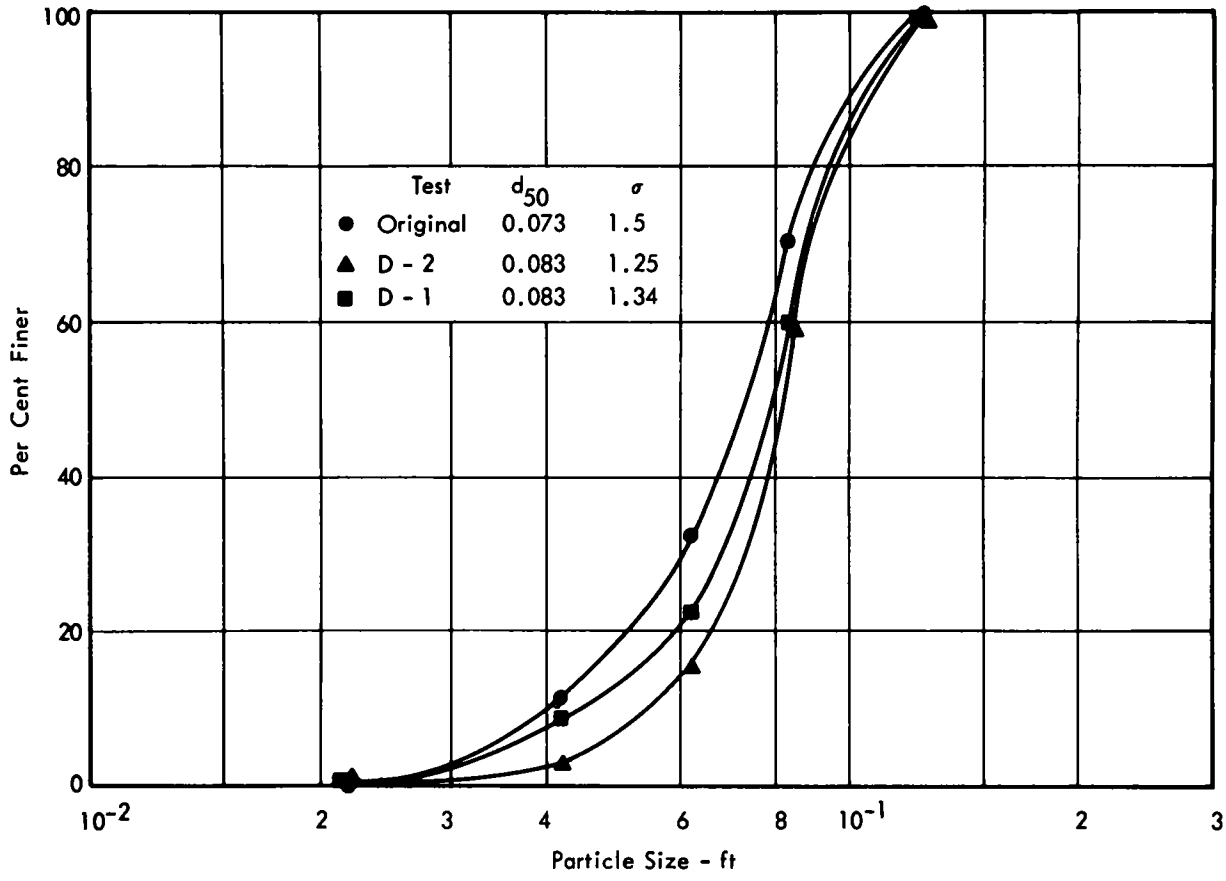

Figure 67. Size distribution of transported riprap (D Series—Series 1)

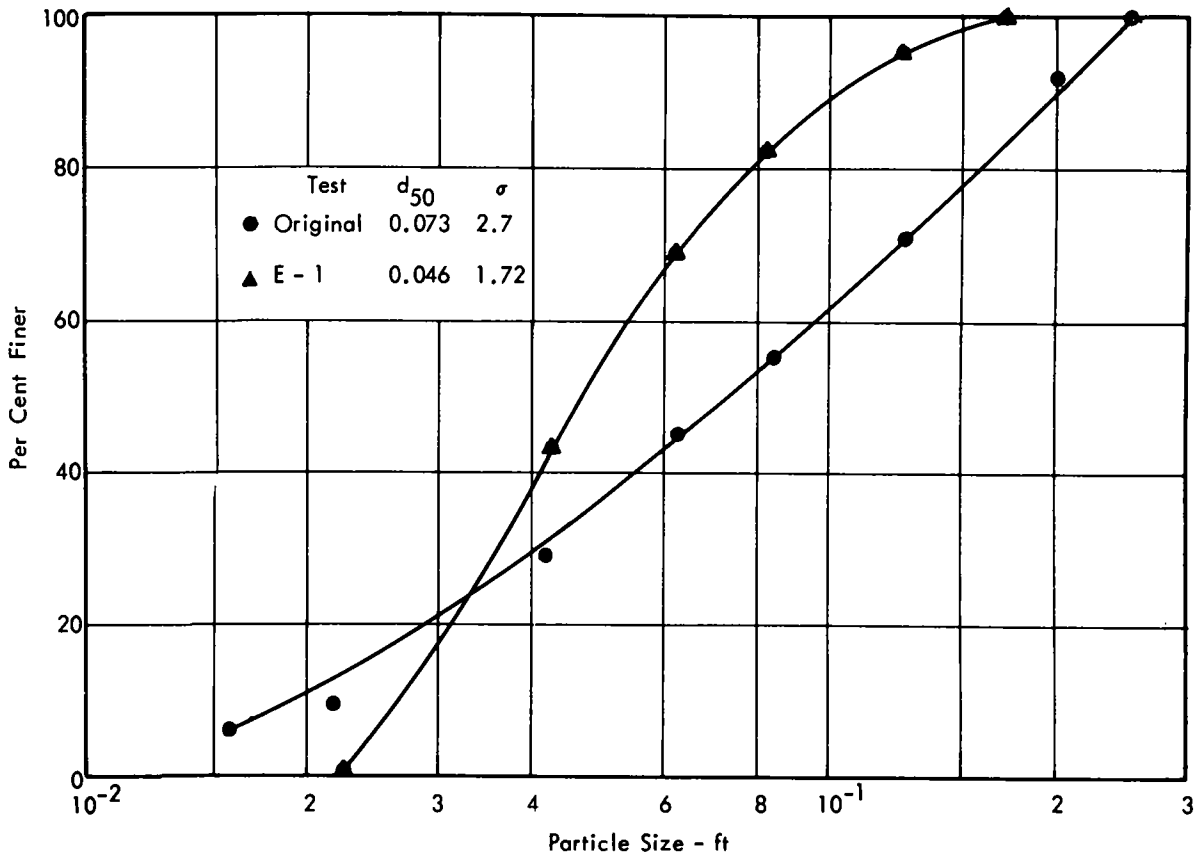

Figure 68 Size distribution of transported riprap (E Series—Series 1).

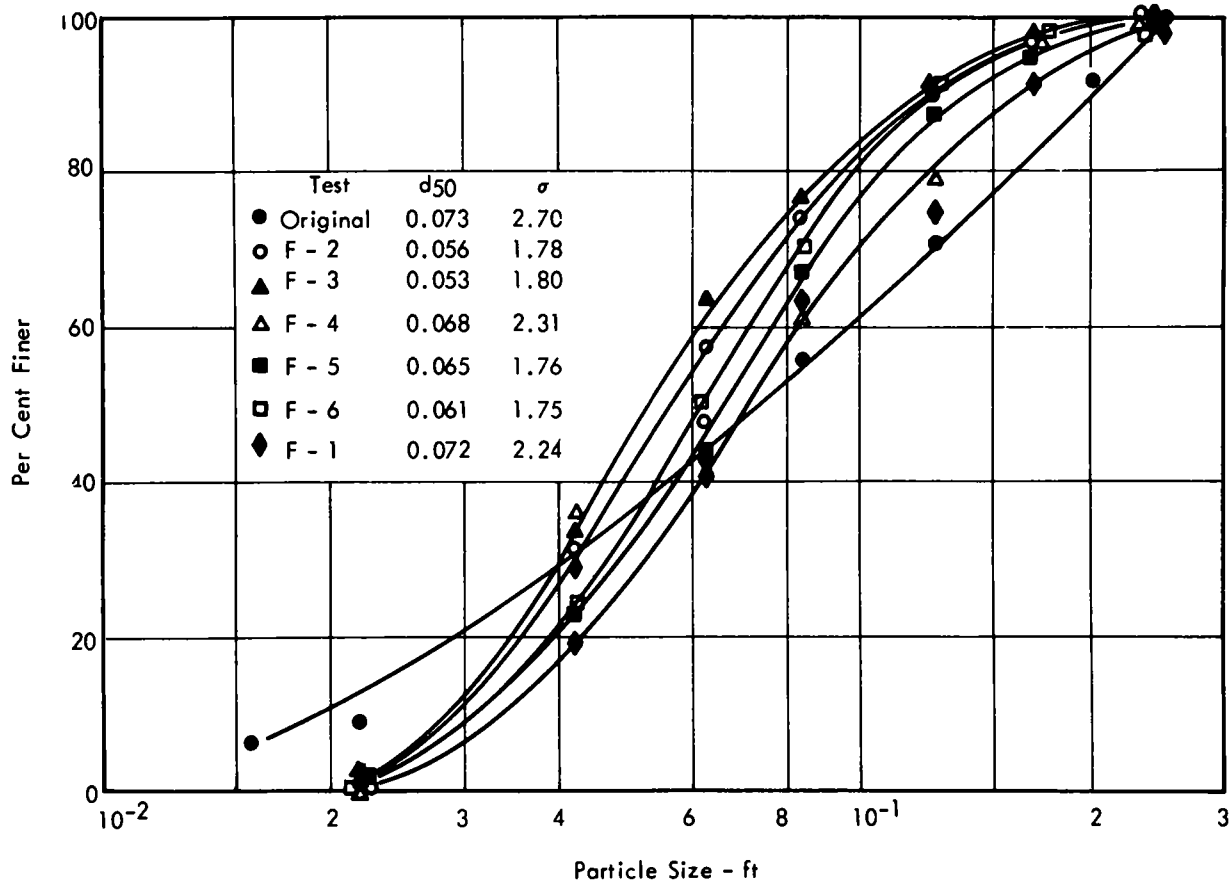

Figure 69. Size distribution of transported riprap (F Series—Series I)

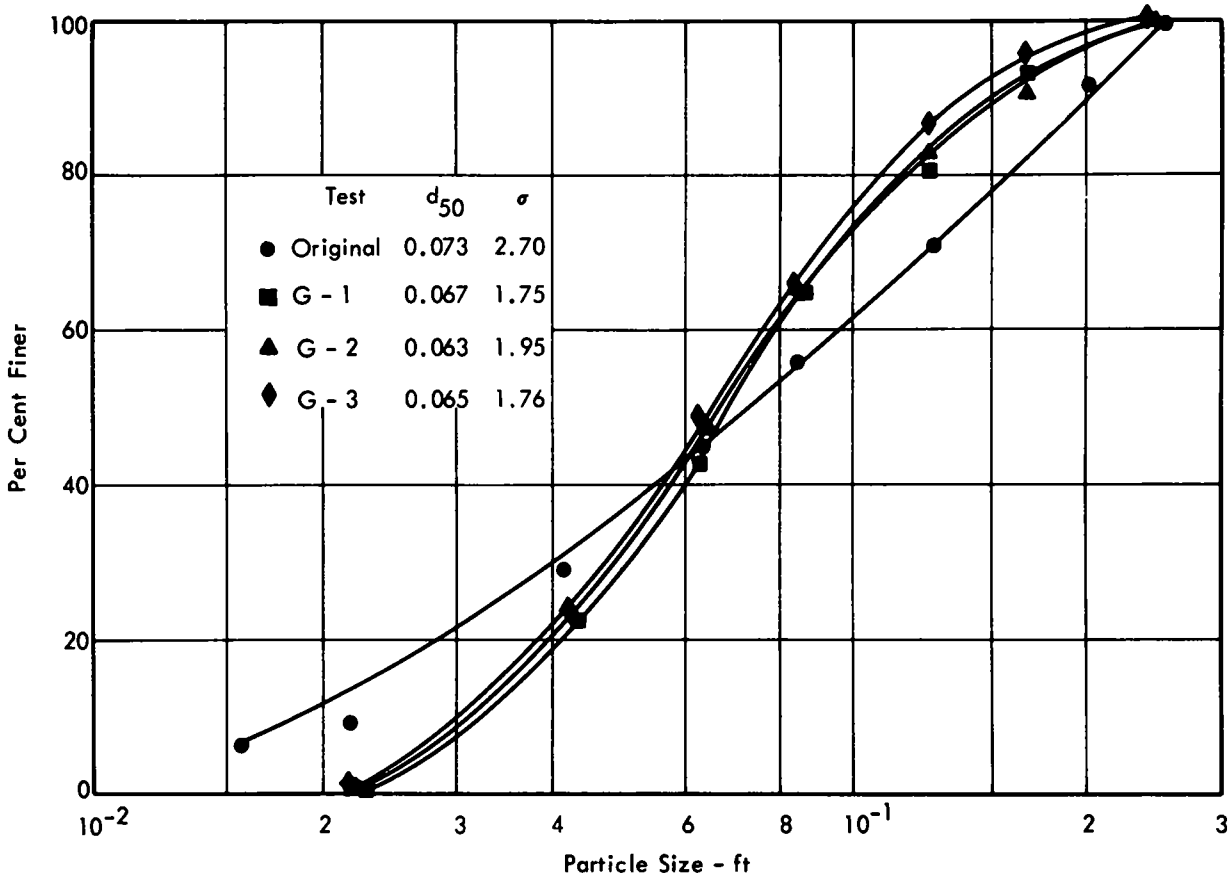

Figure 70. Size distribution of transported riprap (G Series—Series I)

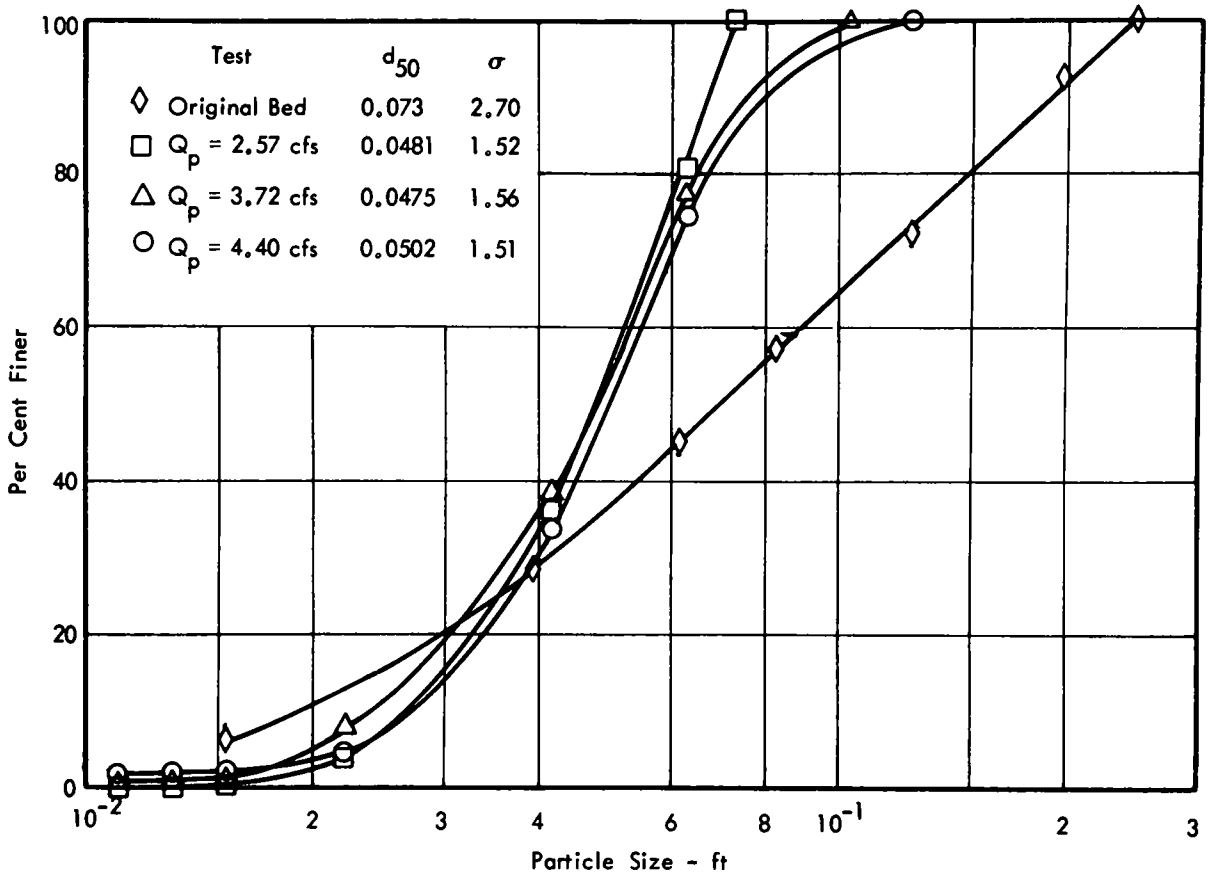

Figure 71 Size distribution of transported riprap—Series II.

scribing the weight of gravel per unit area. These thicknesses varied from zero to 1.6 times the effective diameter of the riprap. For each thickness, various flows could be discharged over the riprap layers to generate various boundary shear stresses. The channel was then divided into four portions, and on each a riprap layer of a particular thickness was placed. Near the end of each portion a small hopper equal to the channel width was inserted into the bed so that any sand transported through or over the riprap layer was trapped. The transport rate was determined by the amount trapped and the duration of the test This arrangement permitted the performance of four experiments at the same time.

The shear stress on the bed for each discharge was determined from the depth of flow and the channel slope.

Leaching Characteristics of Thin Riprap Layers

In these experiments the object was primarily to obtain qualitative information on the effect of the armor layer on the transport rate of the underlying base material when the thickness was less than one diameter. The results of these experiments appear in Figure 75, which shows the transport rate of the base material through riprap layers of various thicknesses in terms of the boundary shear stress Included in the figure is a line that indicates the transport rate of the gravel riprap in terms of the shear stress. The curves are well defined for each value of riprap thickness and show that the rate of transport of the base material decreases with increasing thickness of the armor layer and decreasing shear stress The data also suggest that for low shear stresses the transport rate of the riprap material is independent of the thickness of the riprap layer, that is, each particle moves independently of the others that may be in the bed.

The decrease in sand transport, defined as the difference between sand transport without riprap protection and sand transport with riprap protection, appears to be proportional to the thickness of the armor layer Figure 76 is a plot showing the transport rate for the sand of the base material as a function of a flow parameter as

$$q_s = f(\tau_o k^n) \tag{56}$$

in which q_s is the transport rate in pounds per foot per second, τ_o is the bed shear stress, n is the thickness of the riprap layer, and k is a constant ($k = 0.17$). Only those points that are part of the systematic family of curves in Figure 75 are included. The function in Figure 76 shows that the transport rate is proportional to a power of the shear stress and is reduced as the thickness of the riprap layer increases. This expression represents a qualitative relationship between the property of the riprap layer, the shear stress, and the transport rate, and is suggestive of the manner in which the various parameters influence the channel stability.

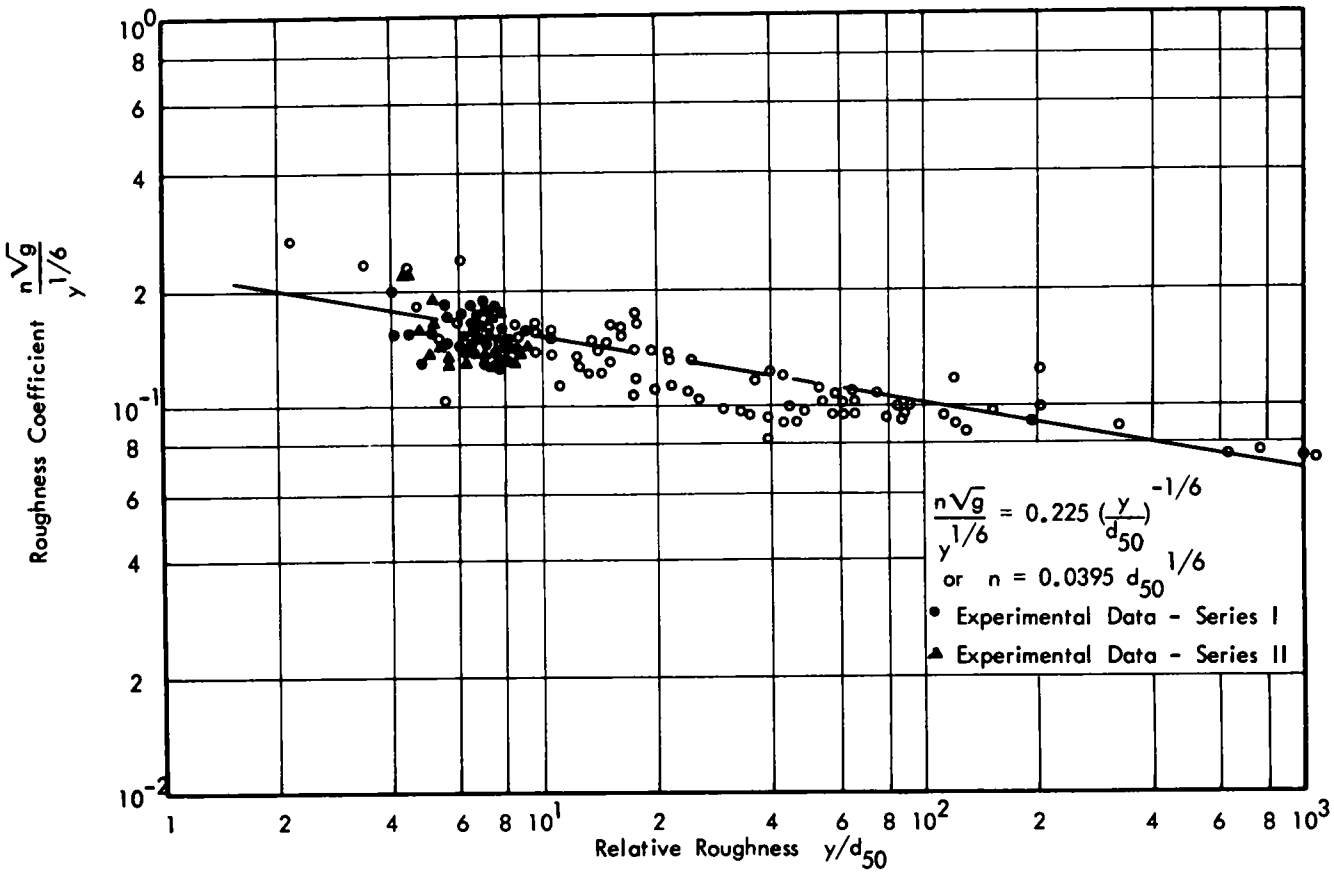

Figure 72. Variation of Manning's n *with relative roughness*

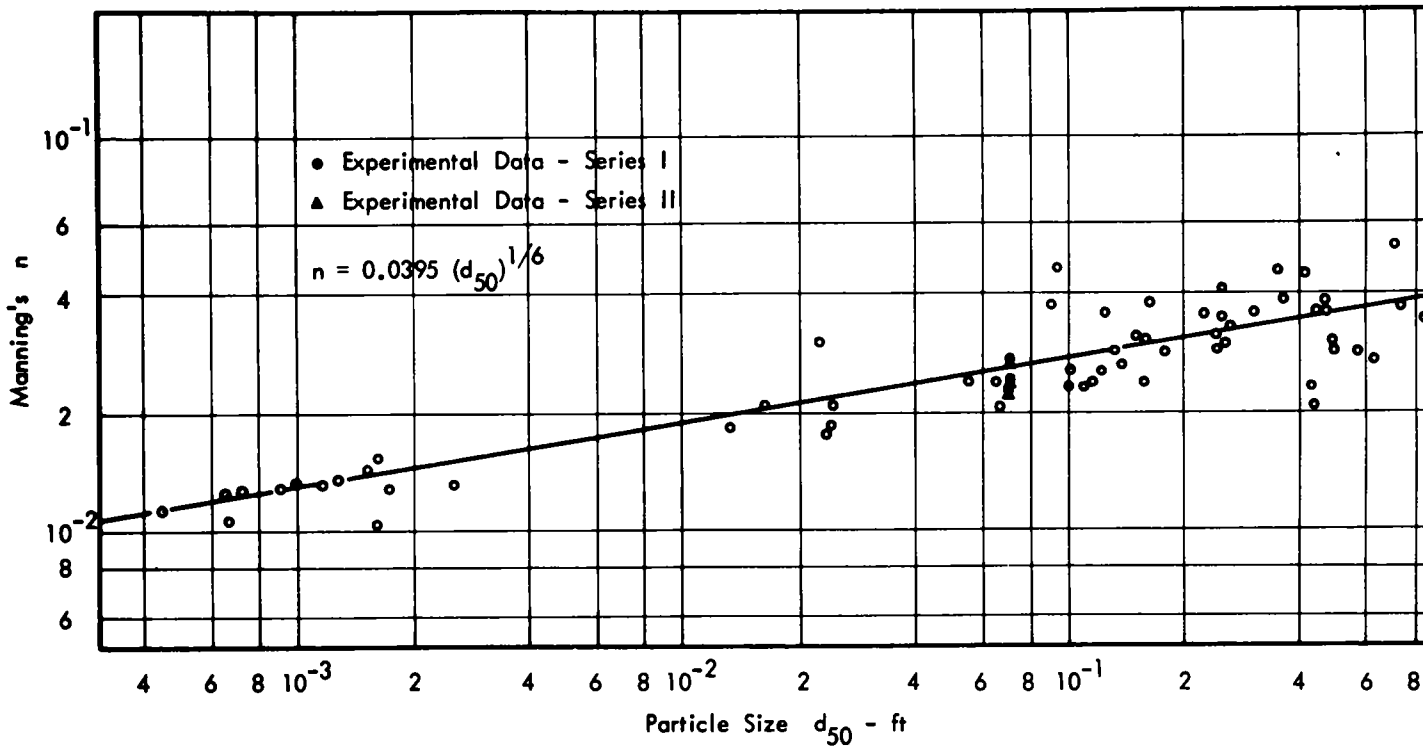

Figure 73. Variation of Manning's n *with particle size.*

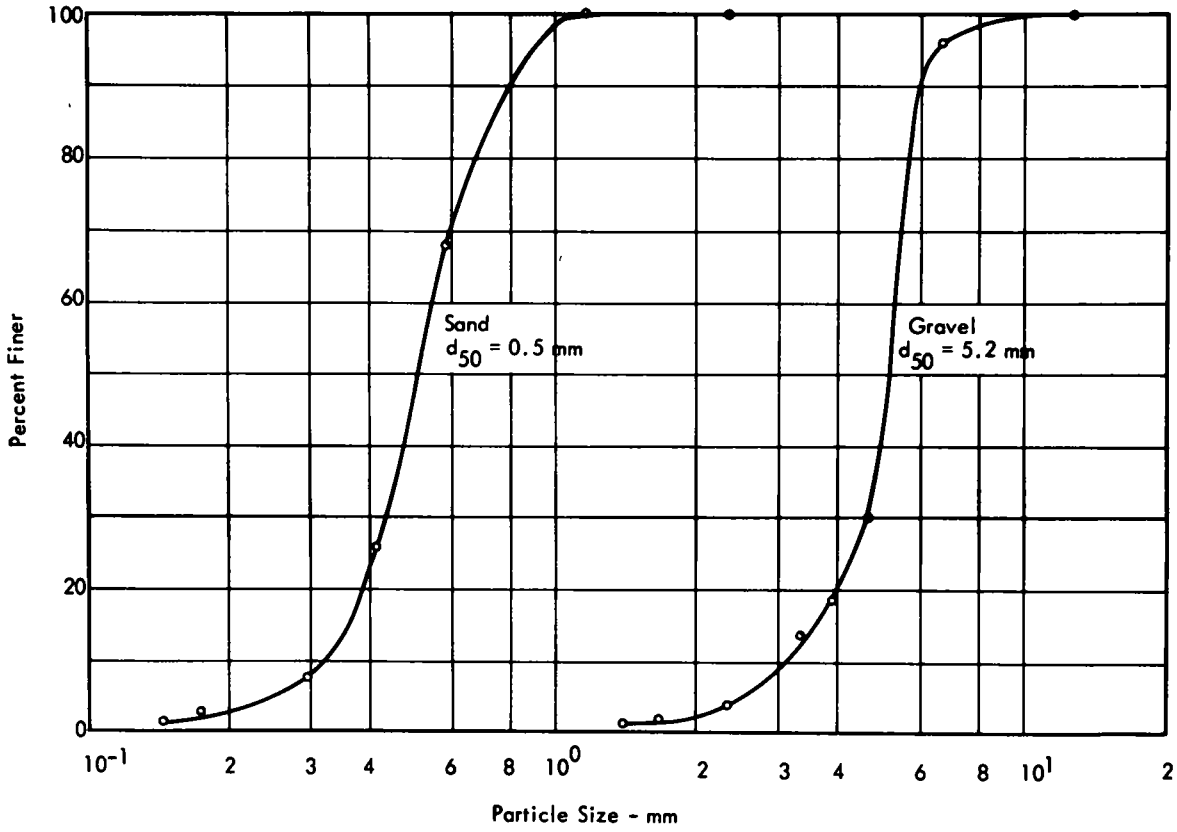

Figure 74 Size distribution of base material (sand $d_{50}=0.5$ mm) and riprap (gravel $d_{50}=5.2$ mm) for leaching experiment

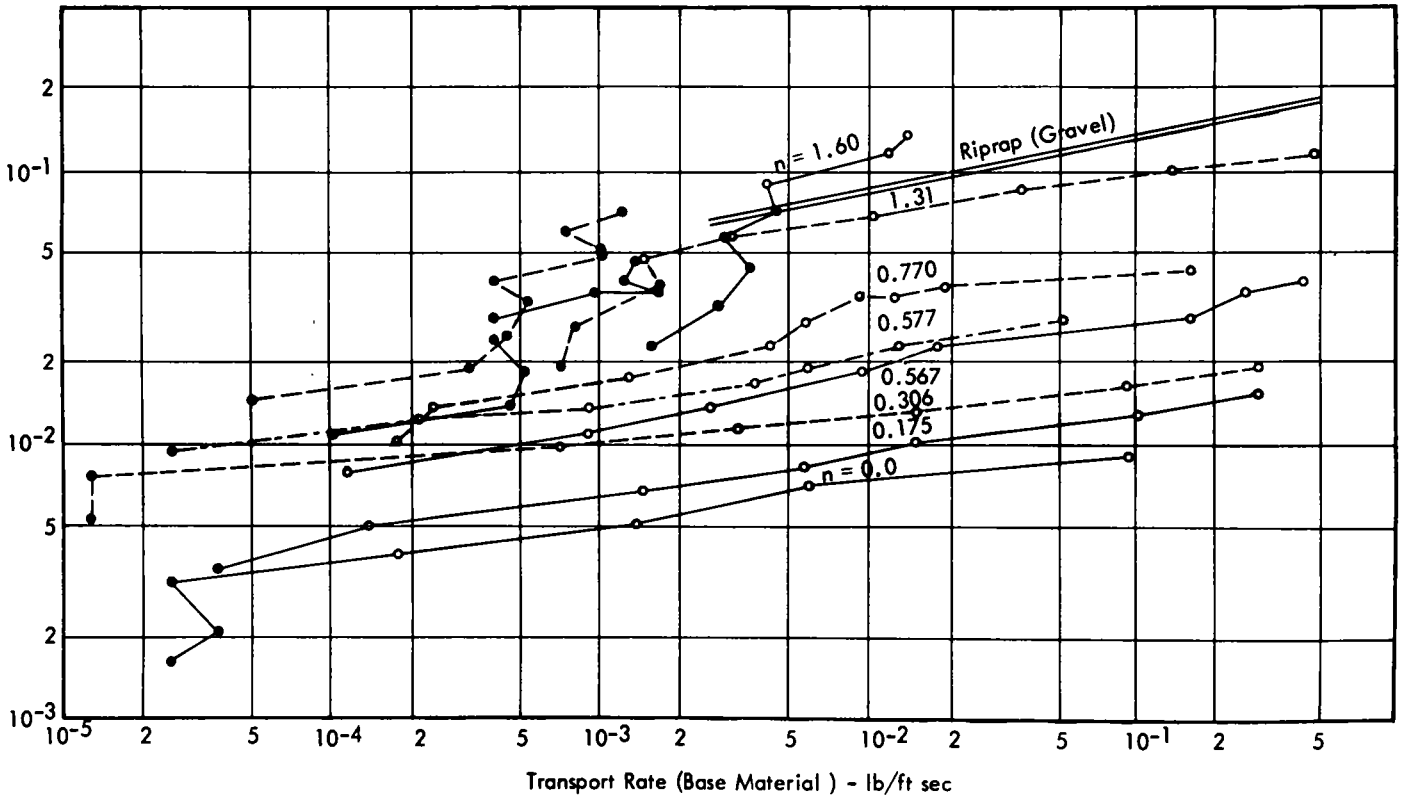

Figure 75 Transport rate of base material in terms of boundary shear and thickness of riprap layer

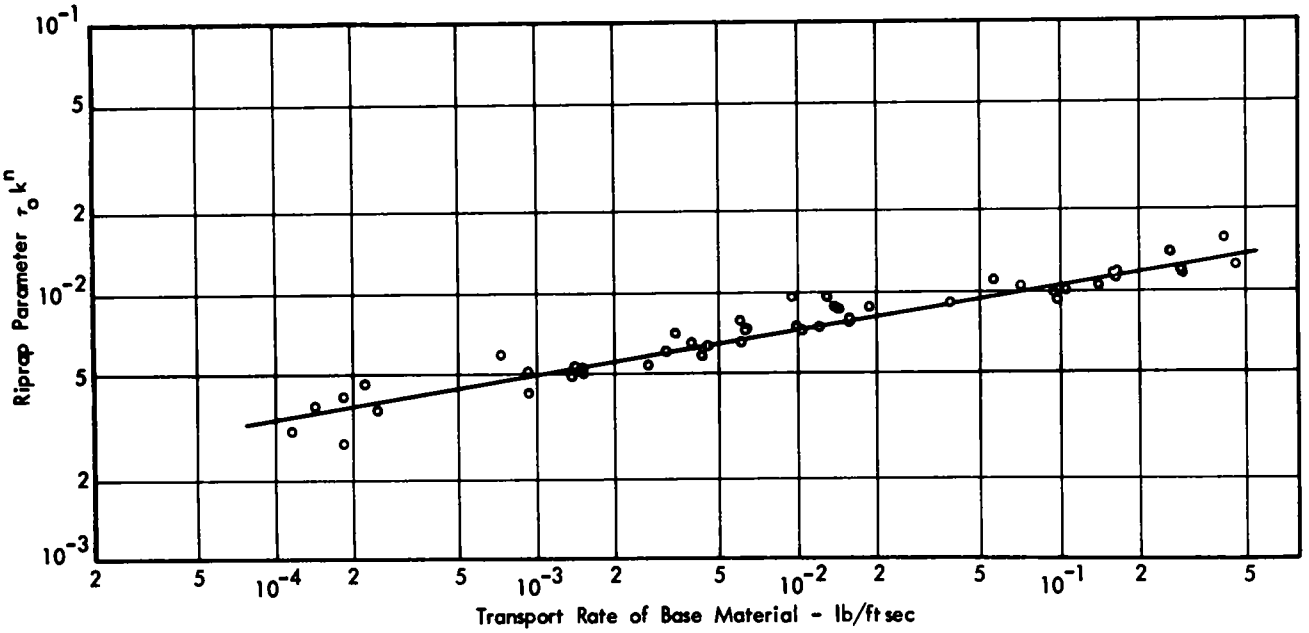

Figure 76 Variation of riprap parameter in terms of transport rate of base material

Effect of Thick Riprap Layers on Leaching of Base Material

In this set of experiments the rate of transport of the base material from or through a riprap layer consisting of layers of carefully defined particles was measured. They were made in the same flume as the previous experiments. The bottom of the flume was now covered with gravel (d_{50} = 16 mm) to a thickness of about 6 in. and placed at a longitudinal slope of 0.001. For these experiments the sand that was to be protected against leaching was placed in a small, flat vessel and its surface was screeded smooth. The vessel and the sand representing the base material are shown in Figure 77. Over the sand a layer of fine gravel was placed; it consisted of particles either 4 mm or 2 mm in size, depending on the experiment. The thickness of this layer was also established by placing a prescribed weight per unit area. The sub-layer of smaller gravel is shown in Figure 78, which also shows the vessel in place in the bed of the channel surrounded by the upper layer of coarse riprap Finally, the entire container was covered with the coarse upper layer consisting of gravel 16 mm in size (Fig 79). Considerable care was taken to cover the surface of the sample and the surrounding riprap as uniformly as possible. The same riprap particles were used for each test so that the degree of protection of the various segments of the riprap layer was the same for each experiment. The sample was then covered with a metal plate and the flume was filled with water from the downstream end. The required discharge was established and permitted to reach equilibrium and become steady before the plate was removed and the riprap was exposed to the shear stresses. After an appropriate time the flow was stopped and the sample was removed from the bed. The sample of base material was then dried and weighed. The amount of leaching that had occurred then was the difference in weight of the sample before and after the experiment.

Seven grades of uniform material—having diameters (d_{50}) of 16, 4, 2, 1, 0.5, 0.25, and 0.125 mm—obtained by sieving were used in various parts of the experiments. The 16-mm gravel was used as riprap (top protective layer). The particles having sizes of 1, 0.5, 0 25, and 0.125 mm were used as base materials, and the intermediate gravel between 2 and 4 mm was used, at different times, both as the base material and the intermediate protective covering. The experiments were conducted at two values of the boundary shear stress that were determined from the velocity profile. Forty different combinations of flow, riprap, and base material were tested, with each experiment repeated five times. The average value of the characteristic parameters was computed and was plotted in the figures. The results of the experiments are shown in Figures 80, 81, and 82. It is obvious from these figures that the effect of the protective layer depends strongly on the number of layers in the protective blanket and not too strongly on the diameter of the base material. It is presumed that the boundary shear stress is greater than the critical shear stress for the base material, so that any particles that are exposed will be removed. The results indicate that it is necessary to use only enough coarse material to create a protective layer to reduce the transport of the base material. The minimum diameter that can be used depends not only on the flow condition but also on the position in the layer that is created. The riprap is supposed to consist of many layers, with the average size of the material increasing with increasing elevation within the layer. It appears that the riprap layer

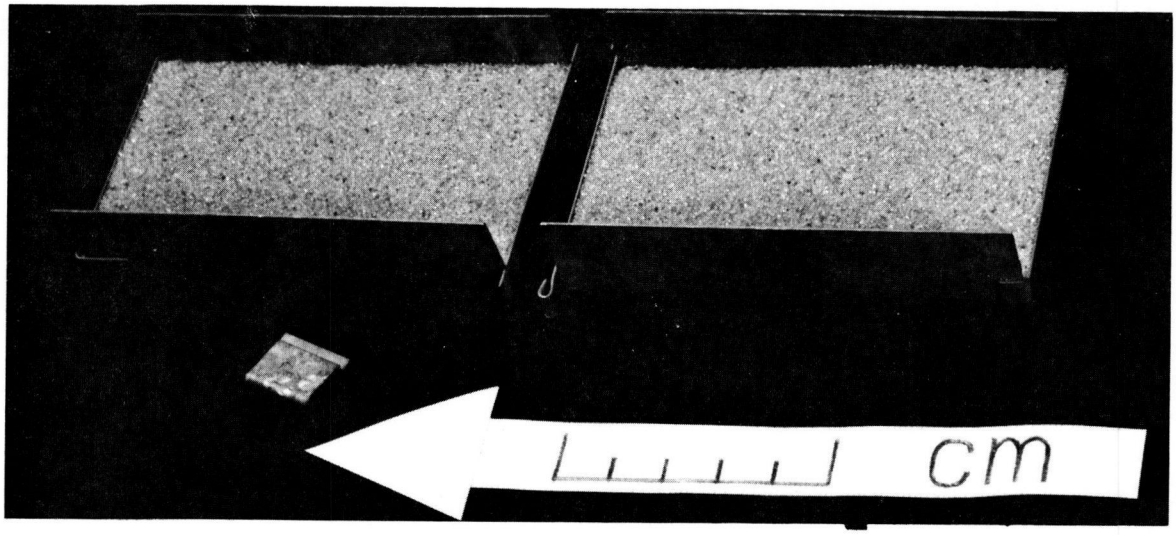

Figure 77.

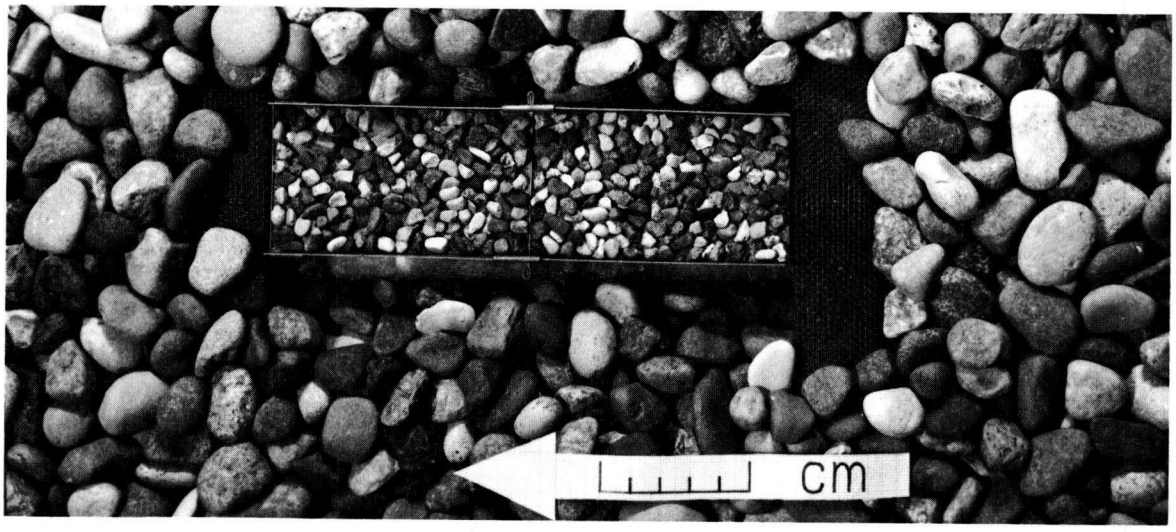

Figure 78.

Figure 79.

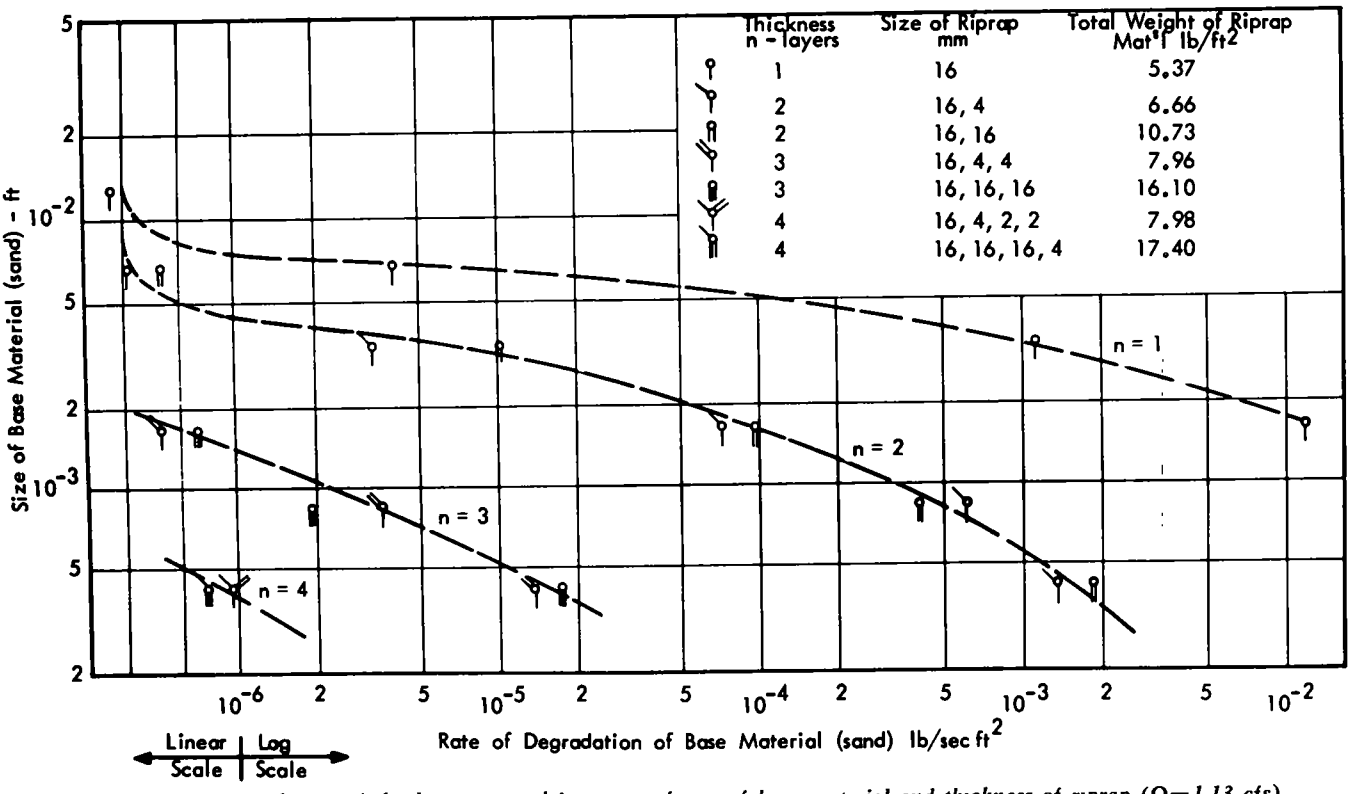

Figure 80 Rate of degradation of the base material in terms of size of base material and thickness of riprap (Q=1.13 cfs)

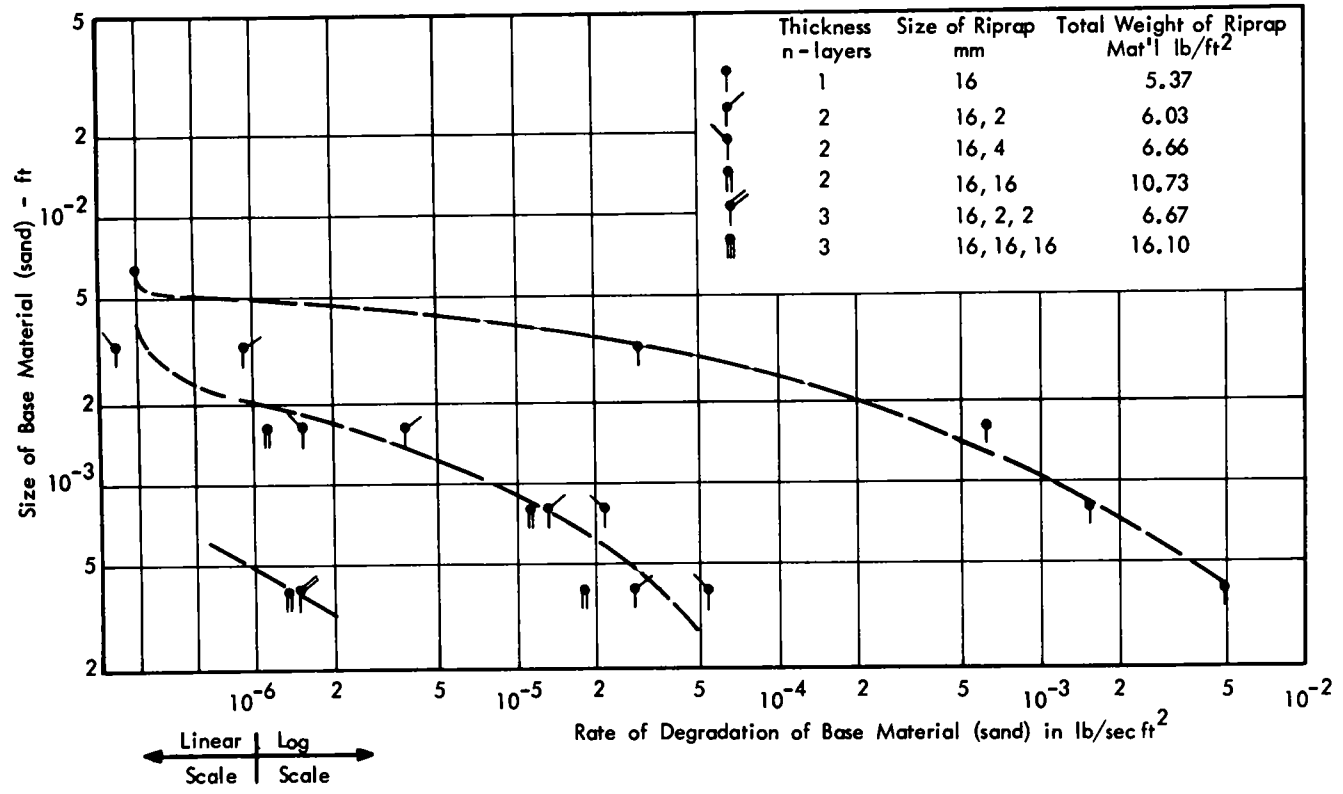

Figure 81. Rate of degradation of the base material in terms of size of base material and thickness of riprap (Q=1 13 cfs)

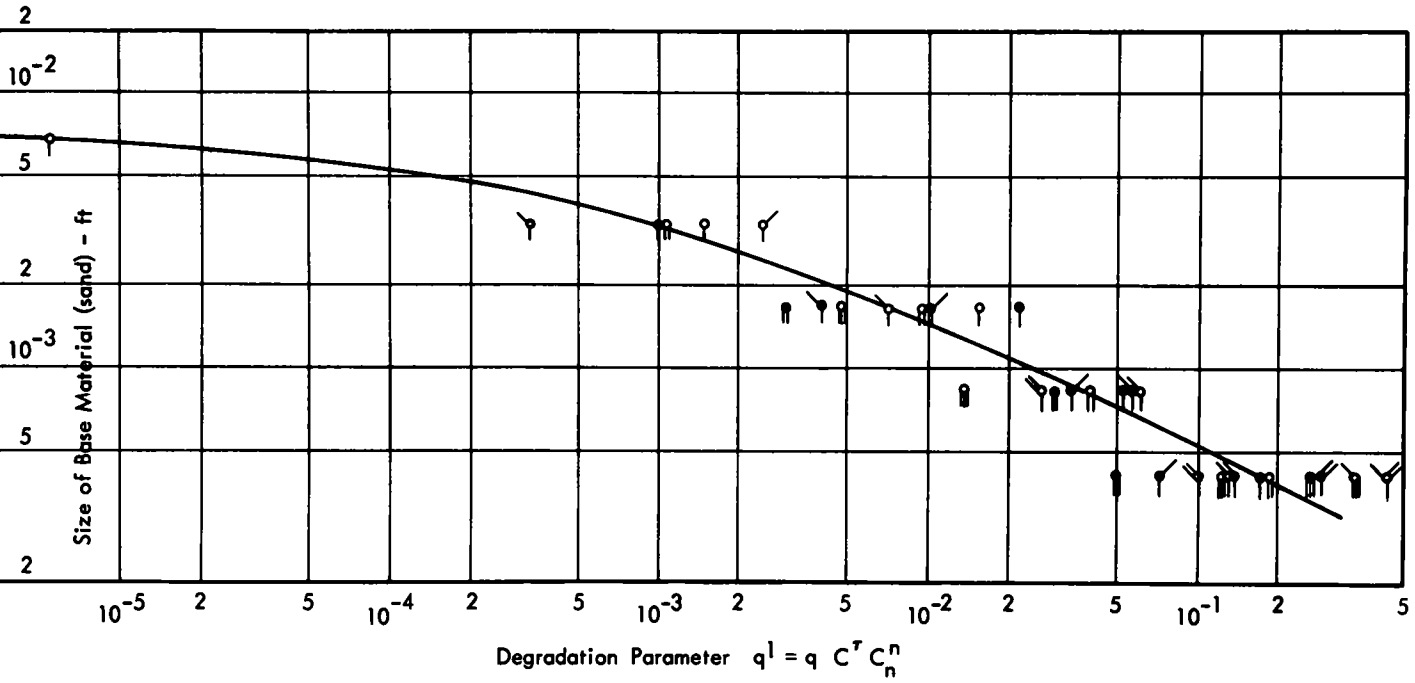

Figure 82. Base material degradation parameter in terms of size of base material. q = *transport rate of base material in lb/ft-sec;* τ = *unit shear in lb/sq ft;* n = *number of layers; and* C *and* C_n = *constants.*

can act as a filter to prevent the fine base material from being removed. In Figures 80 and 81 separate curves are drawn through the data corresponding to a specific number of layers in the riprap blanket. It appears that other curves would exist for intermediate values of thickness. In other words, the relationship between the size of the base material and the transport rate is a function of the effective thickness of the riprap layer. It further appears that the protective layer can reduce the transport rate very greatly but cannot prevent all transport. The reduction in the rate of scour in terms of the total number of layers that compose the protective layer is exponential, and the results suggest that each layer of protective material reduces the rate of degradation about 75 times.

CHAPTER THREE

APPLICATION OF DESIGN CHARTS TO CHANNEL DESIGN

In Chapter Two some examples of the use of the design charts to establish channel dimensions satisfying the prescribed discharge and slope are discussed. It must be borne in mind in the use of these charts that they are only graphical representations of the equations that were developed in the preceding chapters and that the equations themselves can be used in lieu of the charts or to extend the charts beyond the range for which they were drawn. The chart limits were determined primarily from the fact that the channels were to provide drainage for highways. For the trapezoidal channels the maximum discharge was set at 1,000 cfs, because larger channels would generally require engineering experience as well as design charts to accomplish a good design. The upper limit of the triangular drainage channels was set at 100 cfs, because it is not likely that greater discharges will be met.

The use of the charts as an aid to channel design can perhaps best be shown through the specific examples given

CHAPTER FOUR

RECOMMENDATIONS FOR FURTHER RESEARCH

The study on the design of riprap-lined highway drainage channels reported here represents what appears to be the initial phase of the solution of a problem of considerable magnitude. In this initial phase useful techniques that have been developed for the design of a rather large class of highway drainage channels may well serve as a basis for further investigations in this area The study and the results obtained suggest the direction of research for further useful results. This chapter attempts to outline some of the areas in which further research would be of considerable value

FIELD TESTING

The ultimate test of any analytical development or laboratory result is its operation in practice and perhaps at scales considerably larger than any that can be produced in a laboratory. Prototype drainage channels should be designed on the basis of the tentative procedures for various purposes and in various sizes to test not only the applicability of the procedures to highway practice but also the validity of the design assumptions and the experimental data incorporated in the procedure. This will require a considerable period of time for construction to be completed and to yield test data, because any such test depends on hydrologic circumstances for the discharges that will appropriately stress the system. In order to further this study, a continuing program by some organization having surveillance of highway practices would be desirable.

CHANNELS OF LARGE CAPACITY

Although the design procedures are not limited to the range of discharges for which the design charts were drawn, further consideration should be given to the extension of the design procedures to discharge perhaps an order of magnitude greater than those initially suggested Such a study would involve the search for and analysis of application of riprap in which the large rock particles are subjected to high velocities. Hydraulic structures of such magnitude are usually out of the area of routine design and require a considerable amount of engineering experience and judgment. The equations relating the four variables—discharge, slope, channel shape and size, and riprap properties—are of course applicable to such large structures, but it may be necessary to incorporate larger factors of safety as the structure becomes more important.

LABORATORY RESEARCH

Both fundamental and applied research in this area should be carried on By fundamental research is meant the mechanics of two-phase flow or flow over boundaries of discrete particles, the interrelationships between the flow and boundaries consisting of a wide range of particle sizes, the leaching phenomenon, shear distribution in bends, and the concept of a critical shear applied to a gradation of riprap particles By applied research is meant the further testing of various aspects of the design procedures. This includes testing of the stability and the nature of the forces acting on riprap placed on side slopes and in the neighborhood of the junction of the sides and bottom of trapezoidal channels Research should be carried out to determine the precision with which various geometrical or hydraulic properties can and should be computed Laboratory research can provide additional facts where data are limited, such as more precise determinations of the angle of repose of materials of various sizes, shapes, and textures. Much of this research should be carried on on a rather large scale so that the problems of extrapolation to prototype sizes of riprap may be minimized. The scale of such research is determined by a balance between the value of such results and the cost and time involved

REFERENCES

1 SEARCY, J K , "Design of Roadside Drainage Channels." *Hydraulics Design Series No. 4,* Bureau of Public Roads (May 1965).

2. CAMPBELL, F B., "Hydraulic Design of Rock Riprap." *Misc. Paper No. 2-777,* Waterways Experiment Station, Corps of Engineers, U.S. Army, Vicksburg, Miss. (Feb 1966).

3 REE, W O., "Flow of Water in Channels Protected by

Vegetative Linings." *USDA Tech. Bull. 967,* Soil Conservation Service (Feb. 1949)

4. VENNARD, J K., *Elementary Fluid Mechanics* Wiley, 4th ed. (1961).
5. KING, H. W., and BRATER, E. F., *Handbook of Hydraulics.* McGraw Hill, 5th ed (1963).
6 CHANG, Y. L., "Laboratory Investigation of Flume Traction and Transportation." *Trans. ASCE,* Vol. 104 (1939).
7. GILBERT, G. K., "The Transportation of Debris by Running Water." *U.S. Geological Survey Professional Paper 86* (1914).
8. LANE, E W., and CARLSON, E. J., "Some Factors Affecting the Stability of Canals Constructed in Coarse Granulated Material." *Proc. Minn. Hydraulics Conf.* (Sept 1953).
9 U.S Waterways Experiment Station, "Studies of River Bed Material and Their Movement with Special Reference to the Lower Mississippi River" *USWES Paper 17,* Vicksburg, Miss. (Jan. 1935).
10. SIMONS, D. B , *Theory and Design of Stable Channels in Alluvial Materials. Report CER No 570BS17,* Col. State Univ., Dept. of Civil Eng. (May 1957)
11. KELLERHALS, R , "Stable Channels with Gravel Paved Beds." *J. Waterways and Harbors Div., ASCE,* Vol. 93 (Feb 1967)
12. SCHNACKENBERG, E. C., "Slope Discharge Formulas for Alluvial Streams and Rivers." *Proc. New Zealand Inst. of Civil Eng.,* Vol. 37 (1957).
13. GARDE, R J , "Discussion of 'Discharge Formulas for Straight Alluvial Channels,' by H K. Lui and S. Y. Huang." *Trans. ASCE,* Vol. 126, Part I (1961).
14. KRAMER, H., "Sand Mixtures and Sand Movement in Fluvial Models." *Trans. ASCE,* Vol. 100 (1935).
15 SHIELDS, A., "Anwendung der Aehnlichkeitsmechanik und der Turbulenzforschung auf die Geschiebebewegung *Mitteilungen der Preuss Versuchsanstalt fur Wasserbau und Schiffbau,* Part 26, Berlin (1936).
16. NEILL, C. R., *Stability of Coarse Bed-Material in Open-Channel Flow.* Research Council of Alberta, Highways Div., Edmonton (Jan 1967).
17. MAVIS, F. T., Ho, L., and TU, Y C , "Transportation of Detritus by Flowing Water." *Studies in Eng., Bull. 5,* Univ. of Iowa (1935).
18. U.S. Corps of Engineers, *Bank Protection Studies* Linton Hydraulic Lab , Portland, Ore. (1938).
19. MEYER-PETER, E., and MULLER, R., "Formula for Bed Load Transport" *Proc IAHR,* Stockholm, Sweden (1948).
20. TINNEY, E. R , *A Study of the Mechanics of Degradation of a Bed of Uniform Sediment in Open Channels.* Ph.D. Thesis, Univ. of Minn. (1955).
21. LANE, E. W., "Progress Report on Results of Studies on Design of Stable Channels" *U.S. Bureau of Reclamation Hydraulic Lab Report No. Hyd-352,* Denver, Col. (June 1952).
22. Department of the Army, "Criterion for Graded Stone Riprap Channel Protection." *Draft Report 20,* Office of Chief of Engineers (Apr. 1966)
23 ISBASH, S. V , *Construction of Dams by Depositing Rock in Running Water.* Second Internat. Cong. on Large Dams, Wash., D C. (1936).
24. California Division of Highways, *Bank and Shore Protection in California Highway Practice.* Dept. of Public Works (1960).
25 PETERKA, A J., "Hydraulic Design of Stilling Basins and Energy Dissipators." *U.S. Bureau of Reclamation Eng. Monograph No 25*
26. OLSEN, O. J , and FLOREY, Q. L., "Sedimentation Studies in Open Channels—Boundary Shear and Velocity Distribution by the Membrane Analogy, Analytic, and Finite Difference Methods." *U.S. Bureau of Reclamation Structural Lab. Report No SP-34,* Denver, Col. (Aug. 1952).
27. REPLOGLE, J. A , and CHOW, V. T., "Tractive Force Distribution in Open Channels." *J Hydraulics Div., ASCE,* Vol. 92, No. HY2 (Mar. 1966).
28 IPPEN, A T., DRINKER, P. A , JOBIN, W. R., and SHEMDIN, O. H., Stream Dynamics and Boundary Shear Distributions for Curved Trapezoidal Channels." *Hydrodynamics Lab. Report No. 47,* MIT Jan. 1962).
29 LEOPOLD, L. B , BAGNOLD, R. A., WOLMAN, M. G., and BRUSH, L M , "Flow Resistance in Sinuous or Irregular Channels." *U.S. Geol. Survey Prof. Paper No 282 D* (1960).
30. YEN, B. C , *Characteristics of Subcritical Flow in a Meandering Channel* Inst. of Hydraulic Research, Univ. of Iowa (1965)
31 HARRISON, A J. M., "Design of Channels for Supercritical Flow" *Proc Inst of Civil Eng.,* London (Nov. 1966).
32. STRAUB, L. G., *Report on Experimental Studies of Gravel Stabilization Blanket for Stream Bed-Arkansas River Project.* Univ. of Minn., St. Anthony Falls Hydraulic Lab. (Nov. 1960).
33. Bureau of Reclamation, "The Use of Laboratory Tests to Develop Design Criteria for Protective Filters." *Earth Lab. Report No E M-425,* Denver, Col (June 1955).
34. U.S. Waterways Experiment Station, "Soil Mechanics Fact Finding Survey, Seepage Studies." *Tech. Memo No 175-1,* Vicksburg, Miss. (Mar. 1941).
35. LINDNER, W. M., "Stabilization of Streambeds with Sheet Piling and Rock Sills" *Proc Fed. Inter-Agency Sedimentation Conf.,* USDA Misc Pub. 970 (1963)
36. Bureau of Reclamation, *Lining for Irrigation Canals.* 1st ed. (1963).
37. STRAUB, L. G., *Report on Experimental Study of Gravel Stabilization Blanket for Stream Bed—Arkansas River Project.* Prepared for Div. Eng., Southwestern Div., Corps of Engineers, Dallas, Texas (Nov. 1960)
38 HARRISON, A. S., "Report on Special Investigation of Bed Sediment Segregation in a Degrading Bed." *Serial No. 33,* Univ. of Cal , Inst. of Eng. Research, Berkeley (Sept. 1950).

APPENDIX A

SIZE DISTRIBUTION AND GRADATION LIMITS FOR EIGHT STANDARD AGGREGATES

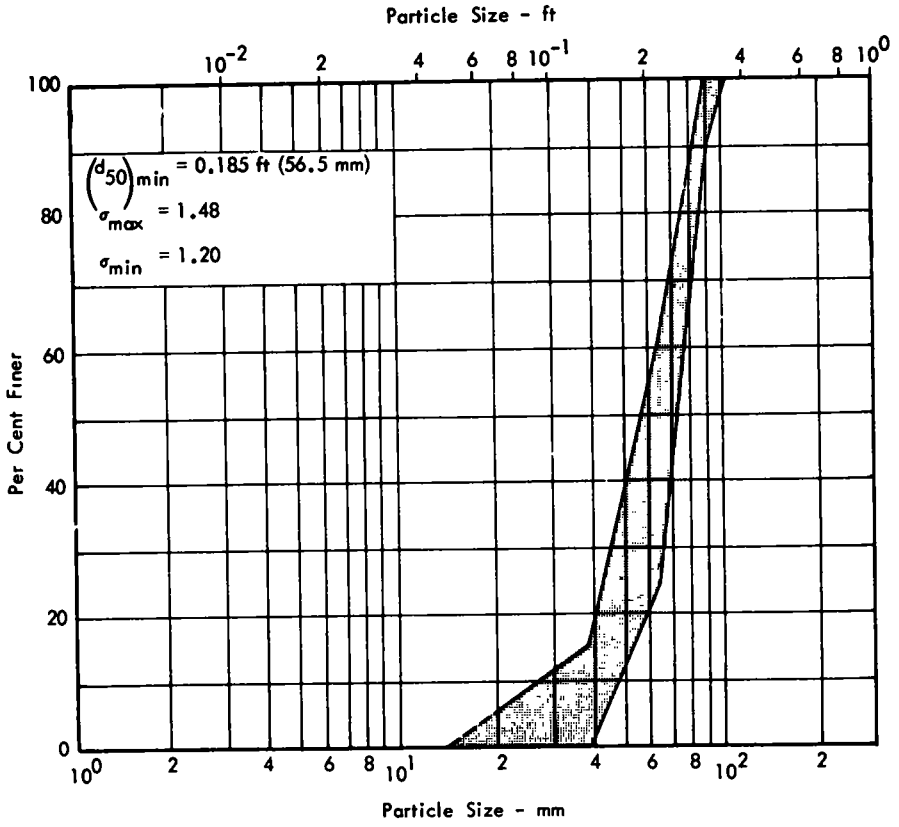

Figure A-1. Size distribution and gradation limits for standard aggregate No. 1, AASHO designation M 43-54.

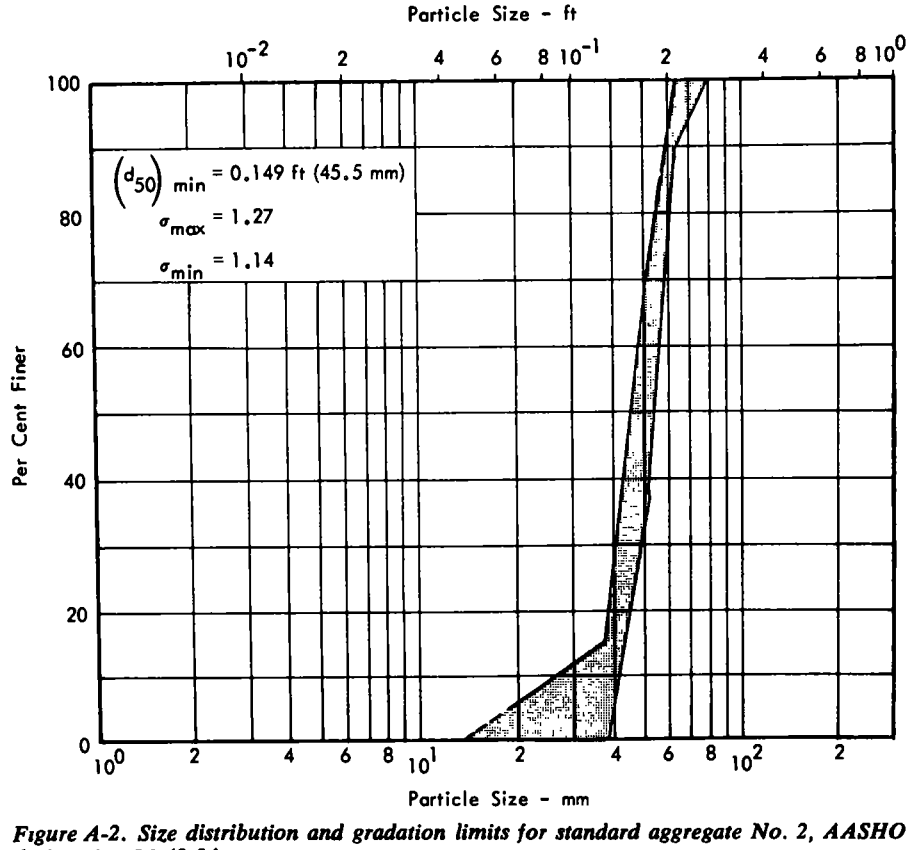

Figure A-2. Size distribution and gradation limits for standard aggregate No. 2, AASHO designation M 43-54

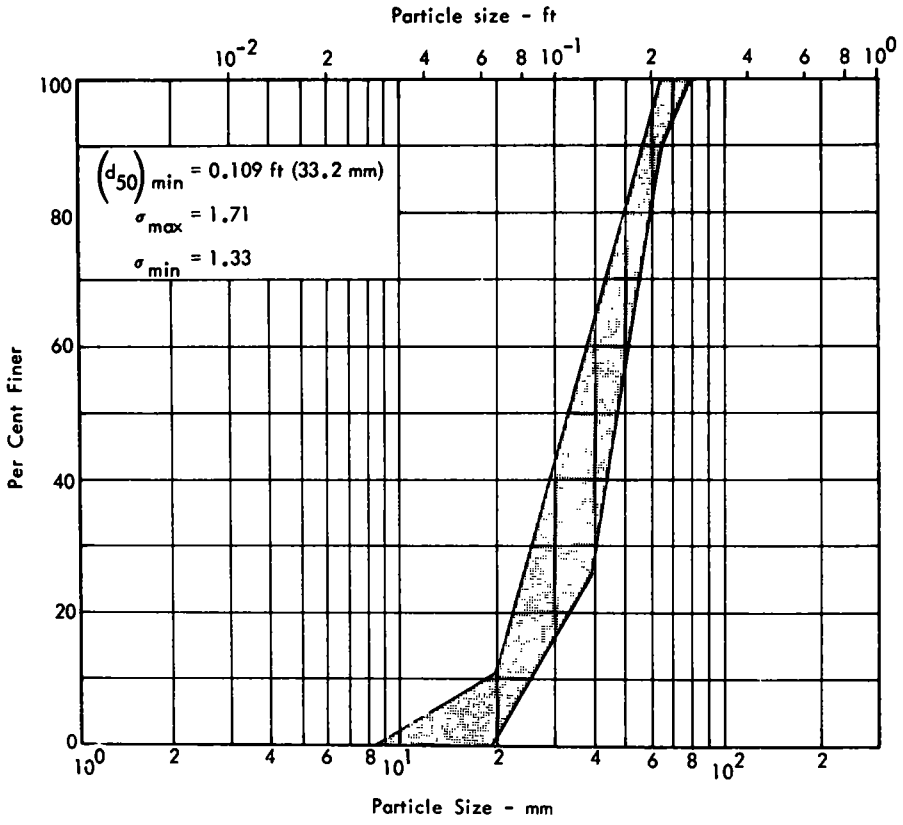

Figure A-3. Size distribution and gradation limits for standard aggregate No. 24, AASHO designation M 43-54.

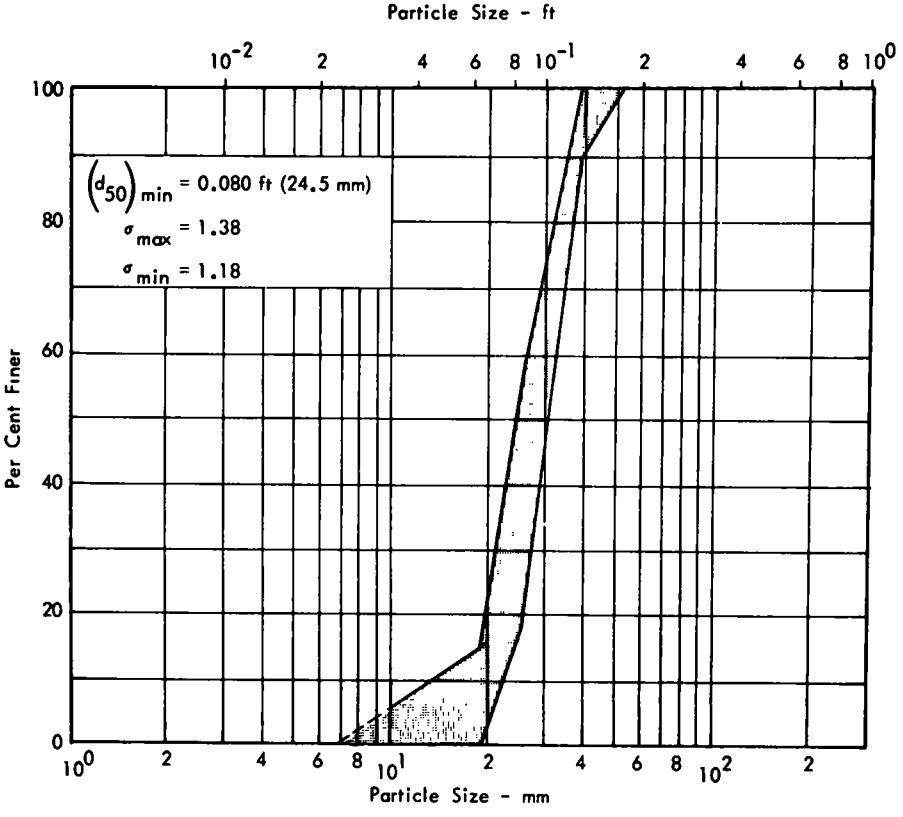

Figure A-4. Size distribution and gradation limits for standard aggregate No 4, AASHO designation M 43-54.

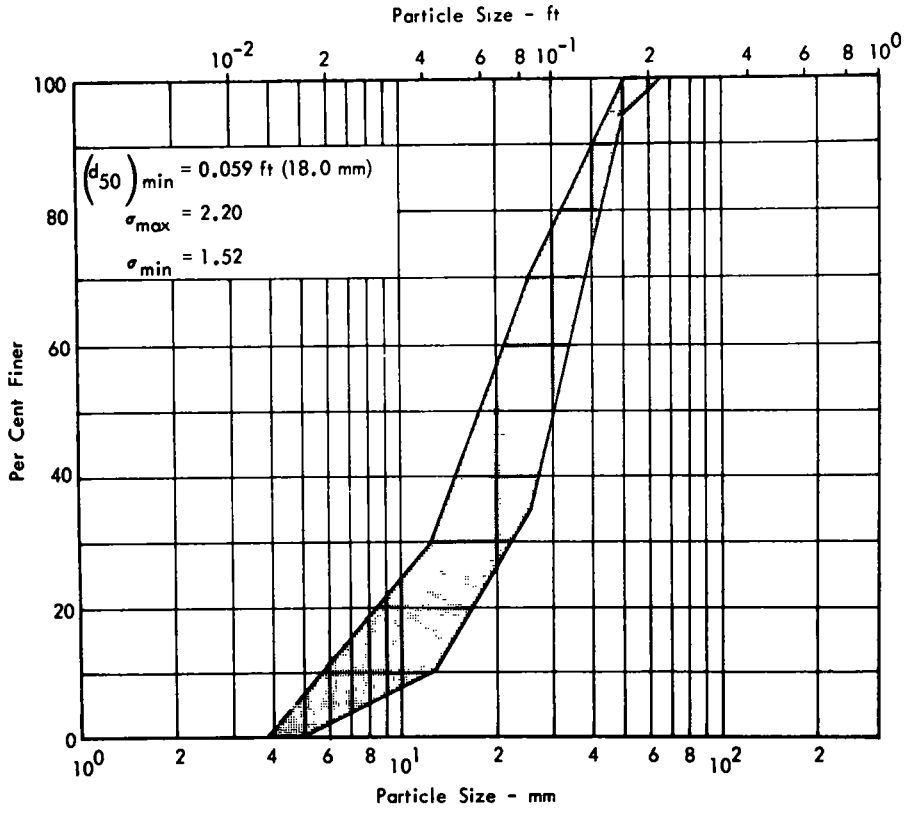

Figure A-5. Size distribution and gradation limits for standard aggregate No. 357, AASHO designation M 43-54.

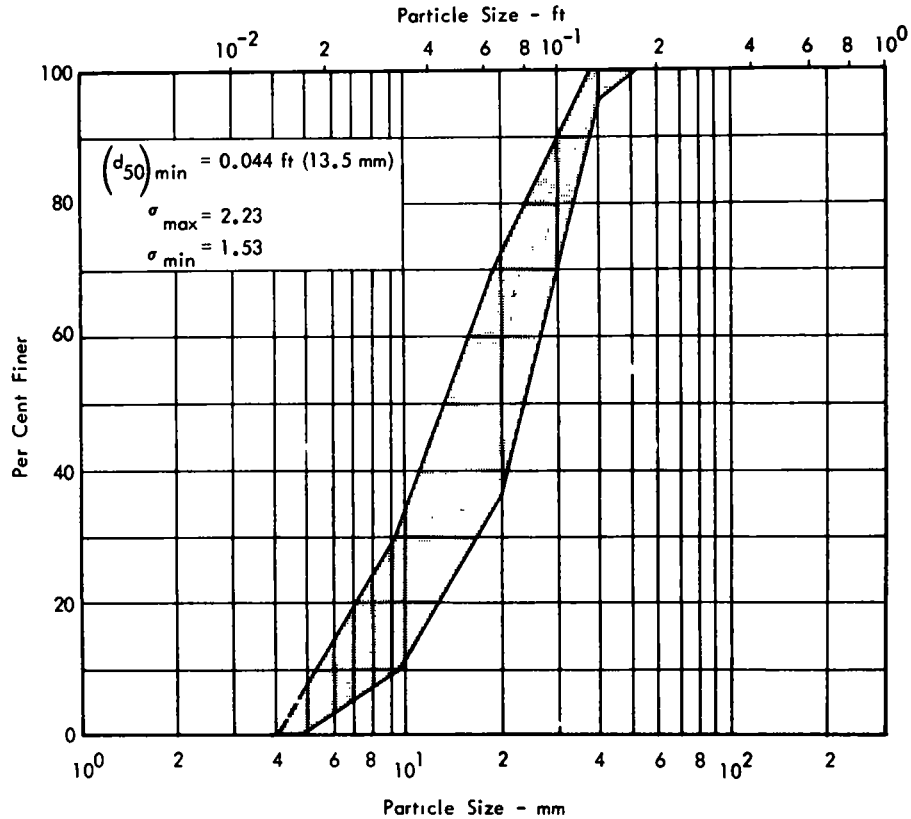

Figure A-6 Size distribution and gradation limits for standard aggregate No 467, AASHO designation M 43-54.

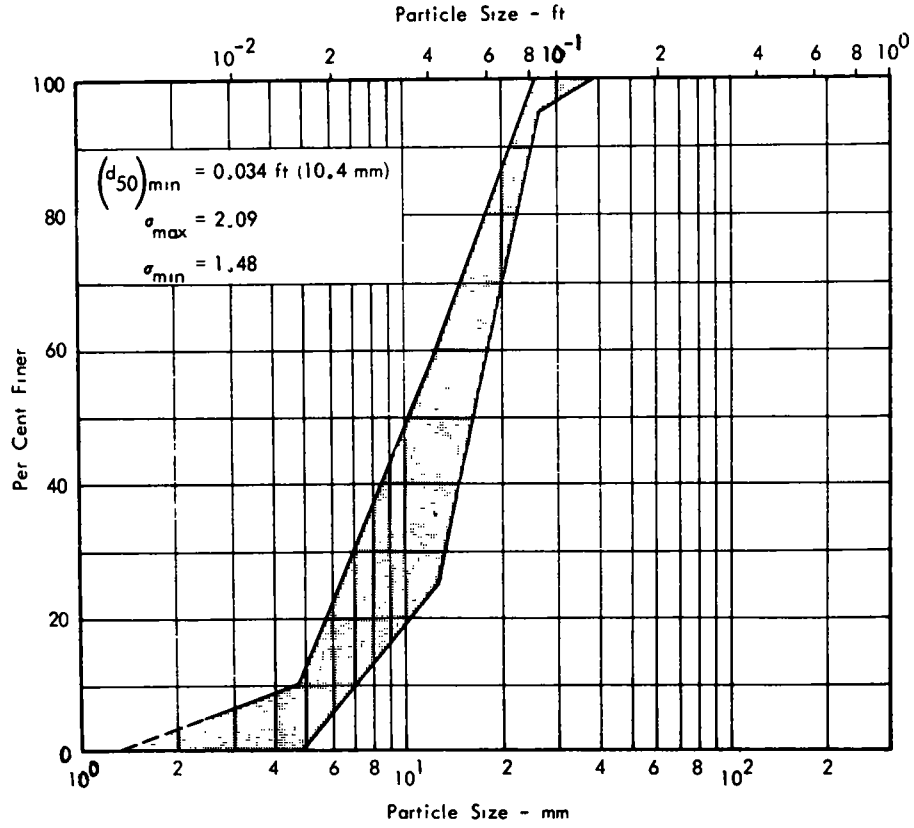

Figure A-7 Size distribution and gradation limits for standard aggregate No 57, AASHO designation M 43-54

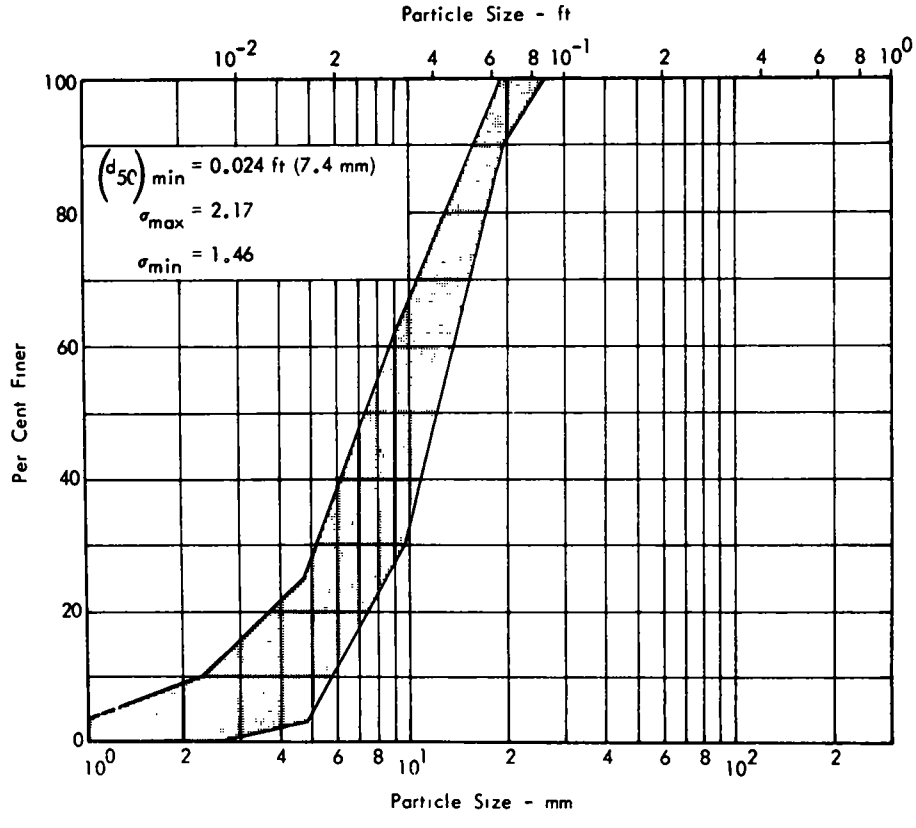

Figure A-8 Size distribution and gradation limits for standard aggregate No 68, AASHO designation M 43-54

Published reports of the

NATIONAL COOPERATIVE HIGHWAY RESEARCH PROGRAM

are available from:

Highway Research Board
National Academy of Sciences
2101 Constitution Avenue
Washington, D.C. 20418

Rep. No.	*Title*
—*	A Critical Review of Literature Treating Methods of Identifying Aggregates Subject to Destructive Volume Change When Frozen in Concrete and a Proposed Program of Research—Intermediate Report (Proj. 4-3(2)), 81 p., $1 80
1	Evaluation of Methods of Replacement of Deteriorated Concrete in Structures (Proj. 6-8), 56 p., $2.80
2	An Introduction to Guidelines for Satellite Studies of Pavement Performance (Proj. 1-1), 19 p, $1.80
2A	Guidelines for Satellite Studies of Pavement Performance, 85 p +9 figs, 26 tables, 4 app., $3 00
3	Improved Criteria for Traffic Signals at Individual Intersections—Interim Report (Proj. 3-5), 36 p., $1.60
4	Non-Chemical Methods of Snow and Ice Control on Highway Structures (Proj 6-2), 74 p, $3.20
5	Effects of Different Methods of Stockpiling Aggregates—Interim Report (Proj. 10-3), 48 p., $2 00
6	Means of Locating and Communicating with Disabled Vehicles—Interim Report (Proj. 3-4), 56 p. $3 20
7	Comparison of Different Methods of Measuring Pavement Condition—Interim Report (Proj 1-2), 29 p, $1.80
8	Synthetic Aggregates for Highway Construction (Proj. 4-4), 13 p., $1 00
9	Traffic Surveillance and Means of Communicating with Drivers—Interim Report (Proj. 3-2), 28 p., $1 60
10	Theoretical Analysis of Structural Behavior of Road Test Flexible Pavements (Proj 1-4), 31 p, $2.80
11	Effect of Control Devices on Traffic Operations—Interim Report (Proj 3-6), 107 p., $5 80
12	Identification of Aggregates Causing Poor Concrete Performance When Frozen—Interim Report (Proj. 4-3(1)), 47 p, $3.00
13	Running Cost of Motor Vehicles as Affected by Highway Design—Interim Report (Proj. 2-5), 43 p., $2 80
14	Density and Moisture Content Measurements by Nuclear Methods—Interim Report (Proj. 10-5), 32 p., $3.00
15	Identification of Concrete Aggregates Exhibiting Frost Susceptibility—Interim Report (Proj. 4-3(2)), 66 p., $4.00
16	Protective Coatings to Prevent Deterioration of Concrete by Deicing Chemicals (Proj 6-3), 21 p, $1.60
17	Development of Guidelines for Practical and Realistic Construction Specifications (Proj. 10-1), 109 p., $6.00
18	Community Consequences of Highway Improvement (Proj 2-2), 37 p., $2 80
19	Economical and Effective Deicing Agents for Use on Highway Structures (Proj. 6-1), 19 p, $1.20
20	Economic Study of Roadway Lighting (Proj. 5-4), 77 p., $3.20
21	Detecting Variations in Load-Carrying Capacity of Flexible Pavements (Proj. 1-5), 30 p., $1.40
22	Factors Influencing Flexible Pavement Performance (Proj. 1-3(2)), 69 p., $2.60
23	Methods for Reducing Corrosion of Reinforcing Steel (Proj. 6-4), 22 p., $1.40
24	Urban Travel Patterns for Airports, Shopping Centers, and Industrial Plants (Proj. 7-1), 116 p., $5.20
25	Potential Uses of Sonic and Ultrasonic Devices in Highway Construction (Proj. 10-7), 48 p, $2.00
26	Development of Uniform Procedures for Establishing Construction Equipment Rental Rates (Proj. 13-1), 33 p., $1.60
27	Physical Factors Influencing Resistance of Concrete to Deicing Agents (Proj. 6-5), 41 p., $2.00
28	Surveillance Methods and Ways and Means of Communicating with Drivers (Proj. 3-2), 66 p., $2.60
29	Digital-Computer-Controlled Traffic Signal System for a Small City (Proj. 3-2), 82 p., $4.00
30	Extension of AASHO Road Test Performance Concepts (Proj 1-4(2)), 33 p., $1.60
31	A Review of Transportation Aspects of Land-Use Control (Proj. 8-5), 41 p., $2.00
32	Improved Criteria for Traffic Signals at Individual Intersections (Proj. 3-5), 134 p., $5.00
33	Values of Time Savings of Commercial Vehicles (Proj. 2-4), 74 p., $3.60
34	Evaluation of Construction Control Procedures—Interim Report (Proj. 10-2), 117 p, $5.00
35	Prediction of Flexible Pavement Deflections from Laboratory Repeated-Load Tests (Proj. 1-3(3)), 117 p., $5.00
36	Highway Guardrails—A Review of Current Practice (Proj. 15-1), 33 p., $1.60
37	Tentative Skid-Resistance Requirements for Main Rural Highways (Proj. 1-7), 80 p., $3.60
38	Evaluation of Pavement Joint and Crack Sealing Materials and Practices (Proj 9-3), 40 p., $2.00
39	Factors Involved in the Design of Asphaltic Pavement Surfaces (Proj. 1-8), 112 p., $5.00
40	Means of Locating Disabled or Stopped Vehicles (Proj. 3-4(1)), 40 p, $2.00
41	Effect of Control Devices on Traffic Operations (Proj. 3-6), 83 p., $3.60
42	Interstate Highway Maintenance Requirements and Unit Maintenance Expenditure Index (Proj. 14-1), 144 p., $5.60
43	Density and Moisture Content Measurements by Nuclear Methods (Proj. 10-5), 38 p., $2.00
44	Traffic Attraction of Rural Outdoor Recreational Areas (Proj. 7-2), 28 p., $1.40
45	Development of Improved Pavement Marking Materials—Laboratory Phase (Proj. 5-5), 24 p., $1.40
46	Effects of Different Methods of Stockpiling and Handling Aggregates (Proj. 10-3), 102 p., $4.60
47	Accident Rates as Related to Design Elements of Rural Highways (Proj. 2-3), 173 p., $6.40
48	Factors and Trends in Trip Lengths (Proj 7-4), 70 p, $3 20
49	National Survey of Transportation Attitudes and Behavior—Phase I Summary Report (Proj. 20-4), 71 p, $3.20

* Highway Research Board Special Report 80

Rep. No.	Title
50	Factors Influencing Safety at Highway-Rail Grade Crossings (Proj. 3-8), 113 p., $5 20
51	Sensing and Communication Between Vehicles (Proj. 3-3), 105 p., $5.00
52	Measurement of Pavement Thickness by Rapid and Nondestructive Methods (Proj 10-6), 82 p., $3.80
53	Multiple Use of Lands Within Highway Rights-of-Way (Proj. 7-6), 68 p., $3.20
54	Location, Selection, and Maintenance of Highway Guardrails and Median Barriers (Proj. 15-1(2)), 63 p., $2 60
55	Research Needs in Highway Transportation (Proj. 20-2), 66 p , $2.80
56	Scenic Easements—Legal, Administrative, and Valuation Problems and Procedures (Proj. 11-3), 174 p., $6.40
57	Factors Influencing Modal Trip Assignment (Proj 8-2), 78 p., $3.20
58	Comparative Analysis of Traffic Assignment Techniques with Actual Highway Use (Proj. 7-5), 85 p., $3.60
59	Standard Measurements for Satellite Road Test Program (Proj. 1-6), 78 p., $3.20
60	Effects of Illumination on Operating Characteristics of Freeways (Proj. 5-2) 148 p., $6.00
61	Evaluation of Studded Tires—Performance Data and Pavement Wear Measurement (Proj. 1-9), 66 p., $3 00
62	Urban Travel Patterns for Hospitals, Universities, Office Buildings, and Capitols (Proj. 7-1), 144 p., $5.60
63	Economics of Design Standards for Low-Volume Rural Roads (Proj. 2-6), 93 p., $4.00
64	Motorists' Needs and Services on Interstate Highways (Proj. 7-7), 88 p , $3.60
65	One-Cycle Slow-Freeze Test for Evaluating Aggregate Performance in Frozen Concrete (Proj. 4-3(1)), 21 p , $1.40
66	Identification of Frost-Susceptible Particles in Concrete Aggregates (Proj. 4-3(2)), 62 p., $2 80
67	Relation of Asphalt Rheological Properties to Pavement Durability (Proj. 9-1), 45 p., $2.20
68	Application of Vehicle Operating Characteristics to Geometric Design and Traffic Operations (Proj. 3-10), 38 p., $2.00
69	Evaluation of Construction Control Procedures—Aggregate Gradation Variations and Effects (Proj 10-2A), 58 p., $2.80
70	Social and Economic Factors Affecting Intercity Travel (Proj. 8-1), 68 p., $3.00
71	Analytical Study of Weighing Methods for Highway Vehicles in Motion (Proj. 7-3), 63 p., $2.80
72	Theory and Practice in Inverse Condemnation for Five Representative States (Proj. 11-2), 44 p , $2.20
73	Improved Criteria for Traffic Signal Systems on Urban Arterials (Proj. 3-5/1), 55 p., $2.80
74	Protective Coatings for Highway Structural Steel (Proj. 4-6), 64 p., $2.80
74A	Protective Coatings for Highway Structural Steel—Literature Survey (Proj. 4-6), 275 p., $8.00
74B	Protective Coatings for Highway Structural Steel—Current Highway Practices (Proj. 4-6), 102 p., $4.00
75	Effect of Highway Landscape Development on Nearby Property (Proj. 2-9), 82 p., $3.60
76	Detecting Seasonal Changes in Load-Carrying Capabilities of Flexible Pavements (Proj 1-5(2)), 37 p., $2.00
77	Development of Design Criteria for Safer Luminaire Supports (Proj. 15-6), 82 p., $3.80
78	Highway Noise—Measurement, Simulation, and Mixed Reactions (Proj 3-7), 78 p., $3.20
79	Development of Improved Methods for Reduction of Traffic Accidents (Proj. 17-1), 163 p., $6.40
80	Oversize-Overweight Permit Operation on State Highways (Proj. 2-10), 120 p., $5.20
81	Moving Behavior and Residential Choice—A National Survey (Proj. 8-6), 129 p , $5.60
82	National Survey of Transportation Attitudes and Behavior—Phase II Analysis Report (Proj 20-4), 89 p , $4.00
83	Distribution of Wheel Loads on Highway Bridges (Proj. 12-2), 56 p , $2.80
84	Analysis and Projection of Research on Traffic Surveillance, Communication, and Control (Proj. 3-9), 48 p., $2.40
85	Development of Formed-in-Place Wet Reflective Markers (Proj. 5-5), 28 p., $1.80
86	Tentative Service Requirements for Bridge Rail Systems (Proj 12-8), 62 p., $3.20
87	Rules of Discovery and Disclosure in Highway Condemnation Proceedings (Proj. 11-1(5)), 28 p., $2.00
88	Recognition of Benefits to Remainder Property in Highway Valuation Cases (Proj. 11-1(2)), 24 p., $2 00
89	Factors, Trends, and Guidelines Related to Trip Length (Proj 7-4), 59 p., $3.20
90	Protection of Steel in Prestressed Concrete Bridges (Proj. 12-5), 86 p., $4 00
91	Effects of Deicing Salts on Water Quality and Biota—Literature Review and Recommended Research (Proj. 16-1), 70 p , $3 20
92	Valuation and Condemnation of Special Purpose Properties (Proj. 11-1(6)), 47 p., $2.60
93	Guidelines for Medial and Marginal Access Control on Major Roadways (Proj. 3-13), 147 p., $6.20
94	Valuation and Condemnation Problems Involving Trade Fixtures (Proj. 11-1(9)), 22 p., $1.80
95	Highway Fog (Proj. 5-6), 48 p., $2.40
96	Strategies for the Evaluation of Alternative Transportation Plans (Proj. 8-4), 111 p., $5.40
97	Analysis of Structural Behavior of AASHO Road Test Rigid Pavements (Proj. 1-4(1)A), 35 p., $2 60
98	Tests for Evaluating Degradation of Base Course Aggregates (Proj. 4-2), 98 p $5 00
99	Visual Requirements in Night Driving (Proj 5-3), 38 p , $2.60
100	Research Needs Relating to Performance of Aggregates in Highway Construction (Proj. 4-8), 68 p , $3 40
101	Effect of Stress on Freeze-Thaw Durability of Concrete Bridge Decks (Proj. 6-9), 70 p , $3 60
102	Effect of Weldments on the Fatigue Strength of Steel Beams (Proj 12-7), 114 p., $5 40
103	Rapid Test Methods for Field Control of Highway Construction (Proj 10-4), 89 p., $5.00
104	Rules of Compensability and Valuation Evidence for Highway Land Acquisition (Proj. 11-1), 77 p., $4.40

Rep. No. *Title*

105 Dynamic Pavement Loads of Heavy Highway Vehicles (Proj. 15-5), 94 p., $5.00

106 Revibration of Retarded Concrete for Continuous Bridge Decks (Proj. 18-1), 67 p., $3.40

107 New Approaches to Compensation for Residential Undertakings (Proj. 11-1(10)), 27 p., $2.40

108 Tentative Design Procedure for Riprap-Lined Channels (Proj. 15-2), 75 p., $4.00

Synthesis of Highway Practice

1 Traffic Control for Freeway Maintenance (Proj. 20-5, Topic 1), 47 p., $2.20

2 Bridge Approach Design and Construction Practices (Proj. 20-5, Topic 2), 30 p., $2.00

3 Traffic-Safe and Hydraulically Efficient Drainage Practice (Proj. 20-5, Topic 4), 38 p., $2.20

4 Concrete Bridge Deck Durability (Proj. 20-5, Topic 3), 28 p., $2.20

5 Scour at Bridge Waterways (Proj. 20-5, Topic 5), 37 p., $2.40

THE NATIONAL ACADEMY OF SCIENCES is a private, honorary organization of more than 700 scientists and engineers elected on the basis of outstanding contributions to knowledge. Established by a Congressional Act of Incorporation signed by President Abraham Lincoln on March 3, 1863, and supported by private and public funds, the Academy works to further science and its use for the general welfare by bringing together the most qualified individuals to deal with scientific and technological problems of broad significance.

Under the terms of its Congressional charter, the Academy is also called upon to act as an official—yet independent—adviser to the Federal Government in any matter of science and technology. This provision accounts for the close ties that have always existed between the Academy and the Government, although the Academy is not a governmental agency and its activities are not limited to those on behalf of the Government.

THE NATIONAL ACADEMY OF ENGINEERING was established on December 5, 1964. On that date the Council of the National Academy of Sciences, under the authority of its Act of Incorporation, adopted Articles of Organization bringing the National Academy of Engineering into being, independent and autonomous in its organization and the election of its members, and closely coordinated with the National Academy of Sciences in its advisory activities. The two Academies join in the furtherance of science and engineering and share the responsibility of advising the Federal Government, upon request, on any subject of science or technology.

THE NATIONAL RESEARCH COUNCIL was organized as an agency of the National Academy of Sciences in 1916, at the request of President Wilson, to enable the broad community of U. S. scientists and engineers to associate their efforts with the limited membership of the Academy in service to science and the nation. Its members, who receive their appointments from the President of the National Academy of Sciences, are drawn from academic, industrial and government organizations throughout the country. The National Research Council serves both Academies in the discharge of their responsibilities.

Supported by private and public contributions, grants, and contracts, and voluntary contributions of time and effort by several thousand of the nation's leading scientists and engineers, the Academies and their Research Council thus work to serve the national interest, to foster the sound development of science and engineering, and to promote their effective application for the benefit of society.

THE DIVISION OF ENGINEERING is one of the eight major Divisions into which the National Research Council is organized for the conduct of its work. Its membership includes representatives of the nation's leading technical societies as well as a number of members-at-large. Its Chairman is appointed by the Council of the Academy of Sciences upon nomination by the Council of the Academy of Engineering.

THE HIGHWAY RESEARCH BOARD, organized November 11, 1920, as an agency of the Division of Engineering, is a cooperative organization of the highway technologists of America operating under the auspices of the National Research Council and with the support of the several highway departments, the Federal Highway Administration, and many other organizations interested in the development of transportation. The purpose of the Board is to advance knowledge concerning the nature and performance of transportation systems, through the stimulation of research and dissemination of information derived therefrom.

HIGHWAY RESEARCH BOARD
NATIONAL ACADEMY OF SCIENCES—NATIONAL RESEARCH COUNCIL
2101 Constitution Avenue Washington, D. C. 20418

ADDRESS CORRECTION REQUESTED